THE ELECTRICAL RESISTIVITY OF EVAPORATED FILMS OF TITANIUM AND ERBIUM AND THE STUDY OF THE RESISTANCE CHANGES OF ERBIUM FILMS OWING TO THE SORPTION OF GASES

by

B. Singh, M.Sc.

Being a thesis

Submitted to the University of Keele

for the Degree of Doctor of Philosophy

Department of Physics,
University of Keele,
Keele, Staffordshire,
England.

July 1971

ORIGINAL COPY TIGHTLY BOUND

SYNOPSIS

This thesis has been written in two parts in order that the reader will be able to follow the different types of experiment and the results obtained in two different vacuum systems.

In the first part of the thesis are described the results on the electrical resistivity and resistance-temperature characteristics of titanium and erbium films, evaporated onto soda glass microscope slides at room temperature in a glass belljar vacuum system at about 5×10^{-8} torr. The films of both the metals varied in their thickness from 40 to 1100 Å, and the resistivity was very high for the thinnest films but for the thickest ones it approached approximately double the bulk value. The measured resitivities for the continuous freshly prepared films of both the metals are too high to be explained on the basis of the size-effect theory[3,4] for diffuse scattering, and are attributed to the gaseous impurities taken down during and after their formation, and to small grain size, porosity, lattice defects etc. The temperature coefficient of resistance was negative for films less than 50-60 Å thick but positive for thicker ones. A bulk mean free path of 285 Å in titanium and 185±15 Å in erbium was calculated at room temperature.

It was very difficult to prepare erbium films for study in the electron microscope, and reasons are given for considering it unlikely that their structure was the same as for the normal films in vacuum. A mass spectrometric analysis of the residual gases showed that in residual vacua of 10^{-6} to 10^{-8} torr, films of both the metals had a large gettering effect on hydrogen and a small effect on other gases. The extremely large gettering effect of erbium on hydrogen (partial pressure decreased from 10^{-8} to 10^{-11} torr in a few minutes) and very small effect on oxygen, raised the author's curiosity to study the

effect of individual pure gases on erbium films from the point of view of their resistance.

The second part of this thesis describes the new apparatus designed for studying resistance changes of erbium films due to sorption of controlled amount of pure gases; representative of which are hydrogen and oxygen. A special adsorption vessel was constructed from pyrex glass with two platinum electrodes sealed into its wall to make electrical contact with the film (deposited on the inside wall of it), and this vessel was connected to a stainless steel ultra-high vacuum (10^{-9} torr or less) line with steel flanges and copper gaskets. The mass of the film was known from the original metal put in the filament, and was checked by quantitative volumetric analysis of the film after the experiment had been completed. The surface area of the films was measured from the physical adsorption of krypton at liquid nitrogen temperature, using the BET method. The total number of surface sites was calculated from a relationship suggested by Brennan et al.[109] for polycrystalline films. The quantity of gas sorbed by the film was calculated from the initial and final pressures of the gas in the reservoir and adsorption vessel and from their previously known volumes (calibrated by expanding helium in them). The measured surface area of the films increased linearly with increase of film thickness, and a mean specific surface area of 71 ± 18 square metre per gram of erbium was calculated.

At room temperature, the surface interaction of hydrogen with erbium was followed by its bulk sorption, and both types of interaction were accompanied by different types of resistance change. Experiments on hydrogen interaction with erbium at temperatures lower than 295°K were made to find out if the bulk sorption could be restricted. From the experiments carried out at 200°K, approximately 130-160°K and 78°K,

it is concluded that a temperature as low as 78°K would be needed to restrict the bulk hydride formation. However, the resistance changes at 78°K were not reproducible, most probably due to a magnetic transition (AFM-PM) of the bulk metal, which takes place around this temperature (78-86°K). At all the temperatures of study (132-145°K, 200°K and 295°K), the oxygen interaction is possibly confined to the measured surface, and for most of the adsorption, the resistance increased monotonically with the amount of oxygen adsorbed by the film. Oxygen is more strongly adsorbed on the film surface than hydrogen i.e. it blocks the surface and makes it completely inactive with respect to both molecular and atomized hydrogen. On the other hand, a film that has previously interacted with hydrogen is still capable of interacting with molecular oxygen.

The different likely mechanisms, which could change the resistance on adsorption, are discussed with simple mathematical expressions. A simple model[79] suggests that both these gases are adsorbed as atoms, and that each gas atom forms one chemical bond with a surface atom of the metal. The magnitudes of the resistance changes on adsorption of both the gases (15-30% due to hydrogen and 25-40% due to oxygen) are too large to be explained by one predominating mechanism or even by all the mechanisms operating simultaneously. The large magnitude of the resistance changes is attributed to the porous structure of the films and diffusion/adsorption on open capillaries, grain boundaries and dislocation lines reaching the film surface.

ACKNOWLEDGEMENTS

I wish to express my gratitude to:

Professor D.J.E. Ingram, for the provision of laboratory facilities.

Dr. N.A. Surplice, for his constant supervision, guidance and helpful discussion throughout the course of this work.

Dr. J. Müller, for his suggestions and general discussion at the second part of this work, and him and Dr. N.A. Surplice for their teaching and assistance in my glass blowing.

My thanks are also due to:

Mr. W. Brearley for his assistance and advice in my use of the electron microscope, and for providing facility for my drawing the diagrams.

Mr. G. Dudley and his workshop staff for their cooperation in constructional work.

Mr. I.V. Mitchell for his lending a small ion pump and my friends in the secondary electron physics group for their general cooperation.

Mr. M.T. Cheney for the photographic work, and Miss S.A. Leese for her typing of this thesis and its duplicating.

Mrs. S.K. Singh for her help in the preparation of readable manuscript.

The Government of India for the award of a scholarship to carry out this work.

CONTENTS

PART ONE

THE ELECTRICAL RESISTIVITY AND RESISTANCE-TEMPERATURE CHARACTERISTICS OF TITANIUM AND ERBIUM FILMS

CHAPTER I

THE ELECTRICAL PROPERTIES OF THIN METALLIC FILMS

1.1 Introduction

As early as 1920 and more extensively since 1950, thin films have been studied from the research and technical points of view. Solids exhibit many unusual physical properties when they are studied in extremely thin layers with thicknesses ranging from a few hundred Angstrom units to several microns. The electrical properties of thin films, which are often different from those of the bulk, are of increasing importance in the field of electronics. The low temperature coefficient of resistance of most of the resistive metal films makes them useful in the fabrication of stable thin-film resistors in thin-film hybrid circuits, and they have the advantage that the high frequency performance is considerably improved by the absence of inductance. Thin films of getter materials are used for achieving good vacuum in electronic valves. The interaction of gases with thin films has also become a subject of interest in the field of physical chemistry from the point of view of catalysis and the understanding of bond formation mechanisms.

In this research films of titanium and erbium metals have been selected for the study of their electrical properties and interactions with gases. Titanium is a typical member of the transition metals with respect to the quantities of gases it can absorb, and is an important material for getters, sputter-ion pumps and sublimation pumps. The metal erbium is a member of the rare-earth group and has been chosen for studying in detail. Since the electronic configurations of all rare-earth metals are so similar to each other, with identical outer electronic shells ($_5d^{0-1}{}_6s^2$) and differ only in their number of

electrons in the $_4f$ sub shell, many of their chemical properties are very much alike. The $_4f$ electrons play almost no part in valency forces but are mostly responsible for the physical properties. Both the metals readily interact with hydrogen and form dihydrides and trihydrides. Tritium and deuterium adsorbed in a thin film of titanium or erbium provide convenient sources of monoenergetic neutrons when bombarded with deuterons or protons.

The measurements of the electrical properties, and the study of the resistance changes of metal films due to their interaction with pure gases, have been made separately in two different vacuum systems according to the nature of the work and convenience. The resistivity and temperature coefficient of resistance have been studied in a belljar system at a pressure of 5×10^{-6} torr, and have been described first. Another stainless steel system has been designed, in which the adsorption vessel could be isolated from the pump for studying resistance changes of the films with measured doses of pure gases. This will be described in the second part.

1.2 Techniques of preparing thin metal films

The choice of film formation technique depends upon the nature of the material and ultimate use of the film. There are various methods of making thin films and these may generally be classified into two separate groups, chemical methods and physical methods.

There are several chemical methods of depositing thin films but only the following two are commonly in use:

(1) Electrolytic deposition.

(2) Pyrolytic deposition i.e. thermal decomposition of volatile metal-organic compounds or metal halides.

Physical methods can also be divided into two, namely:

(1) Vacuum evaporation.

(2) Sputtering.

The structure of a film prepared by these methods is, as a rule, different from the bulk, and is entirely dictated by the deposition conditions. Electro-deposition is a wet process and is governed by the first and second laws of electrolysis. The films have to be grown on a metal cathode and the possibility of secondary reactions exists in the electrolyte. Films of noble metals, like gold, platinum and silver may be deposited on glass, ceramic and other metals by thermally decomposing their volatile organic compounds or halides in solution spread over the surface of the substrate. Firing temperatures of $400^{\circ}C$ or more are often needed and therefore the substrate must be capable of withstanding a high temperature.

Thin films are more widely prepared by the physical methods mentioned above for the study of their electrical properties. Sputtered films are highly unsuitable for adsorption studies, as impurities in the inert gas supply can react with the vapour to give films of oxide, nitride etc. The method of vacuum evaporation has been adopted for preparing thin films of titanium and erbium to avoid possible contamination of these films, which would otherwise readily absorb gases excited and dissociated due to the glow discharge if prepared by the sputtering technique.

The common procedure of preparing thin films by vacuum evaporation is to outgas a small specimen of the solid in vacuum at temperatures just below those at which it becomes volatile, and then to heat it to a slightly higher temperature to form an evaporated film. To avoid scattering due to collisions, the pressure has to be low enough to make the mean free path of the vapour atoms greater than the

dimensions of the vacuum chamber. The structure, purity and properties of the film so obtained will, in fact, depend on the various deposition variables[1], like the substrate temperature, deposition rate, deposition environment and the nature of the substrate. Also on the nature of the film material, nature of impinging gas species, annealing, and the care taken during degassing and depositing the film.

1.3 Electrical conductivity and resistance-temperature characteristic of thin films

At the beginning of the twentieth century Drude (1900) and Lorentz (1909) explained the conducting properties of metals in terms of a free electron gas. Their theory was successful in predicting the Wiedemann-Franz law, connecting the electrical and thermal conductivities, but failed to explain the specific heat of metals. With the advent of quantum mechanics, Pauli and Sommerfeld (1928) applied the Fermi-Dirac statistics to the free electrons in a metal, and obtained the following equations for the electrical conductivity σ_o of the bulk metal:

$$\sigma_o = \frac{n e^2 \ell_o}{m \bar{v}} \quad \text{and} \quad n = \frac{8\pi}{3} \left(\frac{m \bar{v}}{h} \right)^3 \tag{1.1}$$

Combining these two equations and using Gaussian units we get

$$\sigma_o = 7{\cdot}1 \times 10^7 \, n^{2/3} \, \ell_o \tag{1.2}$$

where n is the number of free electrons per unit volume, which is assumed to be of the same order as the number of atoms per unit volume; e is the charge and m is the mass of an electron, h is Planck's constant, $\bar{v}$ is the velocity of an electron at the surface of the Fermi distribution and ℓ_o is the mean free path of the electrons in the metal.

An important consequence of quantum mechanics and the Pauli principle is that only those electrons whose velocities lie near to the surface of the Fermi distribution can be scattered, and therefore apparently it seems that the value of n occurring in equations 1.1 and 1.2 should refer to those electrons with velocity $\bar{v}$, but a rigorous analysis shows that n isthe total concentration of conduction electrons per unit volume, as in equation 1.1.

It is obvious from the inspection of eq. 1.2, that any deviation in n or ℓ_o will bring a change in the conductivity. In metals the variation of n with temperature is negligible, since at ordinary temperature the free electrons form a highly degenerate Fermi-Dirac gas. However, the electronic mean free path ℓ_o is limited by collision processes occurring within the metal, some of which are temperature dependent. Three types of collision are worth mentioning. They are (1) collisions with the atoms which make up the metal (electron-phonon collisions), (2) collisions with impurity atoms or lattice defects and (3) collisions with other electrons. In a perfect crystal, if the lattice atoms are stationary, as they would be at the absolute zero of temperature, there would be no electron scattering, because the wave functions of the conduction electrons can adjust themselves to the perfect geometrical periodicity of the lattice. At room temperature the lattice atoms of the metal are in constant motion due to thermal agitation and thus the conduction electrons would be scattered by them. The mean free path of this type of scattering is inversely proportional to the absolute temperature, provided the temperature is not too low i.e. $T > \theta$ (the Debye temperature). The second type of scattering arises because impurity atoms have a different atomic number from the host atoms, and generally are electrically charged. The conduction electrons experience an electrostatic field which may be either attractive or repulsive, and can be scattered by a process analogous

to the Rutherford scattering of alpha particles by a nucleus. The mean free path for this type of collision depends on the density of impurity atoms and on the velocity of the conduction electrons. Since velocity ($\bar{v}$) is independent of temperature, the impurity scattering is also independent of temperature. Lattice defects such as vacancies can also cause this type of scattering. The third type of collision has no effect on the conductivity because in such a collision the total momentum of the colliding electrons remains the same and the electrons are indistinguishable.

Both the types of scattering mentioned above limit the mean free path and hence change the conductivity of the metal individually, and if they occur simultaneously then according to Matthiessen's Rule the observed resistivity is expressed as the sum of the ideal resitivity (due to lattice vibrations), which is temperature dependent and the residual resistivity (due to impurities) which is temperature independent.

Another type of collision process, which is related to the subject of the present work, is the scattering with the surface of the metal. When one or more of the dimensions is made comparable with the mean free path, as in a thin film or wire, scattering with the boundary surface becomes a dominating factor. This boundary scattering may be 'specular' or 'elastic' i.e. coherent, like the reflection of a ray of light from a mirror, or it may be 'diffuse' or 'inelastic', like the scattering of light from a rough surface i.e. incoherent. In the first case there will be no change in conductivity due to boundary scattering because the component of velocity parallel to the surface will remain unchanged. In the second case conductivity will be changed as the direction of the velocity after collision is not related to that before. Thus the conductivity of a film with rough surfaces i.e. on diffuse scattering, will be different from that

of the bulk metal.

1.3(1) Conductivity of continuous films

The earlier theory of electrical conduction in thin films was given in 1901 by Thomson[2], who considered diffuse scattering of conduction electrons from the surfaces of the film. His expression is only of historical importance as the assumptions used in deriving it have been criticised, especially as it neglects the effect of electron paths which start from the surface.

The general theory of the conductivity of thin films was worked out by Fuchs[3] (1938), and has been reviewed by Sondheimer[4] (1952). According to their theory (size-effect theory) metallic films are regarded as thin sections of bulk material and the effect of film thickness is to decrease the mean free paths of the conduction electrons by collisions with the boundaries of the film. Their expression for the resistivity is complicated and is given by

$$\frac{\sigma}{\sigma_o} = \frac{\rho_o}{\rho} = 1 - \frac{3}{8K} + B(K)\left[\frac{3K}{4} - \frac{K^3}{16}\right] + \left[\frac{3}{8K} - \frac{5}{8} - \frac{K}{16} + \frac{K^2}{16}\right]\exp^{-K} \quad (1.3)$$

where σ and ρ are the conductivity and resistivity of the film respectively, σ_o and ρ_o refer to the bulk material from which the film is derived; $K = \frac{d}{\ell_o}$ where d is the film thickness and ℓ_o the mean free path in bulk; and

$$B(K) = \int_K^\infty \frac{\exp^{-x}}{x}\, dx$$

For films in the limit when the film thickness d is much greater than the mean free path ℓ_o i.e. for thicker films, the approximation to relation (1.3) is

$$\frac{\rho_o}{\rho} = 1 - \frac{3}{8K}$$

which since the correction term is small compared to unity, may be written as

$$\frac{\rho}{\rho_o} = 1 + \frac{3}{8K} \qquad (K >> 1) \qquad (1.4)$$

and for very thin films:

$$\frac{\rho}{\rho_o} = \frac{4}{3K \log (1/K)}$$

A more approximate analysis by Mayer[5] (1959) for thin films gives:

$$\frac{\rho}{\rho_o} = \frac{4}{3K[\log(1/K) + 0{\cdot}4228]} \qquad (K << 1) \qquad (1.5)$$

In describing the above relations, all the conduction electrons are assumed to be diffusely scattered from the inside surfaces of the film. Modifications of these equations exist which take account of partial diffuse scattering in terms of a reflection coefficient P, defined as the proportion of electrons that are specularly reflected i.e. P = 1 for specular reflection and P = 0 for diffuse reflection. The approximation of the modified equations for different magnitudes of K then yields:

$$\frac{\rho}{\rho_o} = 1 + \frac{3(1-P)}{8K} \qquad (K >> 1) \qquad (1.6)$$

and

$$\frac{\rho}{\rho_o} = \frac{4}{3}\frac{1-P}{1+P}\frac{1}{K \log(1/K)} \qquad (K << 1) \qquad (1.7)$$

(equation 1.7 is valid for small values of P).

Later, experimental evidence for partial diffuse scattering has been cited, based on the observed low film resistivities[6,7] approaching the bulk. Lucas[8] (1965) has dealt with a more general case, in which the scattering of electrons is different at each surface of the film.

So far, the structure of the film has been considered the same as that of the bulk, but as a matter of fact, the structure of a film produced by evaporation or other techniques is not the same as that of the bulk, but may be differing in its grain size, crystal orientation, chemical composition and mechanical stresses, and also film surfaces are more often irregular in roughness at lower thicknesses. These will also contribute to the resistivity of the film which has been neglected in the above theory.

Schwarz and Luck[9] (1969/70) have discussed empirically the changes in resistivity of films due to tunnelling and scattering of conduction electrons at the grain boundaries, and showed that for polycrystalline films of aluminium and zinc about one-half of the electrons are tunnelling through the grain boundaries without being scattered.

Recently, Mayadas et al.[10] (1969/70) have theoretically treated the total resistivity of thin films considering simultaneous operation of all types of electron scattering i.e. scattering due to phonon and point defects, due to grain boundaries and scattering due to surfaces. In their expression, the bulk resistivity is derived from scattering due to phonon and point defects and due to grain boundaries, and then the total film resistivity is obtained by imposing boundary conditions due to the external surfaces (as in the Fuchs-Sondheimer theory). They thus concluded that the observed thickness-dependence of the resistivity in thin films, is due to grain-boundary scattering as well as to the size effect, and the

lower resistivities of single crystal films than polycrystalline films are due to the grain-boundary effect rather than differences in the nature of surface scattering.

Recently, Risnes and Sollien[11] (1969) and Risnes[12] (1970) have extended the size-effect theory and formulated an expression which includes a contribution to the film resistivity due to crystal orientation and also predicts the size effect.

These theories are in good agreement with the experimental results in a thickness range of several hundred Angstroms, but the deviation of the theories from the experimental results appears more clearly as the thickness of the film decreases. At lower thicknesses films are more often irregularly rough. With a simple theoretical expression, Namba[13] (1968) averaged the effects in such films by introducing an arbitrary roughness parameter in the Fuchs-Sondheimer theory whose value lies between 0 and 1.

Experimental results will be in good agreement with the predictions of these theories provided the films are free from chemical impurities, mechanical stresses and have a known structure.

1.3(2) Temperature coefficient of resistance (TCR)

According to Matthiessen's Rule, the observed resistivity ρ_o of a bulk metal is expressed as

$$\rho_o \text{ (observed)} = \rho_i \text{ (ideal)} + \rho_r \text{ (residual)}$$

and

$$\frac{d\rho_o}{dT} = \frac{d\rho_i}{dT} \qquad (1.8)$$

If the left and the right hand sides of the equation (1.8) are multiplied by ρ_o/ρ_o and ρ_i/ρ_i respectively, we get

$$\frac{\rho_i}{\rho_o} = \frac{\alpha_o}{\alpha_i} \qquad (1.9)$$

where α_o and α_i represent the observed and ideal bulk TCR. For films, if the contributions to the resistivity due to boundary scattering and due to structure are ρ_b (temperature dependent) and ρ_s (temperature independent) respectively, then the film resistivity may be expressed as

$$\rho = \rho_o + \rho_b + \rho_s$$

and

$$\frac{d\rho}{dT} = \frac{d\rho_i}{dT} + \frac{d\rho_b}{dT} \qquad (1.10)$$

For thick films so that boundary effect is negligible i.e.

$$\frac{d\rho_b}{dT} = 0$$

then

$$\frac{d\rho}{dT} = \frac{d\rho_i}{dT} = \frac{d\rho_o}{dT}$$

and hence

$$\frac{\rho}{\rho_o} = \frac{\alpha_o}{\alpha_f} \qquad (\alpha_f, \text{ the film TCR}) \qquad (1.11)$$

Thus from equation (1.4) we have

$$\frac{\alpha_o}{\alpha_f} = 1 + \frac{3}{8K} \qquad (K >> 1) \qquad (1.12)$$

Approximation of the complicated equation for very thin films yields:

$$\frac{\alpha_f}{\alpha_o} = \frac{1}{\left[\log (1/K) + 0{\cdot}4228\right]} \qquad (K << 1) \qquad (1.13)$$

1.3(3) Conductivity of island films

From studies of electrical resistivity and temperature coefficient of resistance, and from structural studies in the electron microscope, it has been established that the initial deposit of a metal consists of islands completely separated from each other. At moderate temperature of the substrate, the size of the islands will increase rapidly as more material is deposited. Finally, the islands will become so large that they touch and begin to grow together to form a continuous film. For these island films, the resistance will be dominated by the gaps between the islands, and their sizes, and thus none of the theories which has been described earlier may be applied.

Before developing any quantitative theory, the mechanisms of electrical conduction through such films have to be considered. The significant features of these films are that they have very high electrical resistivity and generally negative TCR. The negative TCR suggests that the process of electrical conduction should be an activated one. This observed activation energy has been found to decrease with the increase of particle size i.e. with the thickness of the film. Several models have been proposed to account for these observed characteristics. The most obvious one, suggested by Minn[14] (1960) and others, is thermionic emission. The activation energy would then be a measure of the height of the potential barrier between the islands over which the charge has to be thermally excited. Theoretically, the height of this barrier (i.e. the activation energy) is decreased when two particles are very close (in the few Å range) because of the overlap of the image force potentials, causing a higher current to flow. However, for small gap sizes the calculated current density for thermionic emission is many orders of magnitude smaller than the observed current density, and the measured activation energy is lower than the predicted potential barrier. Because of these,

many authors have rejected thermionic emission as the mechanism of conduction in island films. Recently, van Steensel[15] (1967) has again supported thermionic emission as the principal mechanism of conduction in such films on the condition that electron transfer between islands takes place through the surface plane of the substrate. In his theoretical expression, the barrier height (the activation energy) equals the metal-substrate work function (metal work function minus the energy of the conduction band in the substrate relative to the vacuum level) reduced by the image force potentials of the islands and part of the applied voltage potential. The expression in which the barrier height is very much reduced explains all his experimentally obtained results.

There is an alternative mechanism of electron transfer between the islands, namely quantum mechanical tunnelling. Tunnelling means the penetration of thin potential barriers by incident electrons having insufficient energy to cross over the barrier height. Tunnelling is a temperature independent process. Hence different activated charge formation processes relating to the size of the islands have been suggested to explain the activated nature of the system before actual tunnelling of electrons could occur. Neugebauer and Webb[16] (1962) have suggested a thermally activated charge carrier creation process, involving the removal of an electron from an initially neutral island leaving it positively charged, and then the tunnelling of electrons between the islands through the separating vacuum. The activation energy of conduction is the energy required to transfer charge from one initially neutral island to another, and is of the order of magnitude e^2/r. Charged particles excited at least to this energy above the Fermi level will be able to tunnel. Thus the process is an activated one and leads to an equilibrium number of charged islands proportional to $\exp[(-e^2/r)/kT]$. The tunnelling probability between the islands separated by a distance d

is proportional to $(1/d) \exp\left[-(4\pi d/h)\,(2m^{*}\phi)^{\frac{1}{2}}\right]$. The conductivity is the product of this tunnelling probability, concentration and charge of charge carriers and is of the form[1]

$$\sigma = A\,\frac{(2\,m^{*}\phi)^{\frac{1}{2}}}{h^{2}d}\,\exp\left[-\frac{4\pi d}{h}\,(2\,m^{*}\phi)^{\frac{1}{2}}\right]\,B\,\exp\left[-\frac{e^{2}/\varepsilon r}{kT}\right] \qquad (1.14)$$

where A and B are constants; ϕ is the potential barrier between islands, roughly equal to the work function of the metal corrected for the image forces; e is the electronic charge, m^{*} is the effective electronic mass; ε is the dielectric constant of vacuum-substrate; and r is the average linear dimension of an island. The expression is qualitatively able to explain experimentally observed dependencies, like the change in activation energy with thickness, the negative TCR and the increase of conductivity with particle size. However, in deriving the above expression, they assume some islands are initially charged and neglect the change in potential of the islands involved in the charge transfer.

Recently, Hill[17] (1969) has allowed for the latter effect and adopted the more reasonable neutral island model. On the basis of quantum mechanical tunnelling, and considering the conduction through the substrate, he has derived a theoretical expression for the current density which includes an activation energy depending on the size and the separation of the islands and another temperature dependent term due to tunnelling. The tunnelling current density calculated from his expression, and the thermionic current density calculated from the Richardson-Dushman equation, were equal for an effective barrier height of 1eV and for an island spacing of 40Å. Thus for a spacing more than 100Å the thermionic process is dominant, and for smaller spacing the tunnelling current dominates. However, one of his expressions for large particle and small gap size yields

infinite current when the activation energy is equated to zero. Kiernan and Stops[18] (1969), who adopted the Hill model, derived a similar equation which takes account of the latter.

All these theories agree qualitatively very well with the experimentally obtained results but are not expected to give exact quantitative agreement either due to the unknown structure of the films or the assumptions involved in them.

1.3(4) Temperature coefficient of resistance

If the variations in island spacing (d) with temperature (caused by thermal expansion) are negligible in comparison with the activation energy term $(e^2/\varepsilon r)/kT$ in eq. (1.14), it can be neglected and for this case eq. (1.14) can be written as

$$\sigma = C \exp\left[-\frac{e^2/\varepsilon r}{kT}\right] \qquad (1.15)$$

where C is a constant. The change in resistivity with temperature is given by differentiating eq. (1.15) as

$$\alpha_f = \frac{1}{\rho}\frac{d\rho}{dT} = -\frac{e^2/\varepsilon r}{kT^2} \qquad (1.16)$$

Thus the TCR is negative and depends strongly on temperature.

On the other hand, if the island film is thick i.e. it consists of large islands just about to grow together, then the activation energy term will be very small, and the conductivity will be entirely dependent on the transmission probability term which includes the inter-island spacing parameter. The usual negative TCR and sometimes positive TCR found for these films are explained in terms of the changes in island spacing, which depend on the thermal expansion coefficient of the substrate and the metal, and the adhesive energy (binding energy) between the substrate and the metal islands.

If the metal islands are only loosely bound to the substrate, and the thermal coefficient of expansion of the latter is small, then the increase of temperature would decrease inter-island spacing and again negative TCR would result. Contrary to this, if the metal islands have high binding energy with the substrate and the latter also has high coefficient of thermal expansion, then the inter-island spacing will increase with increase of temperature and positive TCR would result.

1.4 Previous work on the resistivity and TCR of titanium and erbium films

The early measurements of electrical resistivity and TCR of titanium thin films have been reviewed by Hacman[19] (1966). Gerstenberg[20] (1963) first measured the electrical conductivity of sputtered and evaporated titanium films of 200 to 2000 Å in thickness and also their TCR from -185 to +25°C. For evaporated films, he found that the specific resistivity dropped down rapidly in the range between 200 and 400 Å. It levelled off above 500 Å and remained at the same value of about (100±10%) x 10^{-6} ohm cm. up to 1000 Å. For the same thickness the TCR was +23 x 10^{-4}/°C, which was two thirds the bulk value.

Huber[21] (1964) measured the electrical resistance of titanium films (deposited at a very high rate of evaporation) as a function of thickness and temperature. Since he was interested in these films for micro-component devices for integrated circuits he measured their resistance in air and hence they had very high resistivity.

Hacman[19] (1966) studied the optical properties and the electrical resistivity of titanium films, evaporated in a belljar system with a Viton gasket and evacuated by an oil diffusion pump. His resistivity against thickness curve has a peculiar hump between the thickness range of 200-400 Å, and within the range of 10-100 Å the measured resistivity values were on average twice as large as the

calculated ones. Using Nossek's representation he gave a value of 330 Å for the electronic mean free path in bulk titanium.

Chander et al.[22] (1967) measured the resistivity of films of 75 to 350 Å in thickness in vacuum at 2-3 x 10^{-5} torr. The resistivity increased if these were removed from the vacuum system and left in air, and if they were evaporated in an atmosphere of nitrogen at 10^{-5} torr. They have reported negative TCR for films up to 300 Å thick.

Recently, Friebertshauser and McCamont[23] (1969) have measured electrical properties of single crystal and polycrystalline films of titanium as a function of substrate temperature, film thickness and substrate material. Epitaxial growth of titanium was observed on single crystal sapphire substrates in the temperature range of 200 to 400°C. Films prepared on glass and fused quartz, and also on single crystal sapphire at 100°C were polycrystalline. The electrical properties of epitaxial films approached the bulk properties of titanium i.e. their TCR and the ratio of $R_{300°K}$ to $R_{4.2°K}$ were higher than those of the polycrystalline films.

The electrical resistivity and the resistance-temperature characteristic of polycrystalline and single crystal bulk erbium have been reported by Legvold et al.[24], Colvin et al.[25] and by Green et al.[26]. For single crystal erbium[26] the ratio of resistivities measured at room temperature by passing current perpendicular to (along 'a' axis) and parallel to 'c' axis was 1.72. A sharp rise and a sharp minimum was observed at 20.4 and 85°K respectively in 'c' axis resistivity against temperature curve. The latter minimum was also observed in the case of polycrystalline bars at about 80°K. Elliott et al.[27] also observed a maximum at 78°K in susceptibility versus temperature curve. From these, along with specific heat measurements[28] of erbium, it is concluded that the metal is ferromagnetic below 20°K, anti-ferromagnetic between

20 and 78-86°K and paramagnetic above 86°K. No study of electrical properties of films of erbium has been reported in the literature.

1.5 Summary

From the previous study (Sections 1.4 and 5.2) it has been inferred that titanium is an important material both from the point of view of fabrication of micro-component devices (thin-film resistors, capacitors and diodes) in integrated circuits and as a getter for common gases. Also much of the early data lacks in reproducibility of the results due to the work being done in poor vacuum employing oil diffusion pumps. These previous studies suggested the need of further research in better vacuum free from oil vapour and other contaminants.

The peculiar characteristics exhibited by bulk erbium showed it would be of interest to study it in the form of thin films. The next chapter describes in detail the experimental arrangement made for studying electrical and other properties of these metals.

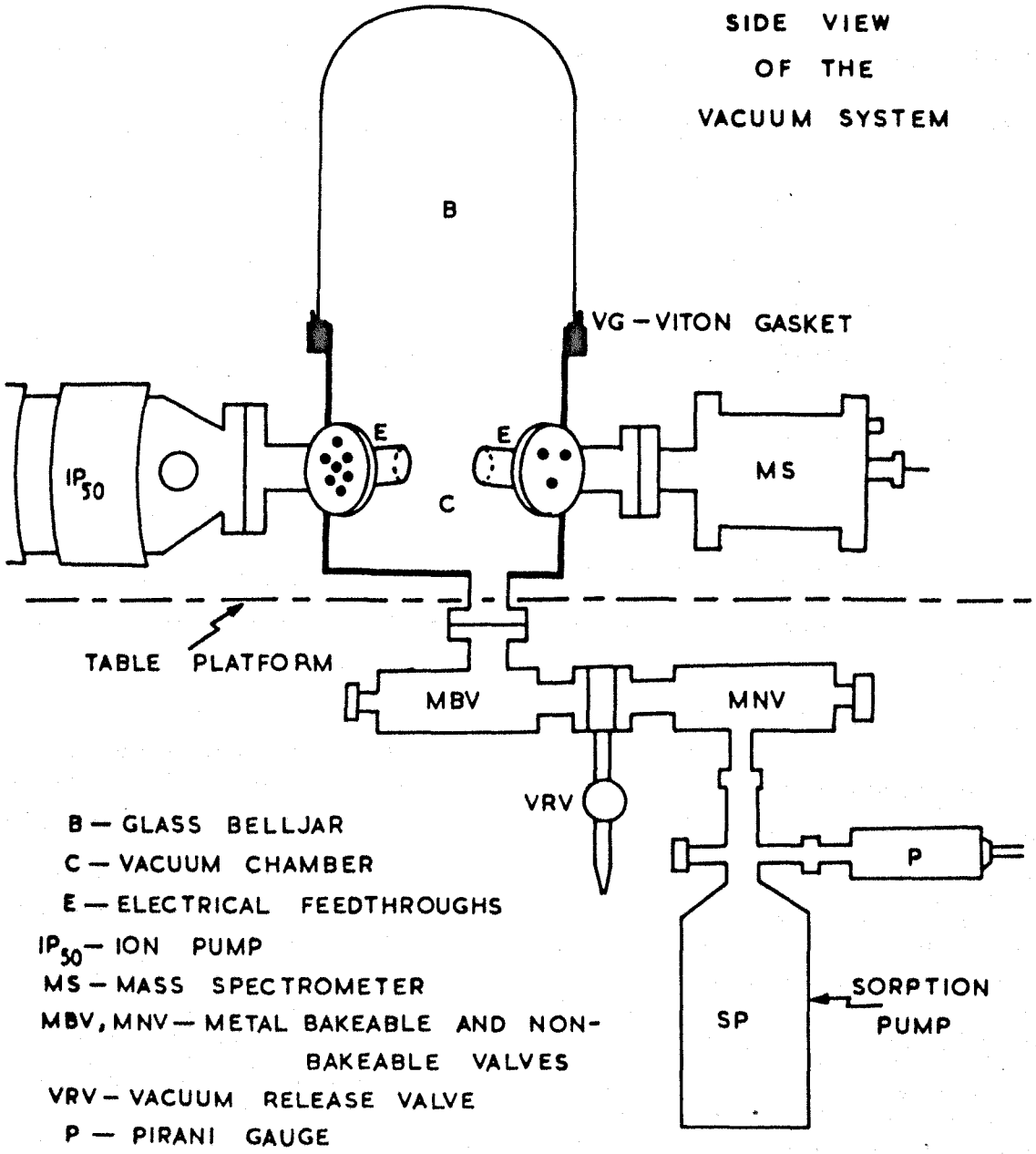
SIDE VIEW
OF THE
VACUUM SYSTEM
B
VG – VITON GASKET
E
E
C
IP50
MS
TABLE PLATFORM
MBV
MNV
VRV
P
SP
SORPTION
PUMP
B – GLASS BELLJAR
C – VACUUM CHAMBER
E – ELECTRICAL FEEDTHROUGHS
IP50 – ION PUMP
MS – MASS SPECTROMETER
MBV, MNV – METAL BAKEABLE AND NON-
BAKEABLE VALVES
VRV – VACUUM RELEASE VALVE
P – PIRANI GAUGE

Figure 1

CHAPTER II

DESIGN OF APPARATUS, EXPERIMENTAL DEVELOPMENTS AND TECHNIQUES

2.1 Introduction

In this chapter, the vacuum system, the technique of preparing experimental films of titanium and erbium, and the methods of film thickness and electrical resistance measurements will be described.

2.2 Vacuum system

A glass belljar vacuum system was chosen for convenience in order to perform frequent experimental runs. From the available apparatus a sputter-ion pump and a zeolite sorption pump were chosen in preference to oil or mercury diffusion pumps to avoid impurity contamination of films due to oil or mercury vapours. Before assembling the system, all its components were cleaned by iso-propyl alcohol and distilled water to remove any grease. The vacuum system consisted of a 6" diameter belljar with a 'Viton' gasket resting on a stainless steel (EN 58B) well which had five side ports for electrical feedthroughs and for pumping, in addition to one at the bottom. The particular ion pump used was FJD 50 (Ferranti) having a pumping speed of 50 litres/sec at 10^{-6} torr and was directly connected to the chamber. The sorption pump was joined to the bottom port of the chamber via two stainless steel bakeable, and one nonbakeable, valves. In between these two another air release valve was introduced to release the vacuum of the system after an experiment was over. A 200 amp feed-through was used on a $4\frac{1}{2}$" diameter flange for supplying high current to the evaporation source. A maximum current of 200 amps could be obtained from a step down transformer at 10 or 20 volts. One of the

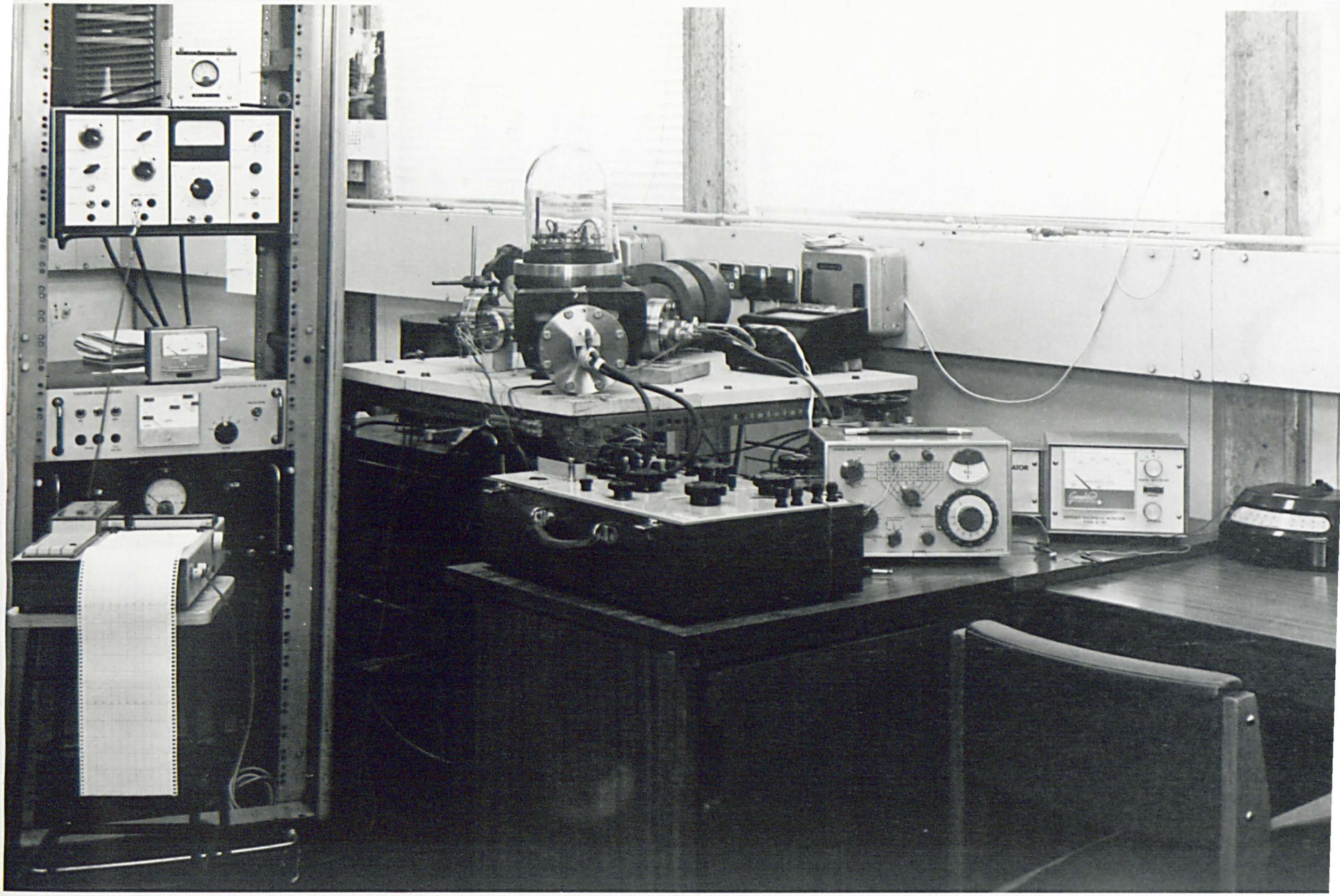

General view of the belljar vacuum system.

Figure 2

side ports was used for the movement of a 2" linear shutter between the source and the substrate. An AEI Mass Spectrometer 'Vacuum MS 10' was connected to the system through a $2\frac{3}{4}$" flange to study the changes in the residual gas composition due to titanium and erbium getter action. The whole of this manifold was placed on a thick asbestos platform of a table made of angle-iron. A simple sketch of the vacuum system is shown in Fig. 1. The actual vacuum system used, with the general electronics for the measurement of various quantities, is shown in photograph 2.

2.3 Design of evaporation system inside the vacuum chamber

In the construction of the main evaporation system inside the well, use of high vapour pressure materials like zinc and brass was avoided, and it was entirely constructed of steel and copper. Two steel discs, one solid and the other in a ring shape, both $5\frac{1}{2}$" in diameter were used with three steel OBA threaded rods to make a framework inside the vacuum chamber to hold the substrate, quartz crystal, thermocouple, evaporation source and heating filaments. One end of the evaporation source (a boat or a filament) was earthed and the other was isolated from the chamber through its holder which was clamped by two pieces of ceramic tubes concentric with glass tube on one of the steel rods. Steel barrel connectors and spring 'bull dog' clips were used as substrate holders. A copper-constantan thermocouple was used as a temperature measuring device, and its junction was pressed closely against the substrate on the same side of it as the film. A quartz crystal thickness monitor was placed adjacent to the substrate, and both were at equal distance from the evaporation source. All these measuring devices were held in position and isolated from the chamber by small, metal-ceramic, T shaped insulators, and were electrically connected through the metal parts of these by copper wires covered with ceramic beads. Two

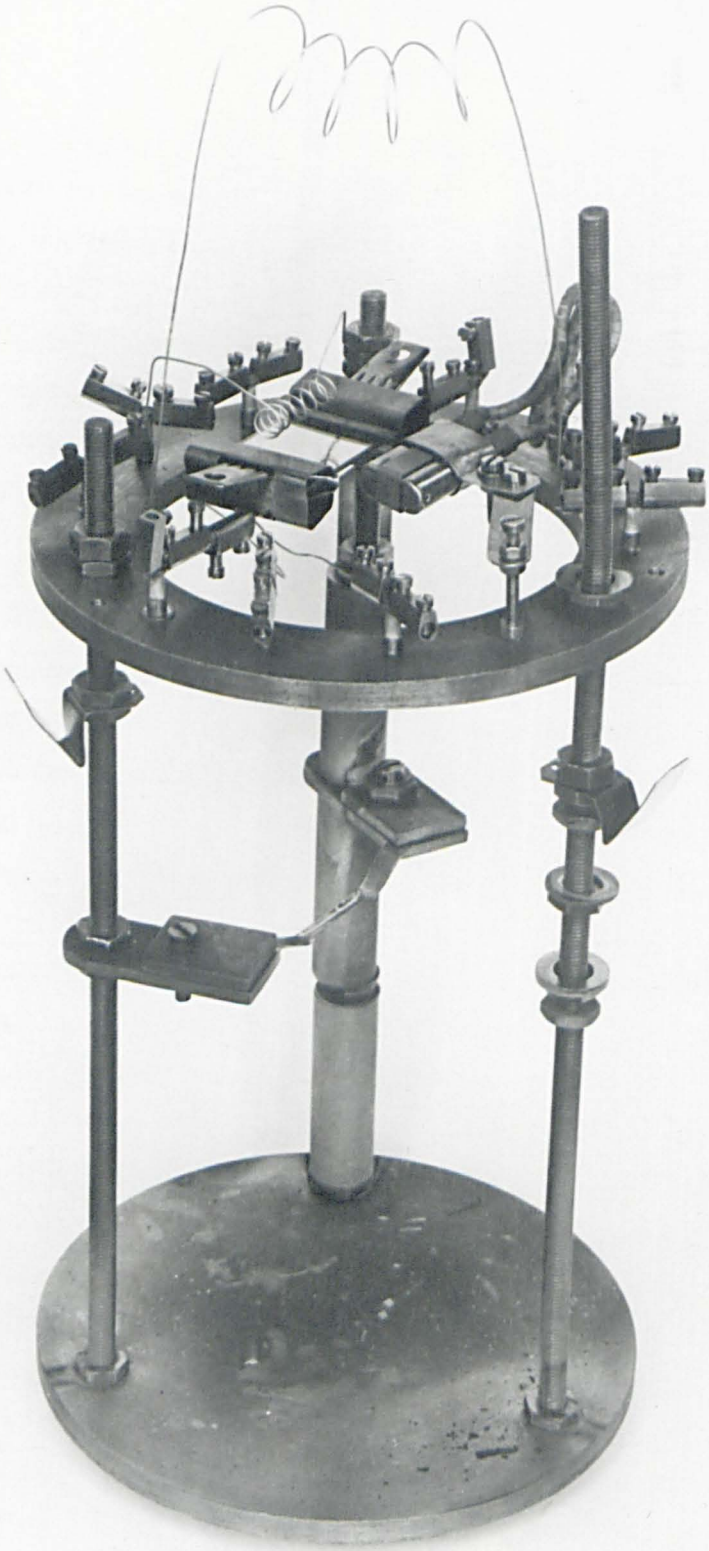

Figure 3

Photograph of the framework inside the vacuum chamber.

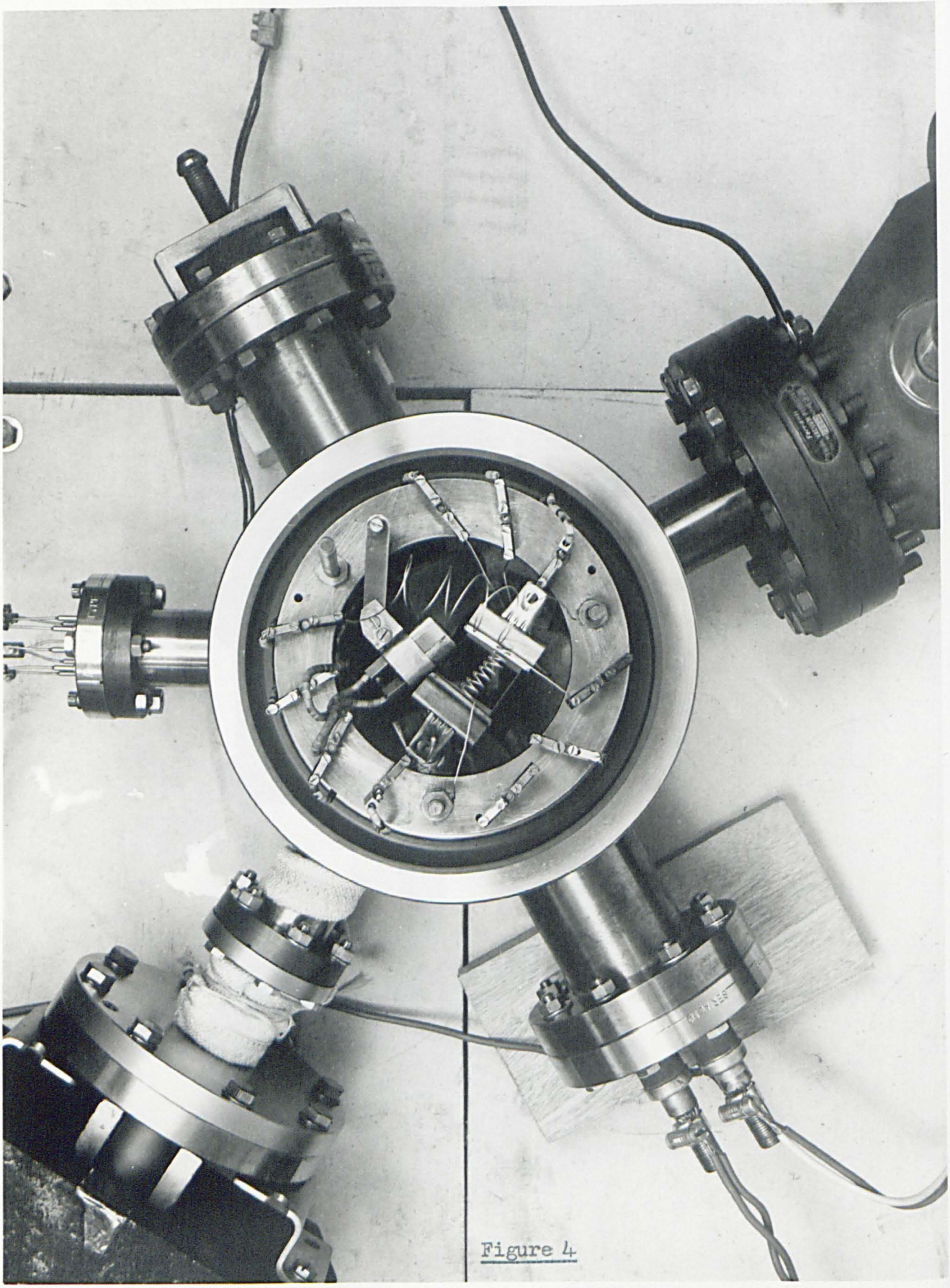

Figure 4

Top view of the experimental arrangement.

molybdenum wire filaments, one for baking the system and another for heating the substrate, were used with one end of each earthed and the others insulated. The whole of the framework was put inside the vacuum chamber and held in a central position by three steel strip clips, each pressing against the wall of the vacuum chamber. The actual framework, holding the substrate and the other measuring devices, is shown in photograph 3 and is self explanatory. The top view of the experimental arrangement with inner assembly is shown in photograph 4.

2.4 Methods of measurement

The electrical resistance of the films, both a.c. and d.c. were measured under various conditions of thickness, temperature and time by a universal bridge T.F. 2700 (Marconi Instruments). The bridge was disconnected from the film between readings to avoid Joule heating by the testing current. A difference in d.c. and a.c. resistance was noticed when the bridge was continuously kept on, even when the leads were disconnected. To test whether the a.c. resistance values (different from d.c.) were due to the frequency of the internal oscillator (1000 Hz), a.c. resistance measurements were made at different frequencies ranging from 20 to 2400 Hz applying an external oscillator, but no effect of frequency in this range on a.c. resistance was observed. The drifting apart of a.c. and d.c. values was also observed when an ordinary carbon resistance was substituted for the film, so it was evidently a fault of the bridge. However, better agreement between a.c. and d.c. resistance values was observed when the bridge was switched off as well as having its leads disconnected between the readings.

The use of a bridge method has the advantage of simplicity and speed, but the disadvantage of including the resistance of the contacts to the films (described in Section 2.6). However, a preliminary experiment with a thick film of titanium showed that the contact resistance was small; i.e. the bridge read 21.7 ohms

on d.c., 21.4 ohms on 1000Hz, and the four point d.c. method gave 20.3 ohms. Since the resistances of nearly all the films studied were at least as high as this (20 - 800 ohms), they were measured by the bridge and d.c. values are quoted throughout.

The film thicknesses were measured with a quartz crystal type of deposit thickness monitor (General Engineering Co., DTM-1). Due to the small size of the vacuum chamber, the original big crystal holder supplied by the manufacturer was not used. Instead a small holder was constructed from the protective case of the crystal. This monitor with the modified crystal holder was calibrated by the method of Fizeau multiple-beam fringes in a separate experiment with a gold film, using the same geometrical arrangement, and is described in the next section.

Other quantities like resistivity, temperature coefficient of resistance and mean free path have been calculated by mathematical relations and graphical methods.

2.5 Calibration of quartz crystal deposit thickness monitor

There are various methods of film thickness measurement, namely physical methods, chemical methods and optical methods; thickness measurement by vibrating quartz crystal devices is common and is straightforward in use. These devices, like the other physical and chemical methods, assume the film density is the same as the bulk density and often require calibration against a standard optical method before their use. Monitoring methods of film thickness measurement have been recently reviewed by Greaves[29].

The quartz crystal monitor, which was used for thickness measurements of the experimental films of titanium and erbium, was calibrated by comparing its thickness reading with the thickness measured by multiple-beam interferometry[30,31]. The test film was deposited, using a commercial oil-diffusion pumped vacuum unit.

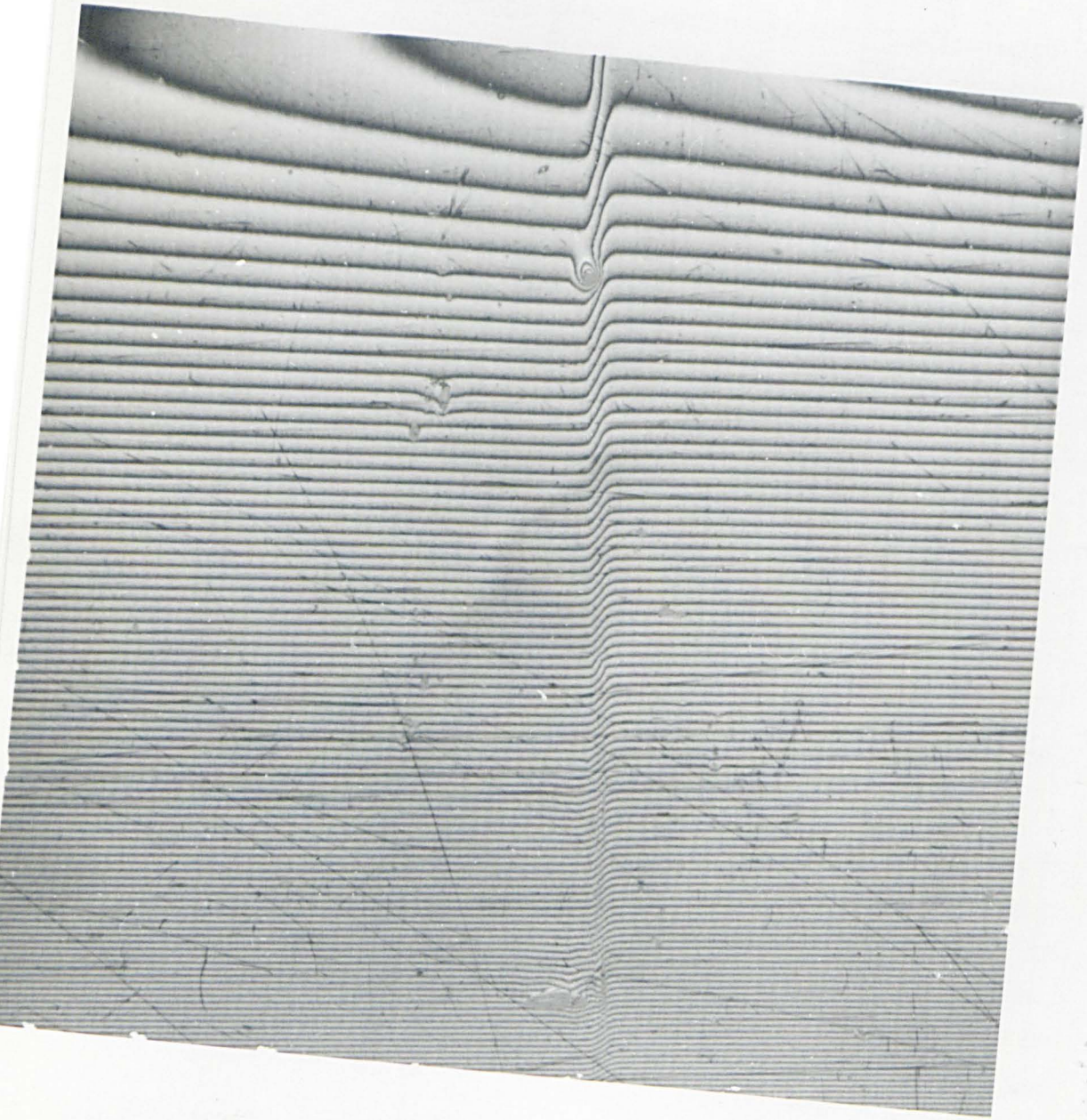

Figure 5

Optical fringe shift photograph for the calibration of the film thickness monitor.

A sharp and thick step of gold film was deposited with a shutter rigidly attached to the substrate, and a thick opaque uniform film of silver was deposited onto the step film. Both the materials were evaporated from separate molybdenum boats. The 'Polaroid' photograph of the fringe shift observed with a sodium light on a Vickers projection microscope was taken with a magnification of x 35, which was further magnified by ordinary photography x 3 to a total magnification of hundred and is shown in Fig. 5. The measurements of the fringe width and the fringe shift were taken by an ordinary travelling microscope, and the calibration factor measured was 1.997 i.e. approximately 2. This means that the deposit thickness monitor read half the actual thickness, which was due to the change of the crystal holder envelope. This caused the following two changes:

(a) A change in the distance of the crystal from the hole in its envelope and

(b) a change in the dimensions of the hole.

The principle of the crystal thickness monitor is the change in the resonance frequency of the quartz crystal with the deposition of mass on its surface, and consequently both the above changes affect the mass deposition for the same thickness. It is to be noted that the calculated thickness assumes the film is uniform and of the same density as the bulk, but as a rule film density is different from the bulk, and the film is of rough surface, consequently the thickness measured is the average thickness of the film.

There is always an error involved in the measurement of the film thickness with the crystal monitor. On the first and the second scales of the frequency meter one division shift of the pointer corresponds to a change of 20 and 100 Hz respectively, and consequently, there are errors of ± 10 and ± 50 Hz in reading the meter

on the two scales respectively, which correspond to error of ± 10 and ± 50 Å for titanium films in the thickness ranges of 1 to 500 Å, and 500 to 2500 Å; and of approximately ± 5 and ± 25 Å for erbium films in the thickness ranges of 1 to 250 Å, and 250 to 1250 Å respectively.

2.6 Substrate electrodes for electrical contact to films

The following three different techniques were tried for good electrical contact of the films with the resistance measuring leads.

Platinum coating

Liquid Bright Platinum (Ga), obtained from Johnson Matthey & Co., London, was painted onto the substrate and was fired for about an hour at 500-600°C. The first layer of platinum-gold alloy left on the substrate was very thin having a high resistance and thus for a thick layer the procedure was repeated several times, which made the substrate contaminated with carbon smoke, organic compounds, and with scratches and uneven edges of the film. For simplicity this procedure was not adopted for the present study.

Vacuum deposition of gold and silver coating

Gold and silver films of 700 to 900 Å thick were deposited onto the substrate by vacuum evaporation, using a commercial vacuum coating unit. The resistance of these films was in the range of 3 to 4 ohms. These films get detached when cleaned ultrasonically and also with a slight movement of the electrical contact leads, consequently substrates were cleaned prior to contact deposition, and were used for limited experimental runs.

Carbon coating

A colloidal solution of carbon in water (Aquadag 660) was painted onto the substrate. One coating gave a low resistance of two to four ohms, and could easily be dried in an oven in 15 minutes at a

temperature above 100°C. The coating was very adherent and was not detached with accidental movement of the electrical contacts, hence these were used for the large part of the experimental runs. However, the carbon paint became detached when the substrates were cleaned ultrasonically, consequently these were also cleaned prior to contact coating and experimental film formation.

2.7 Sources of evaporation for titanium and erbium

Both the metals titanium and erbium have been found to evaporate readily from tungsten, tantalum and molybdenum sources at temperatures below their melting points of 1727 and 1497°C respectively. Titanium is believed to react with tungsten[32], and the films deposited are contaminated with traces of it. Thus tungsten sources were not used.

Boat sources

Several attempts were made to evaporate titanium from tantalum boats but often these burned out. The idea of a tantalum boat was given up for titanium evaporation as it was suggested that tantalum became brittle after being degassed at a high temperature in vacuum[32]. The most successful attempts to evaporate titanium were made from molybdenum boats. These were designed from molybdenum strips of 0.2mm thick and 4mm wide by lifting their side edges up and putting bends in their length to account for thermal expansion. The current required to evaporate it from such a boat at rates of 5 to 10 Å/sec was 60 to 66 amps.

Erbium was evaporated from similarly designed tantalum boats of 4mm x 0.1mm dimensions, and the current required to evaporate from such a boat at a mean rate of 30 Å/sec was 36-40 amps.

Filament sources

Attempts were also made to evaporate both these metals from filament sources. These sources were found more suitable for erbium evaporation and have been adopted for preparing films for their surface-structure and gas adsorption studies (Sections 4.3.3 and 9.6). Erbium was evaporated from helical molybdenum wire filaments. Films were deposited at a mean rate of 30 Å/sec with 20 amps of current, and at 5 - 10 Å/sec with 9 to 11 amps of current, from filaments of molybdenum wire of 0.5mm diameter.

Titanium was evaporated from titanium-molybdenum alloy filaments (Vacuum Generators sublimator filaments) of 1.8mm in diameter, 6.5cms in length, having 85% titanium and 15% molybdenum composition. A two inch long filament of this type has a life of 15 to 30 hours at 35 amps and does not sublimate titanium below 30 amps current through it. The upper limit mentioned for these filaments is 45 amps, and below this value 40% of the titanium in the alloy can be evaporated[33]. The purity of this titanium was quoted as 99.7% with a partial list of impurities of 0.03% iron, 0.08% oxygen, 0.01% carbon and 0.002% hydrogen (Imperial Metals Ltd.). Films of titanium at a mean rate of 1 Å/sec have been deposited by passing 39 - 42 amps of current through these filaments.

2.8 Experimental techniques

Titanium films were prepared by evaporating commercial grade titanium from two different sources onto vacuum baked (130°C for 24 hours) soda glass microscope slides of suitable size, at room temperature. The substrates were cleaned by chromic acid, de-ionised water and ultrasonic agitation, as suggested by Jorgenson and Welhner[34], prior to their assembling in the vacuum system and the film formation. The first source of titanium evaporation was an 85% titanium, 15% molybdenum alloy filament as described in Section 2.7. The second

source was a molybdenum boat containing chips of 99.4% pure titanium for which the typical impurities were quoted as 0.1% iron, 0.18% oxygen, 0.05% carbon, 0.03% nitrogen, 0.004% hydrogen, 0.2% sodium, 0.01% silicon, 0.01% tin, and 0.001% each of calcium, copper, magnesium, manganese and silver (Koch Light Ltd., England). Films of erbium were deposited by evaporating spectroscopically pure ingots of erbium from tantalum boats. The metal was supplied by Rare Earth Products Ltd., England. The purity of erbium quoted was 99.88% with typical impurities of less than 0.1% other rare earth metals and 0.02% other base metals.

In each experimental run, the system was first evacuated by a mechanical pump and a chilled zeolite sorption pump to a pressure of 10^{-3} torr, and then by the sputter-ion pump and was left pumping overnight. It was then baked internally to about 100°C for 24 hours by heating the belljar and the substrate by means of two hot molybdenum filaments, and the mass spectrometer head was baked externally by heating tapes. During the baking of the system, the pressure as measured by the ion pump current was not allowed to increase above $1 - 2 \times 10^{-6}$ torr. After the bake, the system was slowly cooled and simultaneously the evaporation source was degassed, and it was left degassing just below the evaporation temperature of the metals for another 8 to 12 hours. During the baking and this outgassing of the source, the movable shutter was kept between the source and the substrate to keep the substrate free from outgassed impurities. The ultimate pressure after degassing (source still hot) and system at room temperature was about 5×10^{-7} torr. Before the experimental film formation a few films had been deposited onto the shutter. During evaporation of both the metals the pressure had slightly increased, but immediately rapid gettering occurred and within

a few minutes it dropped to the region of 10^{-8} torr. Then the shutter was removed and the experimental films were deposited onto the substrate. The low pressure achieved after film formation persisted for several hours, but rose to about 10^{-7} torr overnight.

A fresh titanium film was deposited onto a separate substrate in each experimental run. Ageing of the films in vacuum and the effect of temperature were studied by measuring their resistance as a function of thickness and time.

Two types of erbium film were studied: the sandwich type that was made by evaporating more erbium on top of an aged and thinner film in a single run, and the fresh films made to a particular thickness in only one process in each separate run. The effect of long ageing in vacuum on both types of film, and the resistance-temperature characteristic of fresh films were studied by measuring their electrical resistance.

For the measurement of the temperature coefficient of resistance of films of both the metals, the substrate was heated (radiation heating) by a molybdenum filament heater on the opposite side to the film, and its temperature was measured by a thermocouple.

The results obtained by this apparatus are described and discussed in the next chapter.

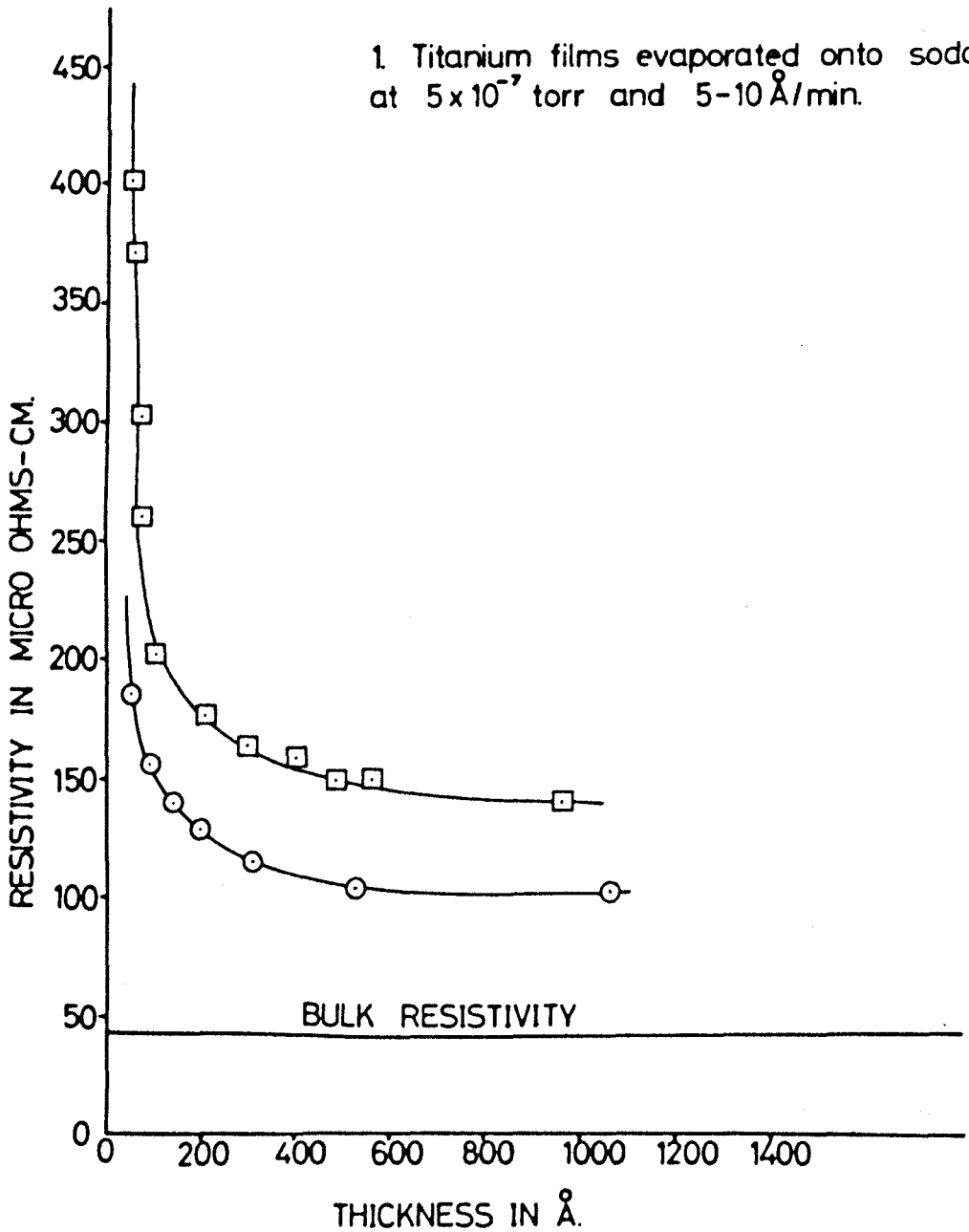

Electrical resistivity of titanium films versus thickness.

Figure 6

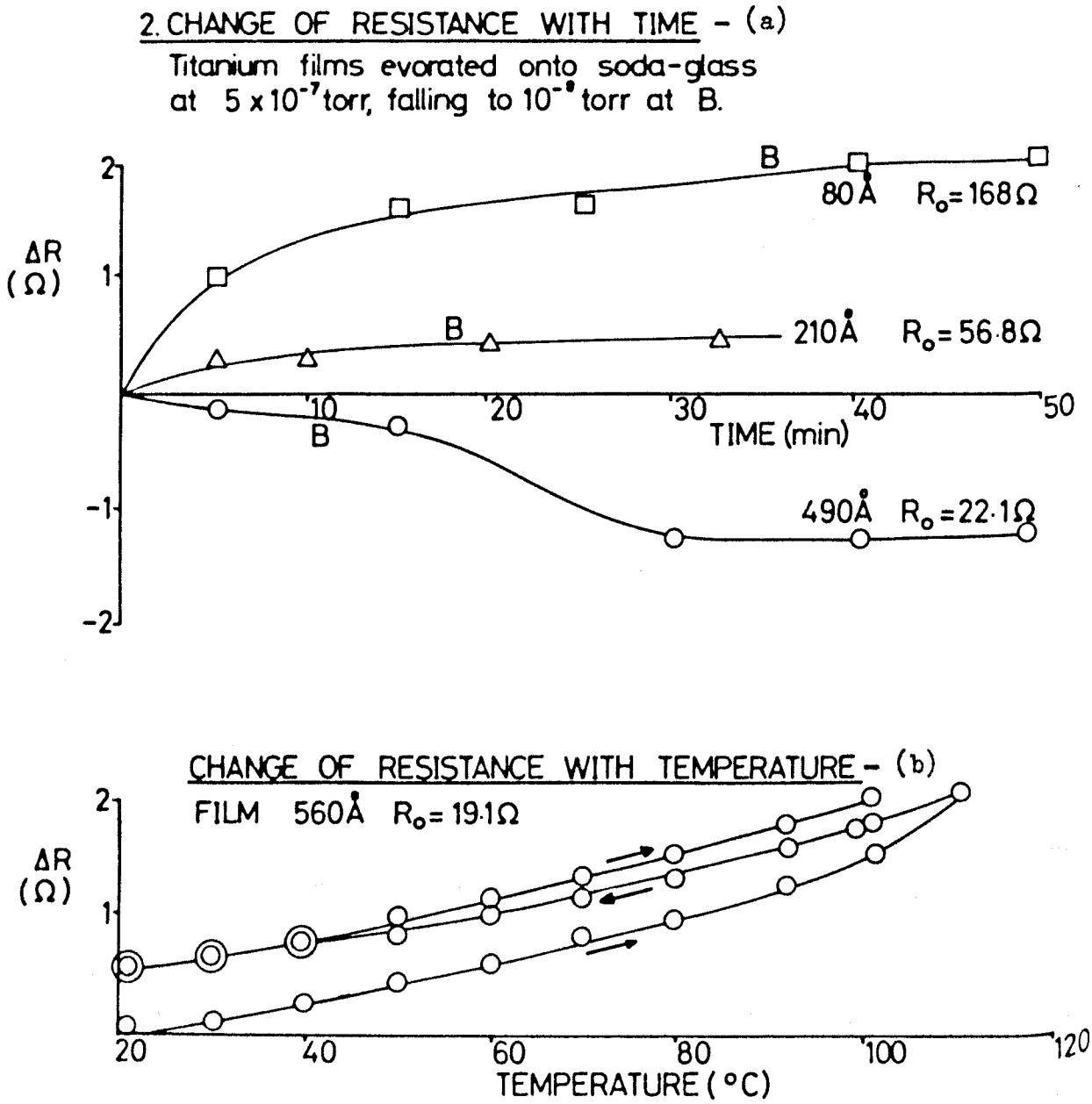
2. CHANGE OF RESISTANCE WITH TIME - (a)
Titanium films evorated onto soda-glass
at 5 x 10⁻⁷ torr, falling to 10⁻⁸ torr at B.
ΔR (Ω)
2
1
-1
-2
B
80 Å R₀ = 168 Ω
B
210 Å R₀ = 56·8 Ω
B
490 Å R₀ = 22·1 Ω
10
20
30
40
50
TIME (min)
CHANGE OF RESISTANCE WITH TEMPERATURE - (b)
FILM 560 Å R₀ = 19·1 Ω
ΔR (Ω)
2
1
20
40
60
80
100
120
TEMPERATURE (°C)

Figure 7

CHAPTER III

RESULTS AND DISCUSSION

This whole chapter has been devoted to the description and discussion of the results obtained on the electrical resistivity and resistance-temperature characteristic of titanium and erbium films. The chapter has been arranged in sections to facilitate reading, and the results for resistivity have been given separately for each metal.

3.1(1) Titanium - Resistivity Results

The electrical resistivities (micro-ohm cm) as functions of film thickness for freshly evaporated films of titanium are shown in Fig. 6, where the squares refer to the films evaporated from the molybdenum boats at 5 to 10 Å/sec, and the circles refer to the films evaporated from the alloy filament at a mean rate of about 1 Å/sec.

The films studied varied in their thickness from 1100 Å down to 50 Å and their resistivity ranged from 100 to 400 micro-ohm cm. The most rapid change in resistivity occurred in the 50-100 Å range; there was very little change in it after 400 Å. For thicknesses over 75 Å, the resistivity of the films evaporated from the titanium-molybdenum alloy filament is 25 to 30% lower than the resistivity of the films evaporated from the molybdenum boat source. The resistance of the films at room temperature (20 - 23°C) in vacuum attained a stable value about an hour after deposition. The effect of ageing in vacuum on some of the titanium films is shown in Fig. 7a. In general, thick films above 300 Å showed a decrease in their resistance (probably due to the sintering or ordering of the structure) and thin films showed an increase in resistance during ageing (probably due to chemical reaction with the residual gases of the vacuum system).

Figure 8

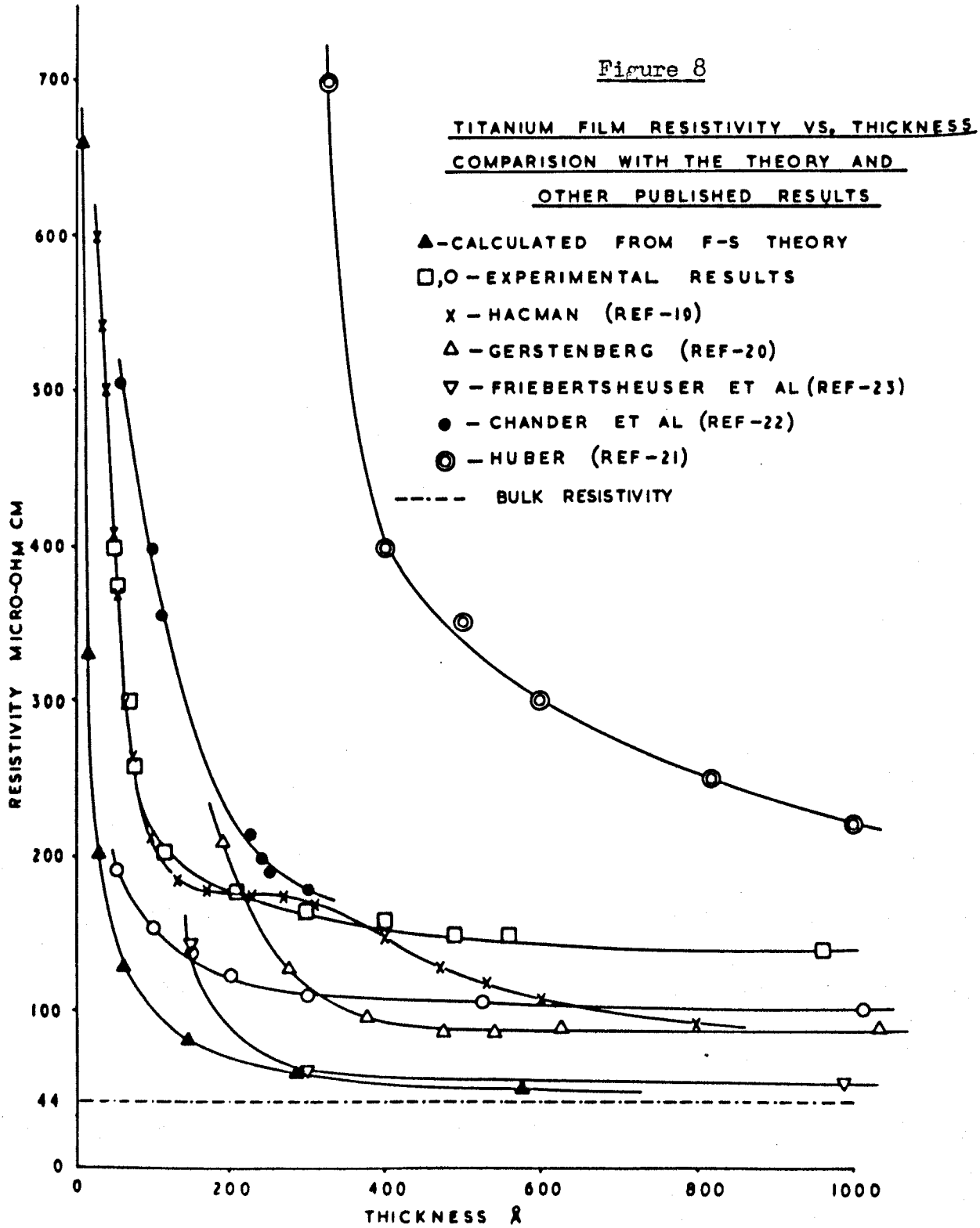
TITANIUM FILM RESISTIVITY VS, THICKNESS
COMPARISION WITH THE THEORY AND
OTHER PUBLISHED RESULTS
▲-CALCULATED FROM F-S THEORY
□,O-EXPERIMENTAL RESULTS
X-HACMAN (REF-19)
△-GERSTENBERG (REF-20)
▽-FRIEBERTSHEUSER ET AL (REF-23)
●-CHANDER ET AL (REF-22)
◎-HUBER (REF-21)
BULK RESISTIVITY
RESISTIVITY MICRO-OHM CM
700
600
500
400
300
200
100
44
0
0
200
400
600
800
1000
THICKNESS Å

The decrease in resistance was greater for thicker films, being about 4% for a thickness of 960 Å, and similarly the increase in resistance was greater for thinner films, being about 2.5% for the film 75 Å thick. This behaviour is in qualitative agreement with that reported by Chander et al.[22], who observed similar changes in resistance of about 5%.

3.1(2) Discussion and comparison with the previous work and with Fuchs-Sondheimer theory

The experimentally obtained resistivity curves are compared in Fig. 8 with the curves available in the literature and with the theoretical curve calculated from the Fuchs-Sondheimer theory.

Gerstenberg's[20] resistivity curve is comparable with the experimentally measured resistivity curves reported here within the thickness range of 200 to 400 Å. For greater thicknesses his resistivity curve is lower and for smaller thickness range it is higher. The lower resistivity at greater thicknesses might be due to the intrinsic high purity of the metal that he mentioned (but unfortunately no data of purity were quoted), and the high resistivity is most likely due to the residual gas interaction (3×10^{-6} torr) with the films which is more probable at smaller thicknesses.

Huber[21] reported much higher resistivity for the same range of thickness, particularly for the thinnest films (not covered in Fig. 8). Both his evaporation rate and the pressure in his experiments were about a hundred times as high as in the present experiments, so the ratio of gas to titanium atoms in both his films and the present films would be about the same. However since he prepared the films for micro-component devices he apparently measured their resistance in air rather than in vacuum, so his results refer to oxidised films.

Hackman's[19] resistivity results are comparable with that of the present films throughout the thickness range investigated, particularly the agreement is excellent at lower thicknesses. The pressure in his experiments was similar to that in the present experiments. A disagreement is the peculiar hump found in his resistivity versus thickness curve and is difficult to explain.

Chander et al.[22] measured the resistivity of titanium films of 75 to 350 Å thickness in vacuum at 2-3 x 10^{-5} torr and these had a higher resistivity than that of the present films. Their evaporation rate is not stated, but on account of their operating pressure it is probable that their films had a higher gas content.

Recently, Friebertshauser and McCamont[23] have reported electrical conductivity of polycrystalline and single crystal films of high purity zone-refined titanium at elevated temperatures on glass, quartz and single crystal sapphire substrates respectively. The resistivity curve in Fig. 8 is drawn from a few points taken from their room temperature (27°C) resistivity data for the films deposited on single crystal sapphire substrates kept at 100°C. The films had a low gas content as they were deposited at a very high rate of evaporation (350 Å/sec). Also because of the good pressure conditions (5 x 10^{-8} torr), high intrinsic purity of titanium and films approaching epitaxial growth, their resistivity is much lower than that of the present (polycrystalline) films and is approaching the theoretically calculated resistivity for thicknesses over 300 Å.

The electrical properties of continuous uniform films have been explained in terms of the mean free path of the conduction electrons by the Fuchs-Sondheimer theory (see Section 1.3.1). The theory assumes the effect of film thickness is to decrease the electron mean free path as is illustrated in Fig. 9. The influence

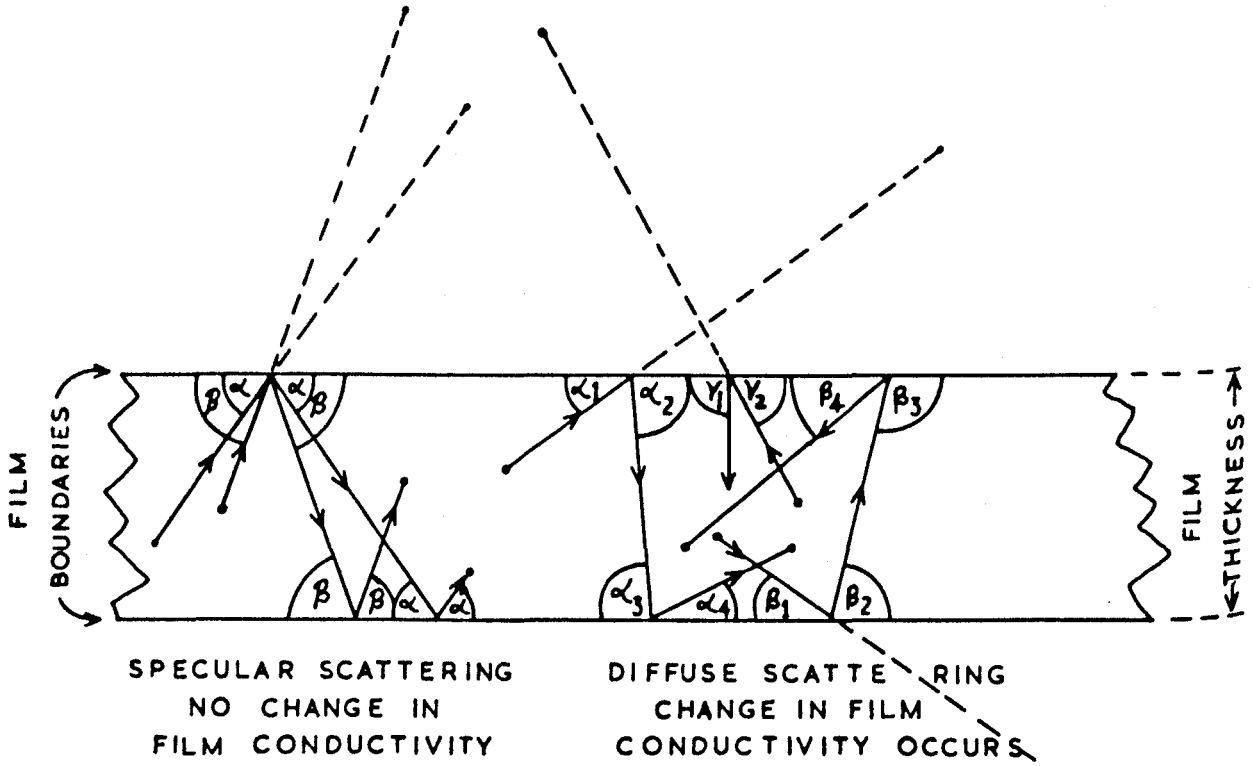

Fig. 9

INFLUENCE OF FILM THICKNESS ON ELECTRON MEAN FREE PATH

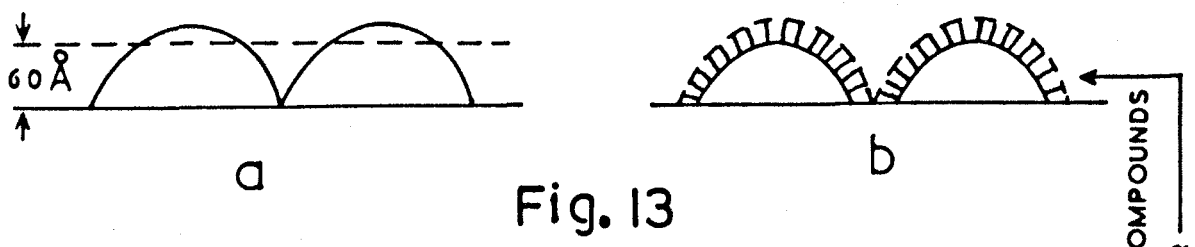

Fig. 13

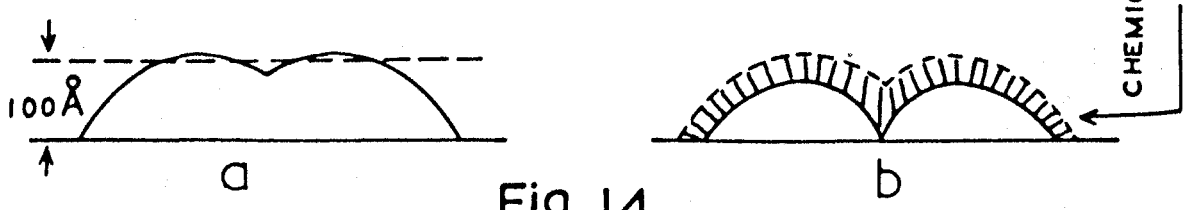

Fig. 14

EFFECTS OF AGEING OF FILMS

of a free surface tends to reflect the electrons back to the body of the film and behaves as another collision mechanism. The overall effect is to decrease the mean free path, thus increasing the ratio of film resistivity to bulk resistivity. For complete diffuse scattering from the boundaries of the film, a theoretical curve calculated from the theory is shown in Fig. 8. For the calculation of the theoretical curve a calculated value of 285 Å (see Section 3.3) for the electronic mean free path and a value[35] of 44×10^{-6} ohm cm for the electrical resistivity in bulk titanium have been used. The measured resistivity of the experimental films is much higher than the calculated one, and a marked difference is observed at lower thicknesses. The effect predicted by the theory is too small to account for these measured resistivities. The disagreement of the experimental results with the theory, suggests that the thin films of titanium should not be regarded simply as thin slices of bulk material, as assumed in the theory.

The higher electrical resistivity observed for the experimental films is possibly due to their different structure from the bulk. The films usually include residual gas atoms which are taken down with the metal during the process of evaporation, and act as additional scattering centres for conduction electrons in the film. Titanium is well known to react chemically with several gases and is also observed to sorb considerable amount of the residual gases in the vacuum system (Chapter V). These sorbed entities form a surface layer of chemical compounds which have different resistivities from the metal. However, better high vacuum conditions will not improve the quality of the film until a high purity metal is used. At 10^{-8} torr and a deposition rate of 5 to 10 Å/sec (2 to 3 monolayers/sec) the gas contamination is only about 0.1% whereas the titanium itself contained metallic and other impurities of 0.3% and

Figure 10

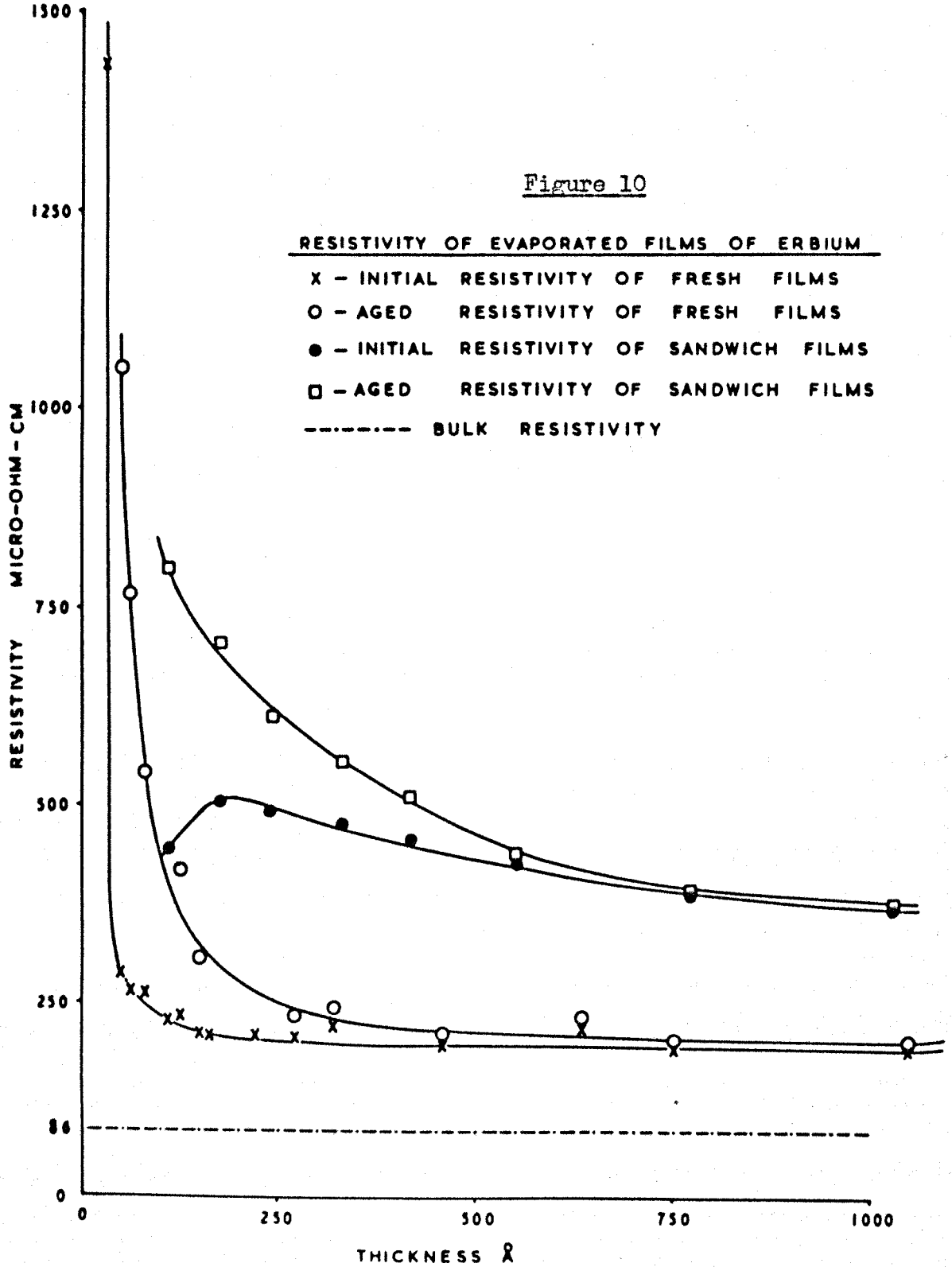
RESISTIVITY OF EVAPORATED FILMS OF ERBIUM
X – INITIAL RESISTIVITY OF FRESH FILMS
O – AGED RESISTIVITY OF FRESH FILMS
● – INITIAL RESISTIVITY OF SANDWICH FILMS
□ – AGED RESISTIVITY OF SANDWICH FILMS
BULK RESISTIVITY
RESISTIVITY MICRO-OHM-CM
1300
1250
1000
750
500
250
86
0
0
250
500
750
1000
THICKNESS Å

0.6% in the two sources. Other factors like the grain size, porosity and lattice defects of the films are mainly responsible for the large observed resistivity. The differences are particularly noticeable for films of less than about 100 Å mean thickness which have negative temperature coefficient of resistance (see Section 3.4) and thus possibly have a discontinuous island type of structure.

The two resistivity curves obtained for two different grades of titanium under similar conditions of pressure and temperature are attributed to the intrinsic purity of the samples. An explanation on the basis of different deposition rates will reverse the situation as a slow rate of evaporation leads to more gas impurities in the films.

3.2(1) Erbium - Resistivity and Ageing Results

The initial and the aged electrical resistivities (micro-ohm cm) as functions of film thickness for both the freshly evaporated and the sandwich films i.e. the films made of the same thickness by evaporating more erbium on top of an aged and thinner film, are shown in Fig. 10. The cross points and the circles refer to the initial and the aged resistivities of the freshly prepared films, and the dotted points and the squares refer to the initial and the aged resistivities of the sandwich films, all evaporated at a mean rate of about 30 Å/sec. Resistivities for fresh erbium films ranged from 190 to over 1350 micro-ohm cm corresponding to thicknesses from 1050 down to 40 Å. The initial resistivity of fresh films increased slowly for thicknesses from 1050 down to 200 Å, rapidly for 200 down to 60 Å and much more rapidly for thicknesses below 60 Å. The aged resistivities of the films increased slowly down to 200 Å and thereafter a rapid increase was observed.

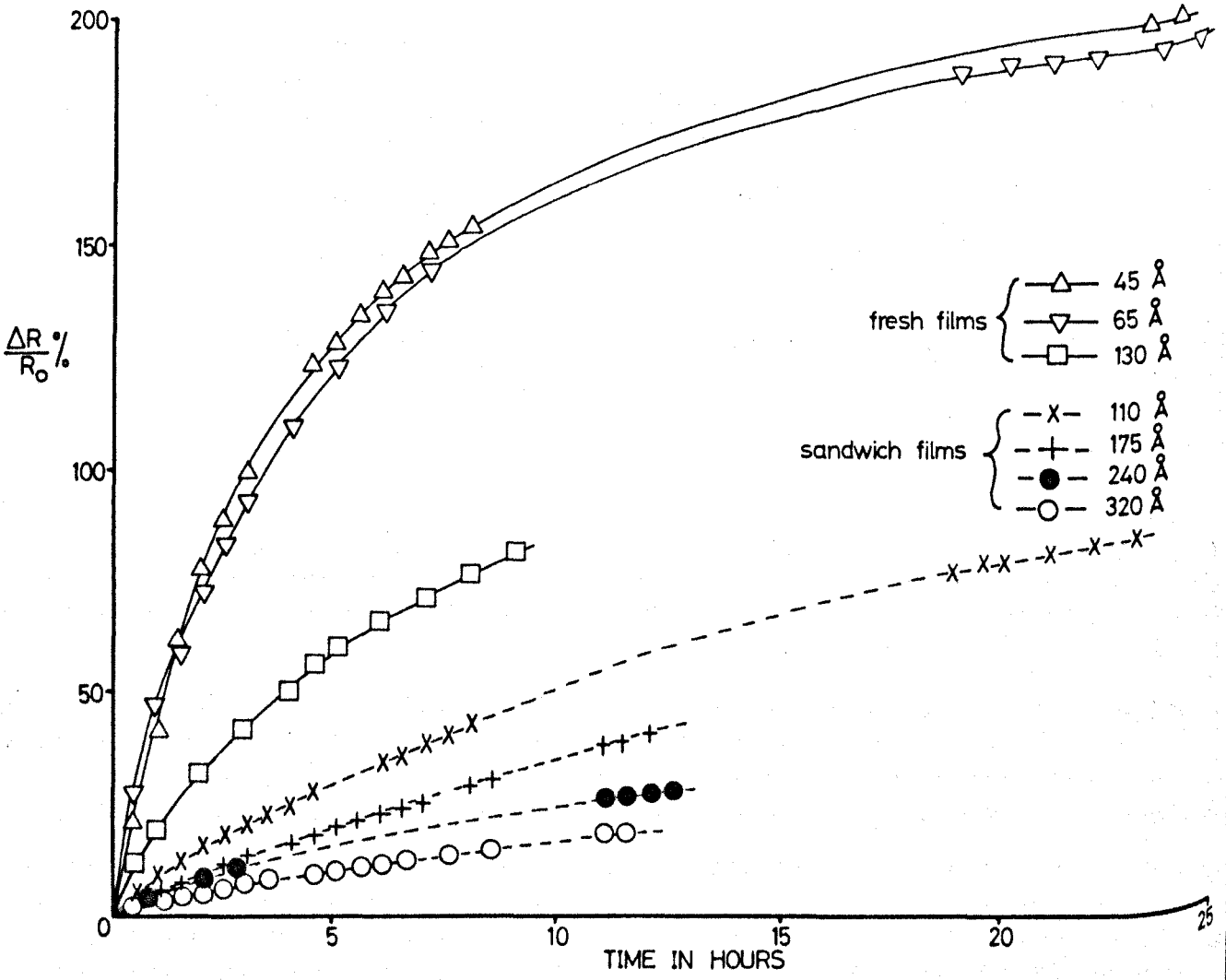

Figure 11 Percentage change of resistance of erbium films as a function of time at pressure of 10^{-8} torr for first hour, rising to 4×10^{-8} torr in 15-20 hours, then staying constant.

Figure 11

The sandwich films studied within the thickness range of 1000 down to 100 Å had a smooth increase of resistivity from 375 to 800 micro-ohm cm, while the initial resistivity of these films increased more slowly from 375 to 500 micro-ohm cm for thicknesses from 1000 down to 175 Å and then decreased to about 450 micro-ohm cm for the first sandwich film of about 110 Å thick. The initial resistivity of these films is essentially dependent on the mode of their production i.e. the number of thickness steps and the time taken for ageing of the previous film.

On ageing in vacuum all films showed an increase in resistance. The percentage rise of resistance ($\Delta R/R_o$ %) versus time of some of the freshly prepared and sandwich films of different thicknesses is shown in Fig. 11. For the fresh films the rate of increase of resistance was fast for a few hours after their formation and then it became slow, but even in thirty hours of ageing the resistance did not attain a steady value. The rate of increase of resistance was much higher for thin films than for thick films. The sandwich films too showed an increase in resistance on ageing in vacuum, but this increase was slow compared to that for freshly prepared films. Except in the case of the first few thinner films, the rate of increase was steady right from their formation and the resistance did not attain a steady value for a period of twelve hours of observation. All this suggests that the erbium films are even more reactive than the titanium films.

3.2(2) Discussion - Resistivity

The observed resistivities of the freshly prepared erbium films are too high to be explained on the basis of the size-effect theory for diffuse scattering. Theoretically, the ratio of the film resistivity to the bulk resistivity (ρ/ρ_o) should vary from 1.08 to 3.00, for the variation of ratio of film thickness to

bulk mean free path (d/ℓ_o) from 5.0 down to 0.2. For the same variation of film thickness to bulk mean free path ratio, the measured film resistivity to bulk resistivity ratio varied from 2.2 to 11.3. In determining the ratios d/ℓ_o and ρ/ρ_o, values of 185 Å for ℓ_o and of 86×10^{-6} ohm cm for ρ_o have been used for bulk erbium[36].

In addition to the size effect some other factors seem responsible for the observed higher resistivity of the films. From the mass spectrometric analysis (Chapter V), it was observed that the residual gas pressure decreased when the film formation started, which means the residual gas atoms or molecules were taken down by the film during its formation. These foreign atoms act as extra scattering centres for the conduction electrons and possibly may form chemical compounds with the film material and thus change the resistivity.

Electron microscope studies (Chapter IV) of surfaces of these films indicated that they had fine grain sizes rather than smooth surfaces. Grain size has a large effect on resistivity, since the electronic mean free path may well be limited by the grain size i.e. the conduction electrons may be scattered from the grain boundaries. Differences in resistivity by a factor of ten or more are not uncommon for films of different grain size but equal film thickness.

Because of the relatively low mobility of metal atoms at the substrate surface at room temperature, erbium vapour atoms tend to condense in the form of a porous film. Also as these films are deposited with a high condensation rate of 30 Å/sec, a deposited layer of atoms is covered by succeeding layers before reaching thermal equilibrium with the substrate, which may involve a large number of vacancies and dislocations being trapped into the film. All these defects are effective in scattering of conduction electrons and

therefore responsible for increased resistivity.

Lastly, due to the low baking temperature (130°C at the substrate) of the system because of the Viton gasket, the water vapour present in the glass substrate may react with the films, as the metal reacts with hot water. This also receives partially favourable support from the fact that the resistance of the thinnest fresh films (film in contact with the substrate) increased rapidly and became about three times their initial value within a few hours of observation, while that of the thicker or superimposed film changed much more slowly (Fig. 11).

The films below 60 Å thick have negative temperature coefficient of resistance (Section 3.4) which possibly suggests that these have an island structure. Thus the extremely high measured resistivity for films of thicknesses below 60 Å is due to their different type of structure which conducts by different processes as reviewed in Section 1.3(3).

The increase and then decrease in the initial resistivity of sandwich films is essentially dependent on the mode of production, and is probably governed by two factors, namely their pre-gas content and their immediate increased thickness. For the first few sandwich films their pre-chemical content is dominant, thereby causing an increase in resistivity, and for the subsequent thick sandwich films the thickness effect is dominant thereby causing a smooth slow decrease of resistivity, with increased thickness. Lucas[37] had observed similar phenomenon on thin gold films superposed by gold and other metal films and explained the results in terms of a specular scattering parameter. The addition of gold atoms to the surface of the specular gold films causes initially an increase in resistance due to a large

fraction of the conduction electrons being diffusely scattered as a result of the increased surface roughness caused by the added gold atoms. With further deposition the resistance begins to decrease as the roughness reaches a maximum and the thickness of the conduction path is increased. In contrast to Lucas's results, Chopra and Randlett[38] have observed that if the superimposed film is of the same material as the base film, then no such changes in the resistivity of the base film occurred for specular as well as diffuse continuous films (> 100 Å). He suggested that at least in the case of further deposition of the same material, the statistical nature of condensation is expected to increase surface smoothness rather than reduce it. In the case of different materials, the formation of a new interface modifies the nature of the surface potential (similar to the phenomenon of modification of surface potential due to adsorption of gases at metal surface), which influences the scattering of electrons near the surface and hence changes the resistivity. None of these explanations seems applicable to the experimental films as the film surfaces are presumably completely rough.

3.2(3) Discussion - Ageing

From the mass spectrometric analysis (Section 5.4) of the residual gases before and after evaporation, it has been observed that the concentration of almost all gases decreased rapidly during and after evaporation and attained much lower partial pressures than before evaporation. This suggests that the films readily take up the gases during their formation and continue to take them for several hours after deposition. These gases diffuse more rapidly through the island boundaries of the discontinuous films, and slowly through the structural defects of thicker films, and form chemical compounds within the film and thus increase the resistance of thinner films rapidly (because of the increase of tunnelling distance between metal

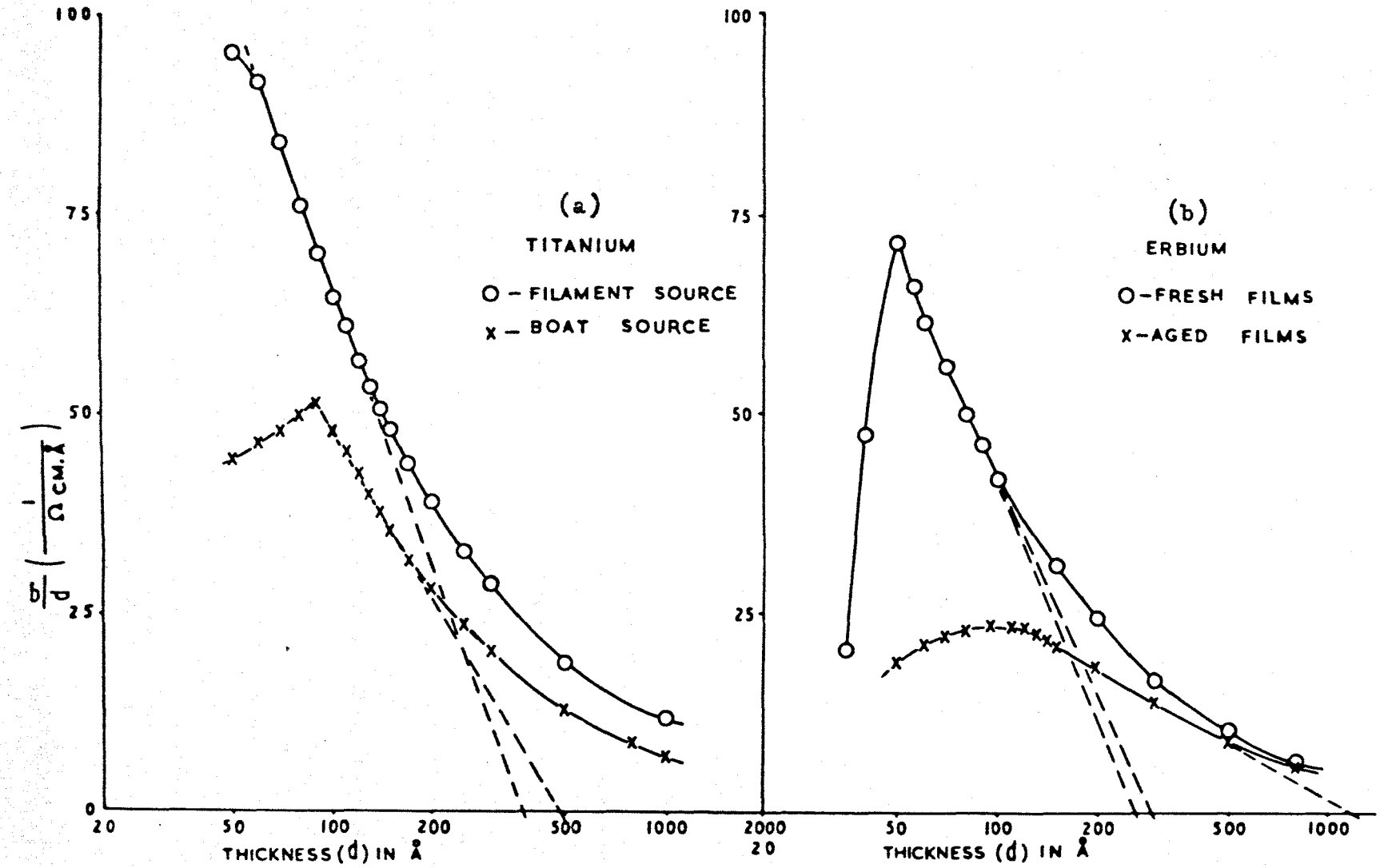
100
75
50
25
0
b/d (1/Ω CM.Å)
(a)
TITANIUM
O – FILAMENT SOURCE
X – BOAT SOURCE
20
50
100
200
500
1000
2000
THICKNESS (d) IN Å
(b)
ERBIUM
O–FRESH FILMS
X–AGED FILMS
CONDUCTIVITY AS FUNCTION OF FILM THICKNESS IN NOSSEK'S REPRESENTATION

Figure 12

islands and also due to decrease in the effective thickness of the metal film), and of thicker films slowly (due to decrease in the effective thickness of the metal film only). This chemical compound layer so formed, decreases the probability of further action of the gases with the metal, and thereby after a few hours the rate of increase of resistance is slowed down. As discussed already, the initial rapid increase of resistance of the thin films might also be due to their reaction with water vapour in the substrate.

Sandwich films are films deposited on thin aged films and consequently as a whole are electrically continuous. The second and third films deposited on the first aged film form sandwiches that have chemically reacted more, and have therefore a smaller probability of further interaction and hence undergo a slow increase of resistance. As the sandwich layers increase in number i.e. the film grows thicker, the content of chemical compounds in the film increases and the further probability of chemical compound formation with the residual gases decreases, and thereby the resistance finally becomes steady.

3.3 Calculation of bulk mean free paths

Rearranging equation 1.5 of the first chapter, one gets

$$\log d = - \frac{4\ell_o}{3\sigma_o} \frac{\sigma}{d} + (0.4228 + \log \ell_o) \qquad (3.1)$$

This when plotted as log d on abscissa and σ/d on ordinate gives a straight line with intercept of length $(0.4228 + \log \ell_o)$ on the abscissa axis. The results are shown in Figs. 12a and 12b, in which values of σ/d from Fig. 6 for the fresh films of titanium (evaporated from both the sources) and from Fig. 10 for the fresh and aged films of erbium respectively are plotted as function of log d. From these plots (Nossek's representation[39]) the following can be seen.

In each figure, the curve initially ascends with thickness and then descends after a particular thickness is reached. The descending part of the curve is characterised by two distinctive features, firstly a straight part, where the relation 3.1 is applicable and secondly a curved part deviating slowly from the straight part and approaching bulk characteristics of the metal. The straight parts of the curves, which are practically straight lines from 60 to 130 Å and 90 to 170 Å for the films of two different grades of titanium, and from 50 to 100 Å and 110 to 500 Å for the fresh and aged erbium films, cut the intercepts at 380 and 490 Å, and 285 ± 15 and 1200 Å for the respective films. From these intercepts bulk mean free paths are calculated of 250 and 320 Å for the two grades of titanium, and 185 ± 10 Å and 785 Å for erbium from fresh and aged films respectively. The mean calculated value of 285 Å for the mean free path in titanium agrees reasonably with the published value (330 Å - Hacman[19]). The anomalously high calculated value of the mean free path in erbium deduced from the aged films, arises because the size-effect theory assumes the only scattering is by the film boundaries and so a higher value of bulk mean free path will give more frequent collisions and therefore a higher resistivity.

The points (thicknesses) where the curves changed the sign of their gradient, probably indicated the stages where the films changed their structure i.e. from a island type of structure to a continuous film structure. These points occurred at thicknesses of 70 ± 20 Å for titanium films and 50 and 100 Å for fresh and aged erbium films respectively. These observations are in agreement with the regions where the titanium and the erbium films changed their TCR values from negative to zero and afterwards positive, as described in the next section. For the erbium films, the region of film thickness for which this transition occurred is much lower for the fresh films than for the aged ones, which is justified by considering

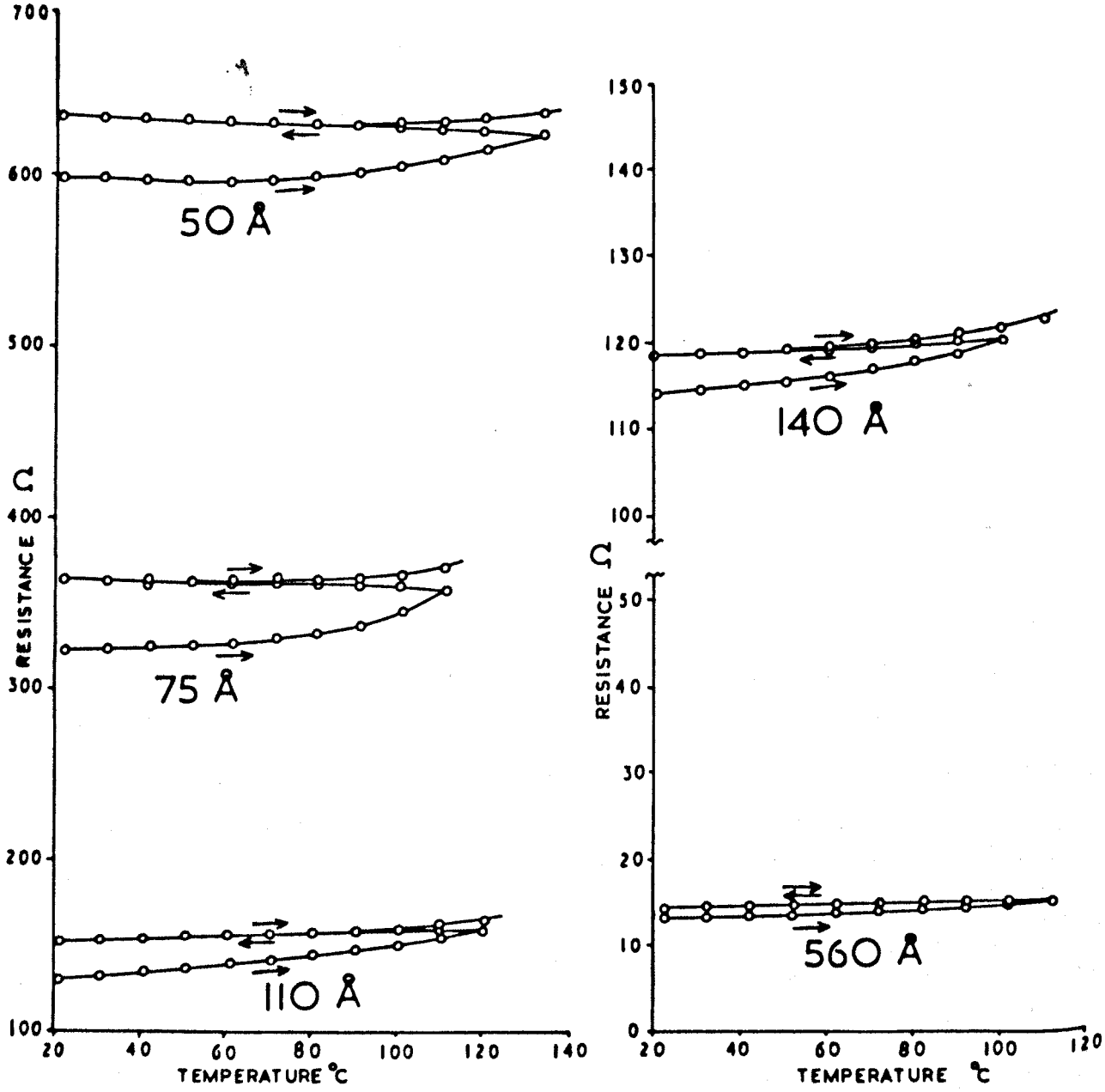

CHANGES IN RESISTANCE OF TITANIUM FILMS WITH TEMPERATURE.

Figure 15

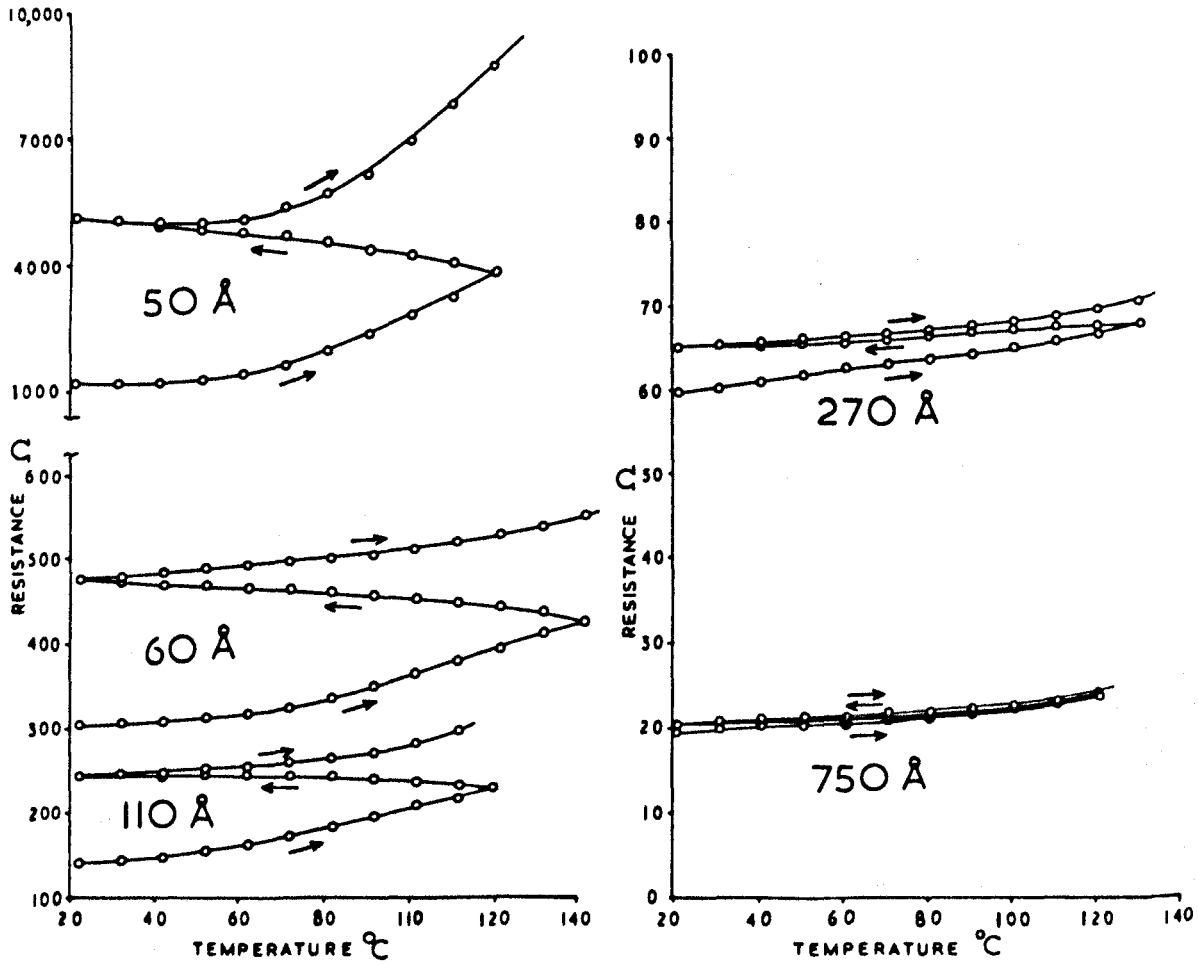

VARIATION OF RESISTANCE WITH TEMPERATURE FOR ERBIUM FILMS.

Figure 16

chemical compound layer formation of the aged films as explained below.

Consider Figs. 13 and 14 where a and b represent fresh and aged chemically reacted (with gases) stages of a film respectively. In Fig. 13a assume that the fresh film just starts forming continuous structure from its islands at a thickness of 60 Å. Then on gas interaction (i.e. on ageing) with this film, its upper layer will form a chemical compound by the mechanism described in Section 3.2(3), that will result in an increase of island to island distance as shown in Fig. 13b. Thus this film will become discontinuous at the same thickness. Similarly in Fig. 14a, where a fresh film is perfectly continuous say at 100 Å, it remains just continuous due to the same mechanism.

3.4 Temperature coefficient of resistance - Results and Discussion

Figures 15 and 16 show the variation of resistance as function of temperature on heating the fresh films of titanium and erbium twice above the room temperature, at heating and cooling rates of 2 - 3°C per minute respectively. Figure 7b shows the change in resistance with temperature for the thickest film of titanium on magnified scale. The second heating was started immediately after the film was cooled to room temperature. The increase of resistance with temperature for the first heating was similar for all films of both metals except the thinnest ones of titanium (for which a slight decrease in resistance with temperature was observed). The rate of increase was slow up to 60°C and then more rapid up to 130°C, which was the maximum temperature studied, but for the thicker films of erbium it was almost constant up to 90°C and then a little more rapid afterwards. On cooling the films, the resistance increased for films thinner than 70 and 120 Å of titanium and erbium respectively,

TABLE I TCR OF EVAPORATED FILMS OF TITANIUM AND ERBIUM IN VACUUM

METALS →	ERBIUM		TITANIUM									
AUTHORS →	EXPERIM-ENTAL ONES		EXPERI-MENTAL ONES		GERSTEN-BERG[20] 1963		HUBER[21] 1964		CHANDER ET AL[22] 1967		FRIEBERT-SHAUSER[23] 1969		CALCULATED FROM F-S THEORY	
THICKNESS AND TCR → / FILM No ↓	d	$\alpha^{\bullet}$	d	$\alpha^{\bullet}$	d	$\alpha^{\bullet}$	d	$\alpha^{\bullet}$	d	$\alpha^{\bullet}$	d	$\alpha^{\bullet\bullet}$	d	$\alpha^{\bullet\bullet\bullet}$ $\times 10^{-5}/°C$
1	40	−84	50	−25	200	+100	275	−35	105	−82	150	+34	115	+175
2	50	−36	75	+04	300	+185	390	−23	155	−65	300	+ 66	170	+ 196
3	60	+ 97	110	+ 52	400	+220	670	+ 23	225	−32	1300	+100	230	+ 210
4	110	+123	140	+ 58	540	+230	4500	+100	275	−00	3850	+112	285	+ 230
5	750	+161	560	+ 92	1170	+260			300	00			570	+280
6	BULK	+201	BULK	+300									855	+ 300
CALCULATED BETWEEN	20−100°C		20−100°C		−195−+25°C		20 − 120°C		21 − 100°C		−195−+27°C			

NOTE 1. d FILM THICKNESS IN ÅNGSTROMS.

2. $\alpha^{\bullet}$ AND $\alpha^{\bullet\bullet}$ TEMPERATURE COEFFICIENTS OF RESISTANCE IN $\times 10^{-5}/°C$ AND $\times 10^{-4}/°C$ UNITS, THERE SEEMS AN ERROR OF FACTOR 10 IN $\alpha^{\bullet\bullet}$ VALUES.

3. $\alpha^{\bullet\bullet\bullet}$ VALUES ARE CALCULATED BY ASSUMING BULK M.F.P. 285 Å AND TCR $30 \times 10^{-4}/°C$.

but decreased for thicker films. On reheating, the thinner films showed a decrease in resistance, slightly thicker films showed no appreciable change, while the thickest films showed increases in resistance. In general, on repeating the cooling and heating cycles, the thicker films showed reversible changes, while the resistance of the thinner films continued to rise. When the thinnest films of erbium were heated continuously at constant temperature ($\gtrsim 100^{\circ}C$) their resistance continued to rise, and for one or two films it reached beyond the limit of the bridge measurements (10 Mohms) in a few hours. In all these measurements pressure variations (5×10^{-8} - 3×10^{-7} torr) were noticed during the heating and cooling cycles.

An irreversible increase in resistance during the first heating has also been observed by Chander et al.[22], and by Belser and Hicklin[40] for titanium and other transition metals respectively. The irreversible increase is most likely due to the surface reactions and chemical compound formation. The negative TCR for thin films has also been observed by several authors with titanium (Table I) and other metal films, and this has been explained by considering their island type of structure in which condution occurs by the mechanisms discussed in Section 1.3(3).

The first two columns of Table I show the temperature coefficients of resistance for erbium and titanium films of different thicknesses after the second heating in vacuum (5×10^{-8} - 3×10^{-7} torr). These have been calculated assuming a linear increase of resistance between room temperature and $100^{\circ}C$. It is observed that the TCR is negative for the thinnest films, approaching to zero for films of medium thickness, and is positive for films more than about 100 Å thick. The temperature coefficients of resistance increased with thickness, but were less than that of the bulk values[35] ($3.0 \times 10^{-3}/^{\circ}C$ and $2.01 \times 10^{-3}/^{\circ}C$ for titanium and erbium respectively).

The TCR values for titanium films in the second column are compared with the published values in the other columns of Table I. The reproducibility of the values of temperature coefficient of resistance is extremely poor. In fact the TCR value depends upon the method of its measurement i.e. the range of temperature, and the method and environment of heating, and also on the structure of the film, as it is possible within a certain thickness range to prepare a film of continuous or island type of structure for the same thickness.

3.5 Conclusion

It is unlikely that the Fuchs-Sondheimer theory would apply to the conductivity of such films of these metals, which are highly reactive. The high resistivities of thick films of both the metals are due to their adsorption and chemical compound formation with the residual gases, their fine grain size and lattice defects. In addition, the very high resistivities of thin films are due to their island type of structure, as confirmed by their negative temperature coefficient of resistance, and possibly their reaction with water vapour in the glass substrate.

CHAPTER IV

STRUCTURAL STUDY OF ERBIUM FILMS BY THE ELECTRON MICROSCOPE

4.1 Introduction

In recent years, surface studies, and the knowledge of the nucleation, growth and the structure of thin films have been considerably extended by the use of high resolution electron microscopes. Observations of the initial growth stages of evaporated films of many metals in particular have shown that these deposits generally consist of isolated islands lying on the substrates and not thin continuous layers, as might have been expected. The (average) thickness of these films is defined as the thickness which would be obtained if the deposit were smeared uniformaly over the substrate. The negative TCR of thin films of erbium studied by the author led him to speculate on their having an island type of structure. It was therefore thought advisable to study their structure in an electron microscope for visual evidence. This chapter describes some of the attempts made to study the surface structure of erbium films under a transmission electron microscope. The particular electron microscope used was 'Hitachi' model HS-7S, having a guaranteed resolving power of 8 Å by the Fresnel test.

4.2 General introduction of film growth

The initial stage of growth of most deposited films consists of the formation of three-dimensional nuclei, and the structural changes occur as these nuclei grow and intergrow, as deposition continues, to form a continuous film. The characteristic stages (Pashley[41]) in this sequence are: (1) the formation of a surface distribution of small three-dimensional nuclei; (2) the growth in

size of these nuclei, without any increase in their numbers; (3) further increase in size of the nuclei or islands, accompanied by a gradual but considerable decrease in their numbers; (4) the formation of a connected network of deposit, usually rapidly developing into the channelled structure; (5) a continuous film. The total amount of deposit (i.e. average thickness) for which a given state is reached varies considerably from one system to another and also for a given substrate-deposit combination. It can be affected appreciably by deposition parameters (e.g. substrate temperature, rate of deposition) as well as by contamination.

Films will exhibit monolayer like growth if the substrate temperature is too low for the deposited atoms to diffuse over the substrate surface, or if film growth is so rapid that the deposited atoms do not have time to move over the surface of the substrate. Films grown under these conditions are often polycrystalline or amorphous. The tendency towards cluster formation (i.e. larger grain sizes) is increased by a high substrate temperature, a low deposition rate, a low boiling point of the film material, weak binding forces between film and substrate, a high surface energy for the film material and a low surface energy for the substrate. In some cases it has been observed that contamination by residual gases helps to form a smooth and continuous film at a very low thickness, probably due to decrease in the surface mobility of the metal atoms due to adsorbed residual gases[42]. Oxygen has been found to be most effective in reducing the surface mobility.

Many deposits do not follow the types of growth sequence described, but there is much less systematic work available about them. Many deposits have very fine grain sizes, probably because the initial nuclei grow together without forming larger single crystal islands. Examples of fine grained structures are some oxide layer on metals and

evaporated deposits of higher melting point metals.

4.3 Experimental details

4.3(1) Preparation of supporting film on grids

The island deposits at the beginning of film growth are isolated from each other, so that it is necessary to support them on a continuous film for microscopic examination. In many cases the supporting film will be the substrate itself, but when this is not possible (usually when the substrate cannot be made thin enough for transmission electron microscopy) a thin coating layer can be deposited over the islands, and the substrate is then removed. This technique is essential for studying the growth of epitaxial single crystals or oriented films and it involves certain complications of film stripping, which probably may change the film structure. However, if the effect of substrate surface is ignored (which actually plays a vital role in film growth), then for studying polycrystalline film growth, a thin layer of transparent material can be deposited over copper grids as a supporting film prior to experimental film formation. For this experimental film study the latter technique was adopted.

The grids used were about 3 mm in diameter with a solid periphery, 25-50 micron thick and contained a square mesh (200 per linear inch) with windows 90 micron square and 35 micron bars. The supporting film was prepared from an organic material called 'Formvar'.

4.3(2) Stripping of specimen film from the glass substrate

A few attempts were made to examine films on glass substrates. Some of the carbon coated films were stripped off from the glass substrates by dipping them into distilled water and these floated films were then picked up on the microscope grids. When these were dried on a filter paper in atmosphere, they were found to become brittle following their detachment from the grids. Thus it became a

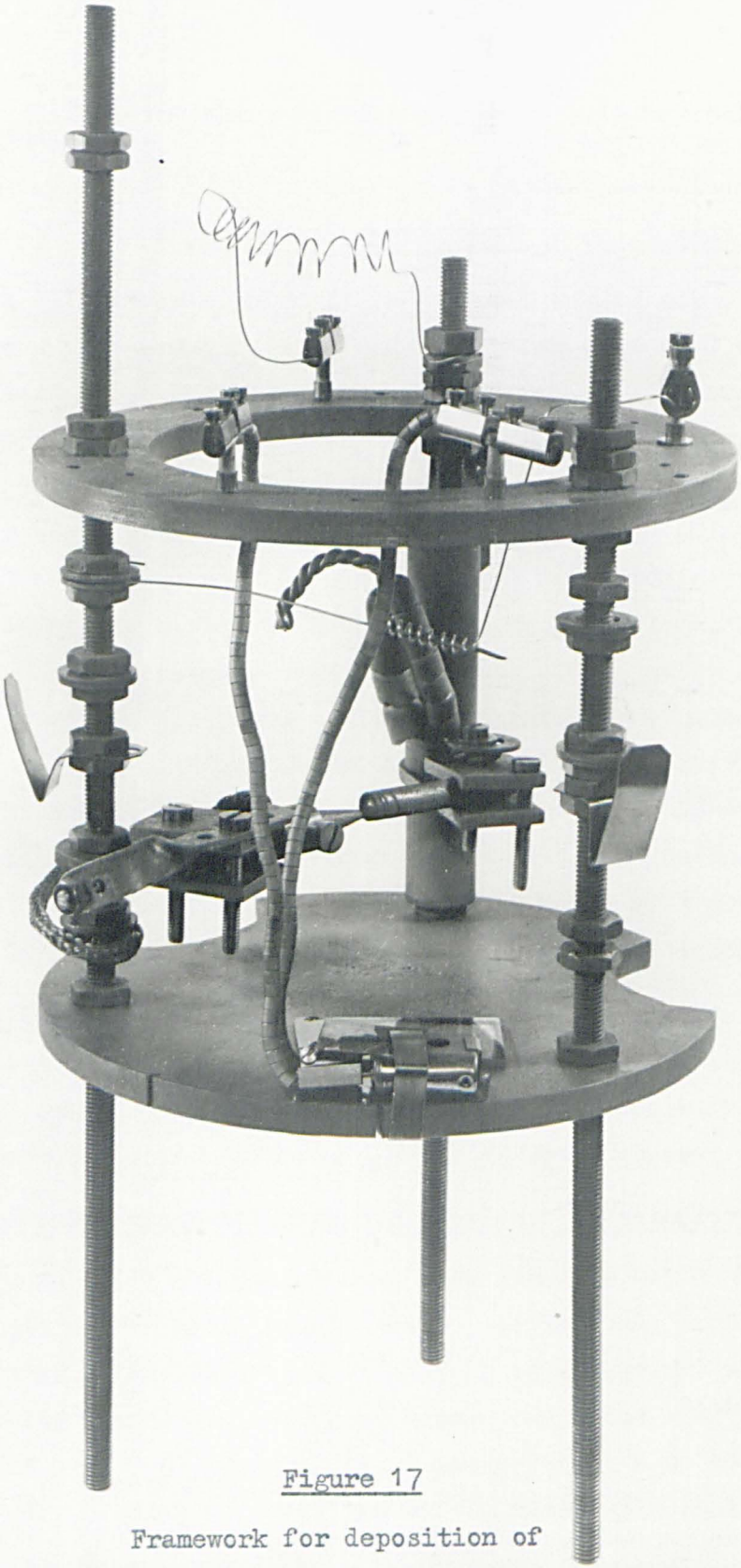

Figure 17

Framework for deposition of metal film and carbon layer.

problem to hold them on the grids. In spite of this complication, a few attempts were made to examine such films in the microscope.

4.3(3) Experimental arrangement

After the films were deposited in the vacuum chamber, they were to be transferred to the electron microscope objective for their surface study. Erbium metal films being highly gettering in nature, may readily absorb residual and atmospheric gases during the period of their transit from the vacuum system to the electron microscope, and consequently change their structure. Therefore, another thin layer of carbon (a low atomic number material) was deposited immediately over the top of the film and sandwiched it between this layer and the plastic film to keep the experimental film free from residual and atmospheric gases.

The vacuum system used was the same as described in Chapter II, but the inside arrangement of the vacuum chamber was slightly modified to hold the copper grids and to provide extra electrodes for the top carbon film deposition. This inside arrangement is shown in Fig. 17. Since the grids had to be on the top of the substrate, the erbium was evaporated from a molybdenum wire filament located above them. The bottom stainless steel circular plate of the inside arrangement, as described in Section 2.3, was raised to about 10 cms, and was used as a platform for holding the copper grids (placed on a convenient size of microscope glass slide) and the quartz crystal. The 200 amp feedthrough was now used for evaporating carbon from the carbon electrodes. One of the carbon electrodes was rigidly fixed to the isolated electrode holder and the other was loosely fixed to the earthed electrode holder by means of a stainless steel spring to keep these electrodes in contact during the entire period of evaporation. These carbon electrodes were arranged at an angle of about 30° to the surface of the grids, and at a distance of about 10 cms to avoid heating

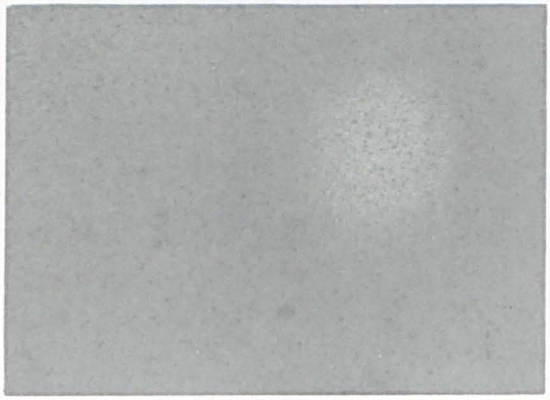

Plate 18a
Film 40Å thick
(magnification x 30,000)

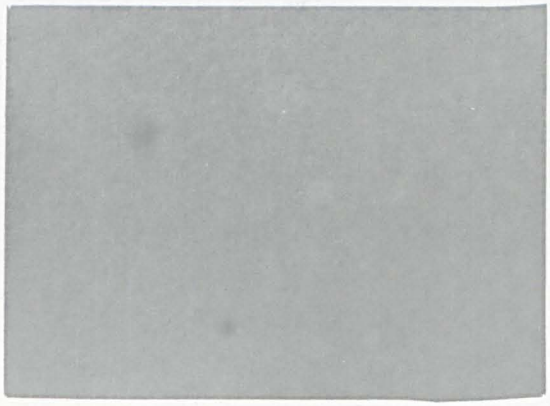

Plate 18b
Film 60Å thick
(magnification x 30,000)

Plate 18c
Film 110Å thick
(magnification x 30,000)

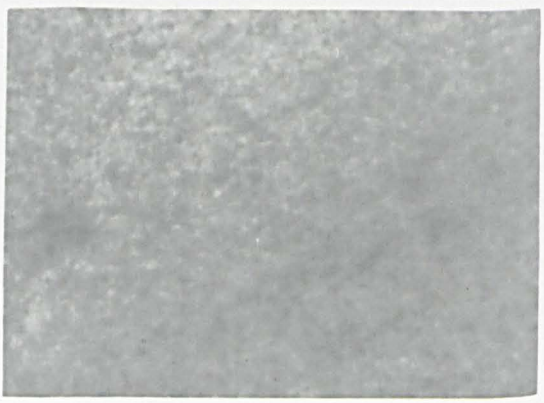

Plate 18d
Film 160Å thick
(magnification x 30,000)

of the films due to the high temperature of the carbon arc. A heavy current of about 60 amps was required through these two pointed carbon rods with the points tightly sprung together to evaporate carbon, but as the evaporation started these points slid adjacent to each other and the carbon arc ceased. It was therefore modified to use one pointed rod (loosely tight with spring) pressing onto a flat end of the other fixed rod, and some control over the direction of evaporation was then obtained. This arrangement was found successful for carbon evaporation and it took about 80-90 amps for its evaporation.

All the grids were placed adjacent to the crystal holder and normally below the source filament for their normal deposition. The source filament took about 20 amps (10 V) to evaporate erbium at the same rate of 30 Å/sec. All these depositions were carried out under similar conditions of pressure as were used for the resistive films studies, i.e. before the electron microscope specimens were prepared, the whole system was baked to about 100°C for about 24 hours. Before evaporation the pressure was in the range of $0.5 - 1 \times 10^{-7}$ torr. However, lots of gases were released during carbon evaporation and the pressure rose up to about 10^{-4} torr and sometimes the pump was automatically switched off (due to pressure rise of up to 5×10^{-4} torr). This immediate rise of pressure was not effectively attended to by the pump. The carbon films deposited were in the range of 200-400 Å in thickness, which were transparent for transmission electron microscopy.

4.4 Results and discussion

Films ranging in thickness from 40 to 270 Å were examined for their surface structure by the electron microscope. Some of the micro-photographs taken are shown in Figs. 18a, 18b, 18c and 18d for films of increasing thickness with a magnification of 30,000. Within the thickness range of the films studied, no distinctive stages (i.e. the sequences in the film growth from completely isolated islands to

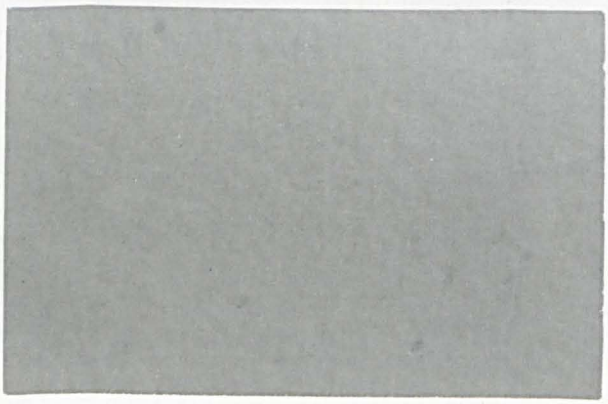

Plate 19a

Film 50Å, prepared on plastic film

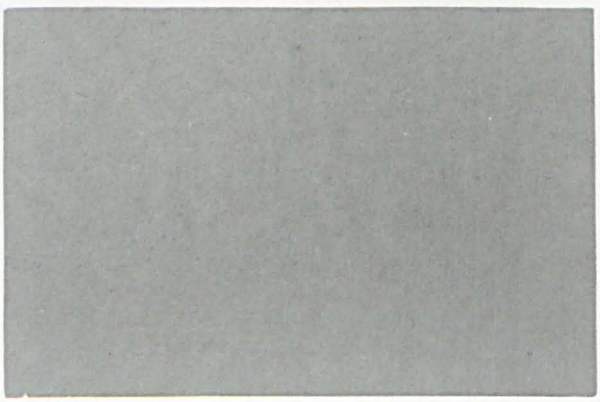

Plate 19b

Film 50Å, stripped from the glass substrate.

channelled structure and subsequently into continuous film formation) were observed. It therefore suggests that the erbium deposits do not follow the types of growth sequence described. However, the deposits have fine grain sizes, probably the initial nuclei grow together without forming larger single crystal isolated islands. Films of small thickness are granular in structure, having small grain sizes as shown in the electron microscope photographs and as the thickness of the film increases, their grain size increases. The films in general are free from big pin holes but have fine grain sizes.

Erbium metal, because of its high heats of fusion and sublimation (4.1 Kcal/mole and 70 Kcal/mole respectively)[43] and therefore presumably low mobility for surface atoms at room tempeature, tends to condense in the form of a porous film with a high surface area. Because of the low mobility for surface atoms and the high deposition rate, films have a fine grain structure and are reasonably smooth but have some roughness due to the randomness of the deposition process and the statistical fluctuations in film thickness.

As has already been said, no conclusion can be drawn about the modes of film growth, moreover the film growth sequences studied on the Formvar film may not be the same as on the glass substrate, as it is the free surface energies of the substrate and of the interface between the film and the substrate, which determine the growth sequence. The total amount of deposit (i.e. thickness) for which a given state is reached would be different for the deposit on the Formvar and the deposit on the glass. However, no appreciable difference was observed between the surface structures of the films prepared on the glass substrates and on the Formvar films, except for a slight change of grain size (compare photographs 19a and 19b of same film simultaneously deposited on the Formvar film and on the glass substrate respectively).

Unfortunately water is expected to change the film structure due to chemical reaction with erbium, so the idea of studying water-floated films was given up.

The enormous amount of gaseous impurities, which were liberated during the deposition of carbon layer could have changed the surface structure of the specimen films due to chemical compound formation. Oxidation of the thin films of erbium has been studied by Murr[44] in the electron microscope and he had observed that as the oxidation content of the film increased, it changed its structure from fine grain size to granular crystalline structure. The carbon arc also raised the temperature of the films to about 70°C. In Section 3.4 it was shown that the resistance of the thin films changed rapidly above 60°C at 10^{-7} torr, hence is seems likely that the film structure may have been changed by the pressure and temperature changes during the deposition of the carbon layer.

4.5 Conclusion

It is therefore apparent that the fine grained structures shown in Figs. 18 and 19 are those of aged films which have already reacted with residual gases in the vacuum system, and may not be necessarily the same as the structure of freshly deposited films. It is not yet possible to study the structure of clean, freshly deposited films, owing to the technical difficulties described above.

CHAPTER V

MASS SPECTROMETRIC ANALYSIS OF THE RESIDUAL GAS

5.1 Introduction

Studies of film structure were limited by technical difficulties, as mentioned in Chapter IV, and were not continued further. However, the rapid changes in the system pressure during degassing and film formation made it interesting to study the residual gas composition, as the residual gases in vacuum systems have been found to undergo numerous interactions with deposited films that modify significantly their surface and bulk characteristics. The residual gas composition in the vacuum system, and the subsequent changes in its concentration due to degassing of the source and metal and the film formation, were analysed by an 'AEI Vacuum MS 10' mass spectrometer.

A scan of m/e = 12 to m/e = 45 mass range was completed in one minute, giving an approximately 5% reduction in peak height over static conditions. The mass spectrum peaks were either observed manually on the MS10 control unit meter or automatically recorded by a 'Beckman potentiometric' recorder by feeding the output of the meter into the latter. The relative sensitivities (with respect to nitrogen) used for the calculation of partial pressures of different gases are given in the following table, which are approximately the mean of values supplied in the 'Vacuum MS10' manufacturer's handbook[45], and published by Craig and Harden[46] and by Bailey[47] for the MS10 mass spectrometer.

Table for sensitivities relative to nitrogen

hydrogen	1.52	oxygen	0.66
helium	0.35	argon	1.37
methane	1.11	carbon dioxide	0.92
neon	0.29	water vapour	1.50
carbon monoxide	1.07		

absolute sensitivity of nitrogen 5×10^{-4} amp/torr

5.2 Previous work on sorption of gases by thin films of titanium and erbium

Although the general solubility of gases in solids has been known for a long time, it is only in recent years that the take up of gases by thin films of titanium has been investigated. Hass[48] ascertained in 1952 by electron optical methods that a film of titanium evaporated at 2 Å/sec at 10^{-4} torr was composed mostly of titanium oxide and titanium nitride. Later Hass and Bradford[49] found that the pure titanium films of normal density could be prepared at a higher rate of 40 Å/sec at a better vacuum of 5×10^{-6} torr. Letting air in resulted in a progressive oxidation to titanium oxide, and at room temperature the oxide layer reached 17 Å in 2 hours and nearly 35 Å after a month.

Lueckert[50] studied absorption mechanisms for films of 700 - 4500 Å thick at temperatures -185 to +60°C, and established that a layer of 120 sq. metres of surface sorbed 34 torr cubic-cms of oxygen per milligram of titanium, about 1:8 in atomic ratio.

Gerstenberg[20] studying the oxidation of sputtered films of titanium in argon atmosphere with an added oxygen, and Arntz and Chernow[51] studying evaporated films of titanium in oxygen leaked into a vacuum system, have shown that the films would be oxidised as fast as they were formed if the oxygen partial pressure exceeded 5×10^{-5}

torr and 2 x 10^{-5} torr in their systems respectively.

Klopfer and Ermrich[52] in 1960 showed that when titanium getters were heated and evaporated in vacuum, hydrocarbons were formed from carbon and hydrogen impurities in the metal. Later Holland et al.[53], using an omegatron mass spectrometer, found that the evolution of hydrocarbon gases was related to the partial pressure of hydrogen in the system and the carbon impurity in the titanium by a relation of the form of the law of mass action.

Previous experiments on the sorption of gases (especially hydrogen) on erbium have been with the bulk metal only[54], except an oxidation study of erbium films in the electron microscope[44].

5.3 Getter action due to titanium evaporation

Titanium was evaporated from two different sources. The first was an 85% titanium, 15% molybdenum alloy filament and the second source was a molybdenum boat containing chips of 99.4% pure titanium. The impurities of both the sources are mentioned in Sections 2.7 and 2.8. With the first source it was difficult to distinguish the changes caused in the composition of residual gases by the titanium alone from those caused by degassing of molybdenum metal in the filament. However, with the second source, to insure that impurities in the boat did not influence the experimental study for titanium, an empty boat was first degassed alone to the same temperature as for the titanium evaporation and in the same manner as the titanium loaded boat, and the mass spectrum of the gases was taken for comparison.

5.3(1) Titanium-Molybdenum alloy filament source

Partial pressures of different gases in the vacuum system before, during and after evaporation of titanium from the filament are shown in Fig. 20. The composition of residual gases changed rapidly within a period of forty five minutes, including a pre-heating

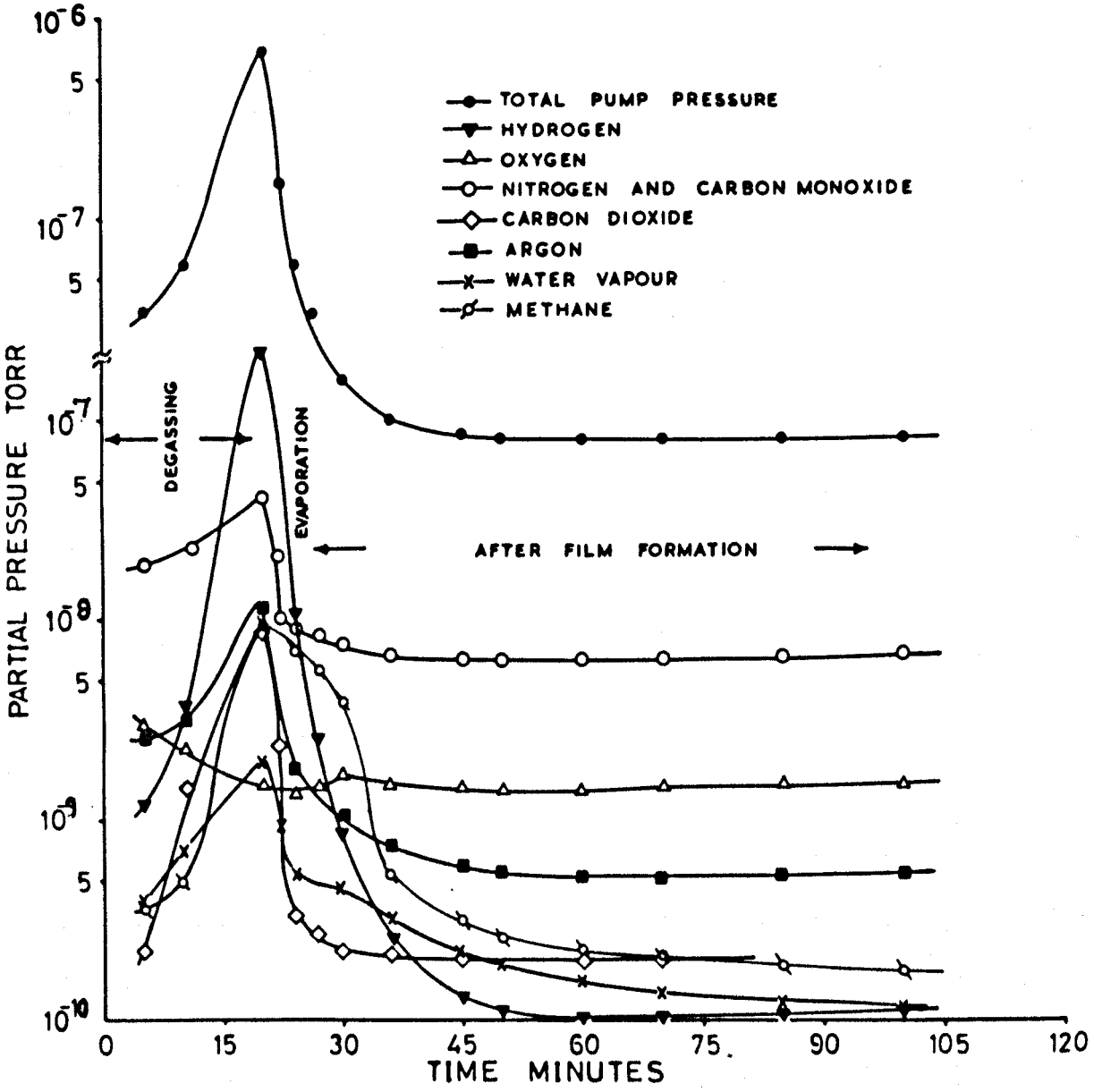

CHANGES IN PARTIAL PRESSURE OF RESIDUAL GASES DUE TO EVAPORATION OF TITANIUM FROM THE TITANIUM-MOLYBDENUM ALLOY FILAMENT.

Figure 20

period of fifteen minutes with increasing source temperature and an evaporation period of ten minutes. The dominant gases evolved during the pre-heating period were hydrogen, carbon dioxide, methane, water vapour, argon and nitrogen (carbon monoxide) and they increased in their partial pressures by factors of 190, 40, 25, 5, 5 and 2 respectively. During this period oxygen decreased in its partial pressure by a factor of 2, probably either due to surface oxide layer formation of the metal, or taken up by carbon impurity in the source to form carbon dioxide and carbon monoxide. Hydrogen increased enormously, as expected, as any hydride content in bulk titanium starts to decompose[55] above 250°C.

During and after evaporation, the partial pressures of all gases, except oxygen, decreased rapidly and within twenty minutes after evaporation they tended to lower concentrations than before evaporation. This shows the gettering nature of titanium, which is also observed by noticing a decrease in total pump pressure by a factor of 90 during this period. The oxygen partial pressure remained almost constant during evaporation and afterwards, probably the oxygen pressure was too low to react with it, or the film was already oxidised and became saturated during and after its formation. Hydrogen underwent the maximum decrease in its concentration, probably either the metal film acted as a very good getter for it, or it was pumped out as the pump was continuously operating during the whole operation of the experiment and the pump has a high pumping speed for it (270%). The pump was not switched off (otherwise it would have desorbed many gases) and because of no isolation valve it was not isolated from the chamber.

5.3(2) Molybdenum boat source

In this attempt, changes in the residual gas composition due to molybdenum boat degassing alone, and due to evaporation of titanium from the same boat under similar conditions of pumping action and boat

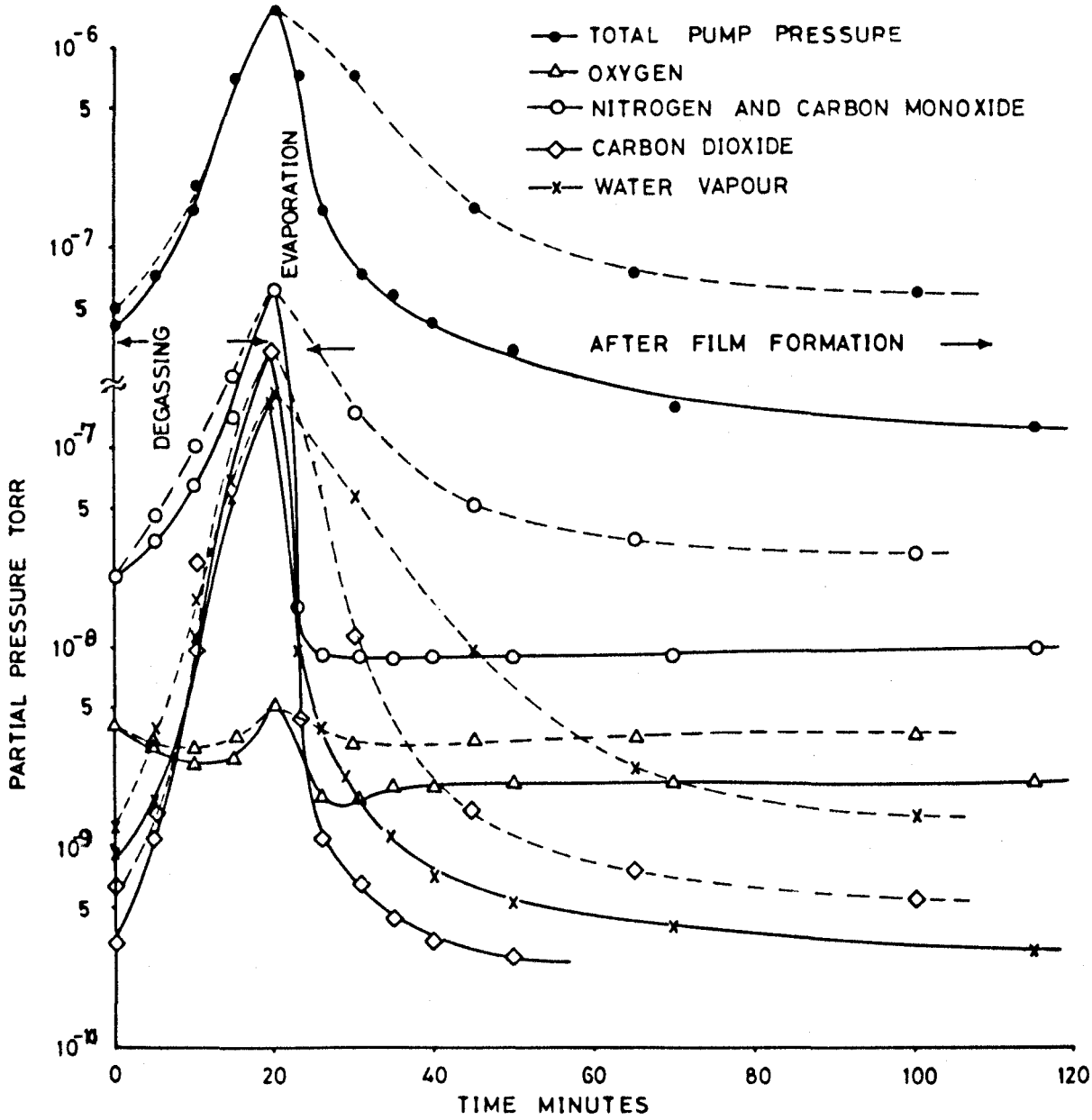

CHANGES IN PARTIAL PRESSURE OF RESIDUAL GASES DUE TO EVAPORATION OF TITANIUM FROM MOLYBDENUM BOAT. BOAT DEGASSING ALONE (- - - -), METAL DEGASSING AND EVAPORATION FROM THE BOAT (——).

Figure 21a

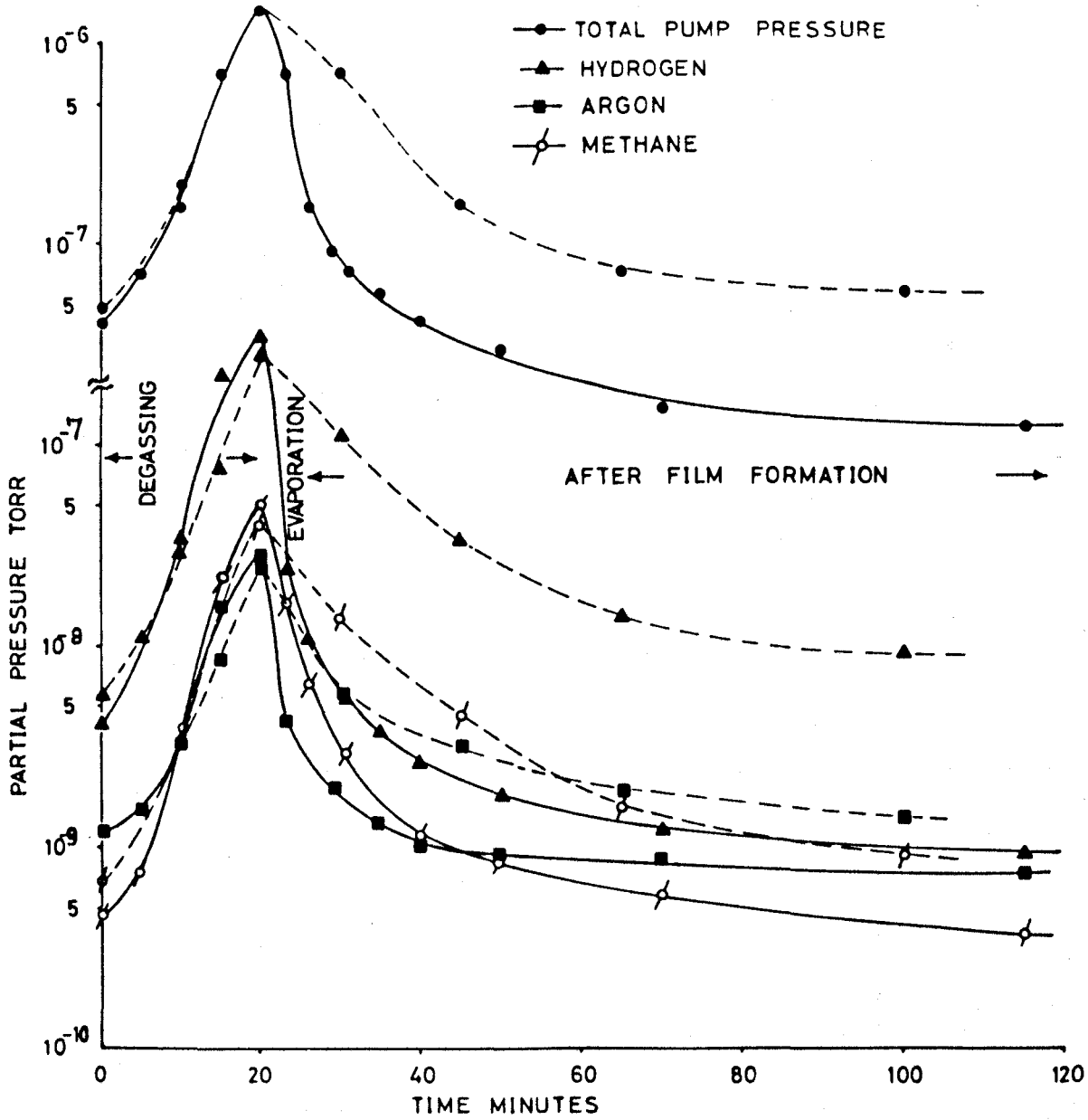

CHANGES IN PARTIAL PRESSURE OF RESIDUAL GASES DUE TO EVAPORATION OF TITANIUM FROM MOLYBDENUM BOAT. BOAT DEGASSING ALONE(- - -), METAL DEGASSING AND EVAPORATION WITH BOAT (———).

Figure 21b

current, were observed separately. Figures 21a and 21b give the simultaneous plots of partial pressure changes of gases hydrogen, nitrogen (and/or carbon monoxide), oxygen, argon, methane, carbon dioxide and water vapour with and without titanium metal in the molybdenum boat under approximately similar conditions, as functions of time, with a degassing period of twenty minutes and an evaporation period of three minutes. The difference of corresponding pairs of curves at any time provides a little real insight into the mechanism of the titanium evaporation alone. In general, pairs of curves coincide during the degassing period and no real information is obtained except that oxygen partial pressure decreased slightly. However, all gases tend to have a lower pressure after the evaporation. Most difference in pairs of curves occurred for the gases hydrogen and nitrogen (and/or carbon monoxide) by factors of 10 and 3.5. Partial pressures for both the gases decreased much more rapidly immediately after evaporation, showing that titanium readily sorbed hydrogen and nitrogen (carbon monoxide). The very little decrease in oxygen partial pressure (by a factor of 1.7 only) suggests that either the pressure was too low for oxidation or the film was already oxidised during its formation, mainly the result of the action of water vapour (partial pressure was reduced by a magnitude of 4) rather than free oxygen.

No siginificant pressure changes were observed in pairs of curves for other gases. Hydrocarbons (principally CH_3 and methane), carbon dioxide and carbon monoxide (m/e = 28, not distinguished from nitrogen) were observed in abundance during degassing and evaporation, and disappeared immediately after evaporation. Hydrocarbons and oxides of carbon are probably formed from carbon and hydrogen impurities in the metals titanium and molybdenum.

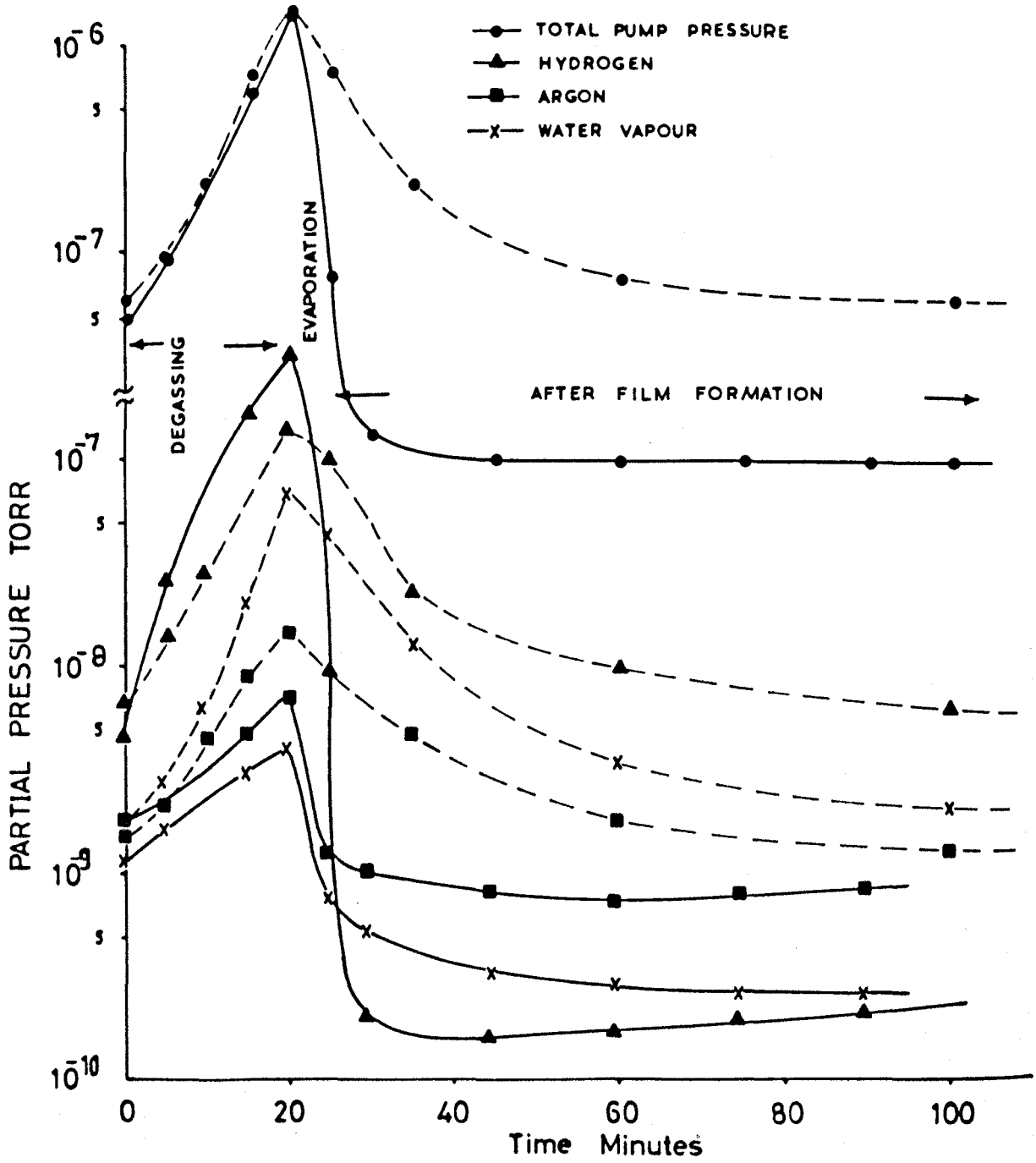

CHANGES IN PARTIAL PRESSURE OF RESIDUAL GASES DUE TO EVAPORATION OF ERBIUM FROM TANTALUM BOAT. BOAT DEGASSING ALONE(— — —), METAL DEGASSING AND EVAPORATION WITH BOAT(————).

Figure 22a

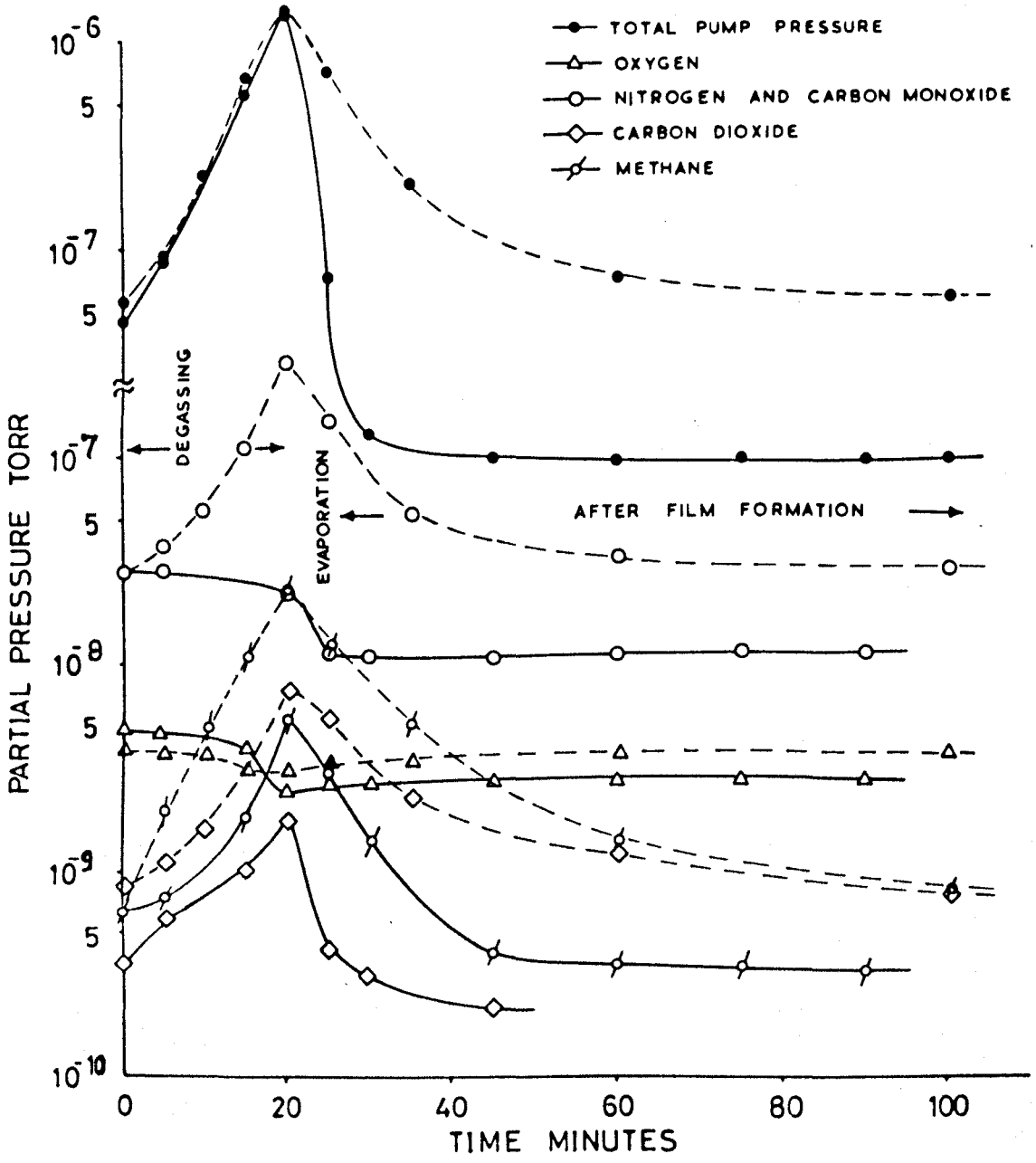

CHANGES IN PARTIAL PRESSURE OF RESIDUAL GASES DUE TO EVAPORATION OF ERBIUM FROM TANTALUM BOAT. BOAT DEGASSING ALONE(– – –), METAL DEGASSING AND EVAPORATION FROM THE BOAT(——).

Figure 22b

5.4 Getter action due to erbium evaporation

Erbium was evaporated from a tantalum boat for studying the electrical resistivity of films in the belljar system, and from a molybdenum filament for the adsorption study of films in the new stainless steel vacuum system. The tantalum boat was expected to evolve hydrogen during its degassing[56], as this metal was annealed in hydrogen during its production. Therefore to study the changes in the composition of the residual gases due to erbium alone, and to distinguish these from those due to tantalum degassing, residual gas analysis was studied separately both from the boat loaded with erbium, and from the empty boat alone. The molybdenum filament containing erbium was degassed at low temperature for a long time and then its temperature was slowly increased to degas and evaporate erbium, and as such three distinctive stages of gas composition were observed.

5.4(1) Tantalum boat source

The main gases which underwent observable changes in their concentrations due to erbium evaporation were hydrogen, nitrogen (and/or carbon monoxide), water vapour, methane, argon, carbon dioxide and oxygen. The changes in the partial pressures of these gases, with and without the erbium loaded boat, under similar conditions of pumping and boat current are shown in pairs in Figs. 22a and 22b, plotted as a function of time (with a pre-heating period of twenty minutes and an evaporation period of five minutes). As before, the difference in pairs of curves gives the change due to erbium alone. During degassing of the metal, the concentration of hydrogen increased and of nitrogen (carbon monoxide) decreased. Hydrogen, which was probably absorbed and chemically combined with bulk erbium, was released on its heating. During evaporation, gases N_2 (or CO), O_2,

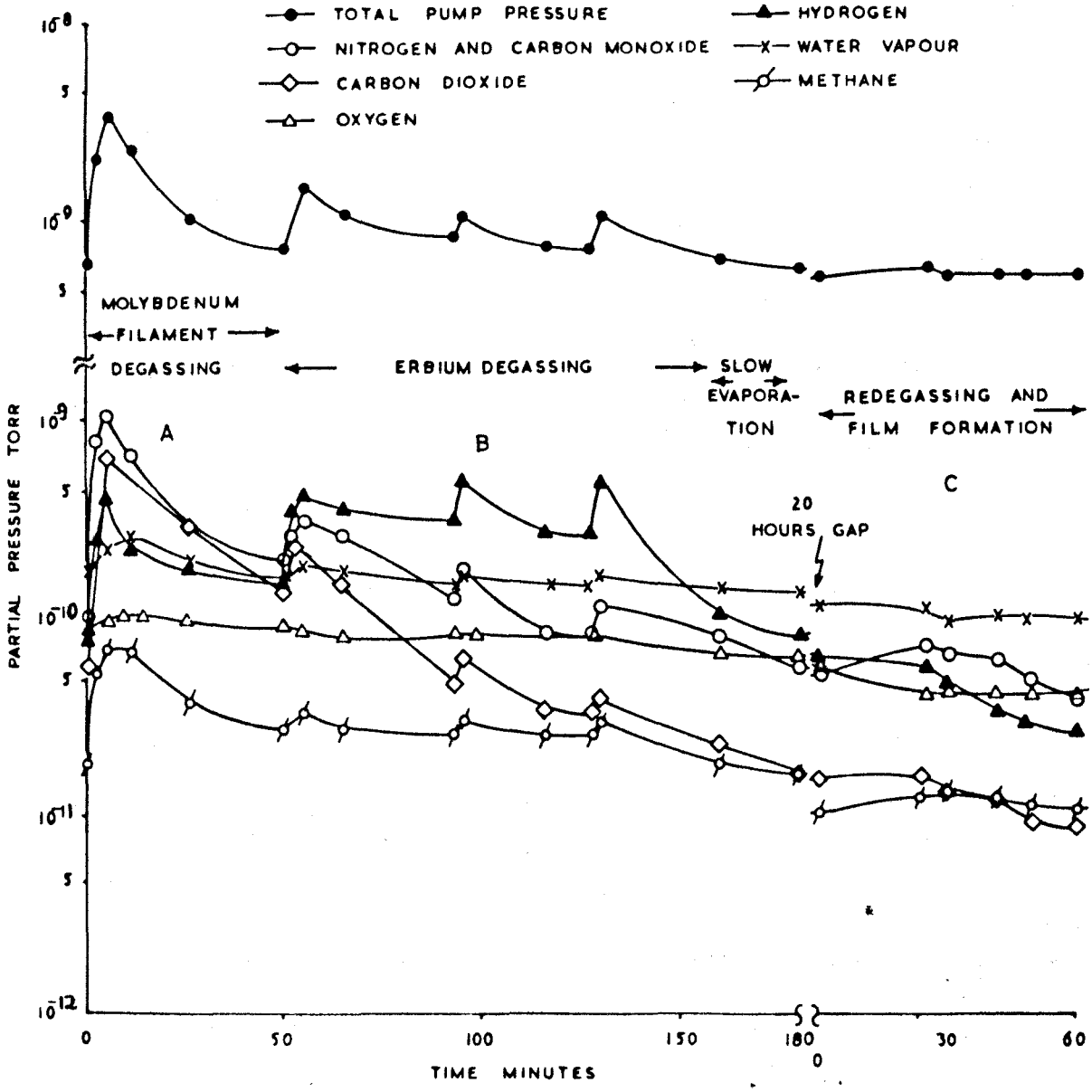

CHANGES IN PARTIAL PRESSURE OF RESIDUAL GASES DUE TO EVAPORATION OF ERBIUM FROM MOLYBDENUM FILAMENT (GAS ADSORPTION SYSTEM).

Figure 23

CH_4 and CH_3 and OH ions (mass No. 15 and 17) decreased slowly and H_2, CO_2, A and water vapour much more rapidly. After evaporation, oxygen and nitrogen remained almost constant in their concentration, while the partial pressures of other gases like CH_3, CH_4 and argon decreased slowly. Hydrogen, on the other hand, decreased much more rapidly and attained its lowest pressure within a period of about fifteen minutes. It therefore appears as if, erbium prefers hydrogen to form hydrides rather than oxygen to form oxide, but the considerable increase of hydrogen pressure, due partly to its liberation from pre-absorbed erbium and from impurity in tantalum, and partly from decomposition of water vapour, suggests that probably the oxygen also liberated from water decomposition might have already oxidised the erbium.film. Hydrocarbons CH_4 and CH_3 (m/e = 15) have also been observed to a little extent during evaporation, these have probably been formed due to the carbon impurity in the metal and the hydrogen availability.

After about half an hour of evaporation, the concentration for all gases became stable and it remained almost constant for many hours, except for hydrogen for which a slow increase was observed, probably due to desorption of it from the walls of the vacuum chamber. Thereafter concentrations of all gases continued to increase slowly, but did not attain the original concentration i.e. that before evaporation for forty eight hours of observation.

5.4(2) Molybdenum filament source

A molybdenum filament was used for depositing films for the adsorption study. In Fig. 23 are shown the partial pressures of residual gases, where three distinctive stages A, B and C represent filament degassing, erbium degassing and the film formation respectively. During the filament degassing, the concentration of all residual gases increased. After pumping for about an hour, the current in the

filament was increased and degassing of erbium started. During the degassing of the metal, hydrogen increased all the time, nitrogen (and/or carbon monoxide) and carbon dioxide increased but were soon pumped out, while methane and water vapour remained practically constant. During evaporation of the metal, partial pressures of all gases decreased, and hydrogen concentration underwent a maximum change. Changes in oxygen concentration were insignificant and its partial pressure was small (10^{-11} - 10^{-10} torr).

5.5 Conclusion

It is not easy to interpret these results with several gases initially present at the same time, e.g. the apparent lack of affinity for oxygen could represent a roughly equal rate of sorption of oxygen and dissociation of water vapour. A new apparatus was therefore constructed in which the film can be isolated from the pump, and the pressure differences measured when known volumes of pure gases (hydrogen and oxygen) are allowed to react with the film. The mass of the film is estimated by physical and chemical methods, and its surface area by the B.E.T. and Point B methods, so that a distinction could be made between monolayer adsorption and bulk solution of gases.

The second part of this thesis describes the electrical conductivity changes due to the pure gas interactions with the erbium films in this new system.

PART TWO

THE CHANGES IN RESISTANCE OF ERBIUM FILMS OWING TO THE SORPTION OF GASES

CHAPTER VI

SURFACE PHYSICS

6.1 Introduction

The physical and chemical behaviour of solids is influenced by their surface conditions. For example, the electronic properties of a single crystal are altered near its surface, because its periodic structure ends abruptly there. Also, the unsaturated bonds of the surface atoms make them much more reactive chemically then the atoms in the bulk.

Electronics is almost entirely based on the control of electrons emitted from surfaces or crossing junctions in thermionic and solid state devices. The catalytic action of surfaces is important in most chemical industries. The gases and vapours are adsorbed on the surface of the catalyst, react there, and finally the products desorb from the surfaces. The activity of certain catalysts has been explained by correlating the surface and internal structure of the catalyst with the molecular structure of the reactants.

From both the scientific and technical points of view, it has become important to study surface conditions and bulk properties of materials, and how these change when exposed to different gas environments.

6.2 Bulk and surface behaviour of solids

Atoms and molecules kept far from each other have ideal distributions of electrons and maintain their individuality. When these atoms or molecules come sufficiently close together, they interact with each other and their electronic energy levels are disturbed. The amount of disturbance depends on the position of

the atom with respect to others, and as an example consider a solid. An atom inside the solid undergoes a much larger and more symmetrical change in its electron energy distribution because of its being completely surrounded by the other neighbouring atoms, as compared to one in the surface plane which is only partially surrounded by atoms. Evidently, the atoms on the surface of a crystal have an electronic environment different from that in the interior of the material. Hence certain properties of the surface atoms will differ from those of the interior ones.

It is not only that the properties of the surface atoms differ from those inside the bulk, but the surface atoms themselves differ from each other also in certain respects depending on the surface plane in which they are situated, as atoms in different surface planes have a different number of neighbouring atoms. Consider the commonly occurring hexagonally closed packed structure, the atoms inside the crystal are surrounded by twelve neighbouring atoms, but atoms on different surface planes have different numbers of nearest neighbours. Atoms on a densely populated plane have the largest number of neighbouring atoms.

Both the physical and chemical properties of a surface differ from the bulk and from one crystal plane to another. The dynamical properties of the surface atoms are different from those of the atoms in the bulk of the crystal. Low energy electron diffraction results indicate[57] that the thermal vibrational amplitude of surface atoms normal to the surface is greater than the vibrational amplitude of atoms in the bulk of nickel crystals.

The emission of electrons from a surface is dependent on the orientation of the surface to the crystal lattice, that is different planes of a crystal have different work function values. For example,

it has been observed that for tungsten the work functions of different planes differ by 1.5 eV, from 4.30 eV for the (116) plane to 5.80 eV for the (011) plane[58].

In chemical reactions different crystal planes of a clean surface may act like different substances. Molecular nitrogen is dissociated and then strongly adsorbed by a clean tungsten surface. The efficiency of this dissociation and adsorption varies considerably from one plane to another[59, 60]. At room temperature the tungsten plane (110), which is the most densely packed does not cause the dissociation and adsorption of nitrogen while the other less densely packed planes are covered with nitrogen.

6.3 Techniques used in the study of surfaces

Techniques used in the study of surfaces could be classified in two categories, the first of which involves the direct or visual study of surfaces and the second involves the indirect study.

The techniques used for the visual study of surfaces observe the effects of particles and electromagnetic radiations emitted or reflected by the surfaces. Until about 1930, the optical microscope was one of the most powerful instruments used in probing surface structures. Late in 1933 Ruska developed a two stage electron microscope with a magnification of 10,000 and resolving power of 500 Å. Modern electron microscopes have a resolving power that is limited to about 5 Å. Such microscopes possibly resolve the atomic lattices of large spacing but not the individual atoms. Field emission microscopes have still higher resolving power and could possibly resolve individual atoms of certain material surfaces.

Low energy electron diffraction (LEED) and Auger spectroscopy are also useful techniques for studying surface conditions of solids.

Measurement of the work function is another tool for investigating the surface characteristics of metals. A slight impurity on a surface i.e. foreign charged particles, could be easily detected by measurement of the work function as it is greatly influenced by these alterations. A review of techniques, with a comprehensive summary of changes in the electronic surface potential of solids on adsorption, has been given by Culver and Tompkins[61], and recently Rivière[62] has reviewed experimental methods of measurement and values of absolute work function of bare metals.

Thin metal films deposited on non-conducting substrates in vacuum provide surfaces for investigation, and if their thickness is of the order of 50 to 80 atomic layers then their electrical resistance measurement may also be used as an indirect means of studying their surface characteristics. There is always a change in the electrical resistance of thin films when these adsorb gases[63]. At room temperature the changes are small, but if the surface to volume ratio of the films is large it may become of the order of 5% for most of the gases. The technique has the added advantages of not changing the surface under investigation, and so can be used to monitor surface reactions.

It is therefore possible to determine from conductivity measurements some of the characteristics of surfaces and how these change as a function of temperature, gas adsorption and crystal orientation. When possible, it is an advantage to use two or more methods to study a particular surface.

As the subject of this research is the measurement of conductivity and adsorption, these will be discussed in detail in the next chapter.

6.4 Mode of production of films, and factors determining surface characteristics

The characteristics of surfaces have been studied under what were considered to be identical conditions, but even until recently, the reproducibility of the experimental results has been extremely poor. In the case of vapour deposited films this lack of agreement was due partly to the residual gases adsorbed by the surfaces and incorporated in the film material during condensation, and partly to their unknown structure.

The residual atmosphere may affect the nature of a surface in two ways. Firstly, the presence of a gas atmosphere during the growth of a thin film can modify the internal structure of the film as the gas atoms would be taken down with the metal atoms if the rate of deposition is slow. Secondly, there is the effect of surface contamination. The residual gases may be adsorbed or may form chemical compounds and they may even diffuse into the bulk material. These would change many of the film properties like the electrical conductivity and work function. Due to the exothermic nature of adsorption, the films may even be sintered if considerable amounts of reactive gases like oxygen are present.

The properties of surfaces are dependent on their microscopic geometry, rough and smooth surfaces of the same material will have different chemical and physical properties. It has been discussed in Section 4.2 how the microscopic structure of a surface depends on its method of production, e.g. for vacuum deposited films on the deposition variables like the rate of deposition, substrate temperature and the nature of the substrate etc. It is difficult to measure the roughness of a surface in an absolute sense, however, it is generally expressed as a "surface roughness factor", which is defined as the ratio of the actual to the geometrical area.

The crystalline properties of films also vary as a function of film thickness, i.e. the nature of the surface is greatly influenced by the nature of the underlying layers and the substrate. The surface microstructure of a substrate can influence the structure of a deposited film i.e. the deposited surface in contact with the crystalline substrate may orient itself to the same crystal plane as exposed by the substrate. This phenomenon of oriented intergrowth between two crystalline materials is called epitaxy.

Film surfaces are highly susceptible to temperature. The process of decreasing the surface area by heating is called sintering. Probably the most common cause is growth in particle size. High temperature causes the small particles composing the film to fuse together into larger ones. This results in a decrease of the surface area. There are other factors besides crystal growth that may bring about sintering. Heating a film to a high temperature may alter not only the extent of its surface area but also the structure. For example, one type of developed crystal face may be replaced by another. Brunauer and Emmett[64] investigated the effect of sintering an iron catalyst on the chemisorption of different gases. Their explanation of their results was that the heat of chemisorption released causes sintering, which does not merely reduce the total surface but also changes loosely packed crystal planes like the (111) face of iron into densely packed planes like the (110) face.

Since the use of too high temperature injures the surface, the films should always be prepared at a fairly low temperature. Too low temperature would result in porous and amorphous film surfaces.

CHAPTER VII

ADSORPTION AND ELECTRICAL CONDUCTION

7.1 Introduction and nature of adsorption

The phenomenon of adsorption was discovered more than a century and a half ago. The uptake of gases by charcoal was first described by C.W. Scheele in 1773 and by A.F. Fontana in 1777.

When a gas or vapour is brought in contact with a solid or liquid surface, the concentration of gas molecules is always found to be greater in the immediate vicinity of the surface than in the free gas phase. This tendency of accumulation of molecules at the surface is called adsorption. Solid surfaces kept in vacuum are very susceptible to this phenomenon.

The atoms or molecules constituting the solid are held together by various forces, namely electrostatic or Coulomb forces, exchange or homopolar valence forces, etc. Whatever the nature of the forces, an atom located inside the body of the solid is subjected to equal forces in all directions, whereas an atom in the plane of the surface is subjected to unbalanced forces, the inward pull being greater than the outward force. This results in a tendency to decrease the surface (a solid has surface tension, similar to a liquid). Any process that tends to decrease the free surface energy (the product of the surface tension and the surface area) occurs spontaneously. Adsorption of gas atoms and molecules saturates some of these unbalanced forces at the surface, thereby decreasing the surface tension. Thus the adsorption phenomenon is spontaneous and results in a decrease of the free energy of the system (ΔF). Prior to adsorption the gas molecules move freely in all three dimensions, but on adsorption they are either held rigidly to the surface or confined to move over the surface in two dimensions and thus lose

degrees of freedom, consequently adsorption is accompanied by a decrease in entropy. Then it follows from the equation

$$\Delta H = \Delta F + T\,\Delta S \qquad (7.1)$$

that ΔH is negative. This means that the adsorption process is exothermic. This decrease in the heat content of the system is called the heat of adsorption. As the adsorption process is always exothermic, the amount adsorbed at equilibrium must always decrease with increasing temperature, according to the principle of Le Chatelier.

The strength of binding forces between the two phases (the solid and gas) depends on many factors such as the nature of substances, temperature, etc. It may be a weak interaction, similar to condensation, or a strong interaction, similar to chemical reactions. The former is called physical adsorption (physisorption) and the latter chemical adsorption (chemisorption).

Physical adsorption is caused by molecular forces also called van der Waals forces. The van der Waals forces are those which give rise to the constant "a" in van der Waals equation:

$$\left(p + \frac{a}{v^2}\right)(v - b) = RT \qquad (7.2)$$

These include: (1) attraction forces caused by the polarization of molecules by static dipole or quadrupole fields of other molecules i.e. Debye's induction effect[65] of 1920; (2) the forces between molecules possessing permanent dipoles or quadrupoles, hence Keesom's alignment or orientation effect[66] of 1921; and (3) the non-polar van der Waals forces (fluctuating forces), also called the dispersion forces, since London[67] discovered the close connection between their nature and the cause of optical dispersion. Including also the

forces between a solid surface and dipole molecules i.e. the electrostatic induction of atoms or molecules by solid surfaces in the definition of van der Waals forces, the energy for physisorption may be put as

$$E_{\text{phys. ads.}} = E_{\text{disp.}} + E_{\text{per. di-quadrupole}} + E_{\text{ind. pola.}}$$

An alternative to the induced polarization, the hypothesis of charge transfer no bond interaction of the type originally developed by Mulliken[68] for complex organic molecules, has also been suggested by Mignolet[69] for physisorption of non-polar molecules and inert gas atoms. The simple picture of physisorption[70] includes all cases in which neutral atoms or molecules interact with surfaces without sharing of electrons taking place, or without exchanging of electrons, thus preserving the individuality of the adsorbed neutral atoms or molecules.

Chemisorption involves sharing or transfer of electrons between the solid (adsorbent) and the gas (adsorbate). The process essentially involves the formation of a chemical compound between the adsorbate and the outermost layer of adsorbent atoms.

The theoretical distinction between the two types of adsorption is therefore clearcut, that electron transfers take place between adsorbent and adsorbate in chemisorption, but do not take place in physisorption. There are certain other differences in the properties of the two kinds of adsorption, namely the heat of adsorption, range of temperature and pressure, activation energy etc, which may be used to decide which type of adsorption is operating[71], but they are often difficult to apply in practice. There is some evidence that the solid surface may not be inert during physisorption, and it affects the arrangement of the adsorbate molecules (see Section 8.3).

Both the phenomena of physisorption and chemisorption are the subjects of the present work, the former for the measurment of true surface area of metal films and the latter for the conductivity changes on adsorption, and thus will be discussed later in detail.

7.2 Conductivity and adsorption

Generally it has been observed that the electrical conductivity of an adsorbent is changed when a gas is adsorbed. These changes are small, amounting to less than 5% for most gases so far studied. Both increases and decreases of conductivity have been observed: but neither can be accounted for by the slight extra conductivity of the layer of adsorbed gas, because the former are too large and the latter are in the wrong sense. These changes are therefore attributed either to (i) exchange of electrons between adsorbent and adsorbate or (ii) modification in surface structure and/or redistribution of charged particles in the adsorbent.

Several measurements have been made on the effect of gas adsorption on the electrical conduction of semiconductors and metals.

Both physical and chemical adsorption have been found to change the electrical conduction of semiconductors. Changes in electrical conductivity due to physical adsorption were reported by Elovich and Margolis[72] for hydrogen, oxygen, carbon monoxide, carbon dioxide, methane and benzene on manganese dioxide, and by Smeltzer and McIntosh[73] for varieties of vapours, gases and hydrocarbons on activated carbon rods. The observed changes in conductivity were explained by postulating that the presence of physically adsorbed molecules on the surface of the carbon semiconductor alters the number of conduction electrons rather than their mobility. Direct evidence of this was lacking, but theoretically it could be attributed to electrons being

trapped in surface states on the free surface of a semiconductor, emphasized by Bardeen[74]. In addition to the impurity levels in the interior of a crystal there may be localised states on the free surface with energies in the 'forbidden' region between the filled and conduction bands. These surface states arise as the surface atoms are in different condition from the bulk. Some of these may result from foreign atoms (i.e. adsorption) on the surface. The conductivity effect due to physically adsorbed vapours may thus be due to shifts of the equilibrium among electrons in surface states and in the conduction and valence bands of the semiconductors.

In spite of the general belief that physisorption does not change the resistivity of metals, some results have been reported[75], but their interpretation is not generally accepted.

7.3 Conduction of metallic films on chemisorption

The effect of chemisorption of gases on metals is usually studied by observing the changes in work function of the metal surfaces. The observed changes in work function on adsorption indicate only an electron shift to or from the adsorbent surfaces. But if the electrons of the adsorbed atoms or molecules become part of the conduction electrons of the metal, or if the free electrons of the metal become part of the electron shells of the adsorbed atoms or molecules, a change in the electrical resistance of the adsorbent will be observed in addition to a change in work function. Chemisorption being a monolayer interaction, the change in conductivity will be appreciable when the surface to bulk volume ratio is very large i.e. the adsorbent is very thin, of the order of 200 to 300 Å thick.

Changes in the electrical resistance of metal films due to chemisorption of different gases, at various equilibrium pressures and temperatures and on bare and pre-covered surfaces, have frequently been described[63], but the results are still in poor agreement.

Quantitative interpretations of the measured changes in electrical resistance on chemisorption have been made, and different models have been proposed to explain the mechanisms of resistance changes and the nature of bond formation i.e. gas-metal electronic interaction.

Some theoretical work has been primarily concerned with the nature of the bond between the adatom and the metal, the various possible sites for adsorption, and the interaction between the adsorbed atoms. It has only secondarily been concerned with the subsequent changes in film conductivity. Horiuti and Toya[76,77] have quantum-mechanically deduced two kinds of chemisorbed state i.e., r states and s states for hydrogen on metal surfaces. The r adatom is situated outside the electron cloud of the adsorbent and above a metal surface atom, and the nature of the interaction bond is similar to the covalent bond with slight negative polarization which increases work function. The resonance between the ground state of the r adatoms and the valence electrons of the metal surface atoms gives rise to considerable electron scattering, thus increasing the resistance of the adsorbent. The s adatom is interstitially located between the electronic surface and the layer of outermost metal atoms; it is dissociated into a proton and an electron in the conduction band of the absorbent, thus decreasing the resistance and also the work function of the latter. However, their theoretical expressions for the resistance change on adsorption due to a change in the nature of surface scattering seem to be invalid as they took a wrong expression for the film conductivity (see Appendix I).

Other theoretical work has been mainly concentrated on the mechanisms for changing the film conductivity, and then the observed magnitude of the changes in conductivity is quantitatively interpreted in terms of electronic interaction between the metal and adatoms.

No one theory has included all likely mechanisms, probably because there is such a variety of possibilities, including the following:

(i) Increase or decrease of the number of free electrons in the conduction band of the metal, due to electron transfer or sharing between the adsorbed gas atom and a metal atom of the surface; the gas atom may act as either donor or acceptor.

(ii) Change of the lattice spacing of the surface due to the formation of the gas-metal compound e.g. if the lattice spacing is increased sufficiently then the band structure of the surface may change from metallic to semiconducting.

(iii) A change in the specular reflection coefficient 'P' at the surface (see Section 1.3.1 on the F-S theory).

(iv) In polycrystalline films some gas atoms may not remain on the surface but may move along capillaries, grain boundaries and possibly dislocation lines which reach the surface, thus producing regions of high resistance between the micro-crystals of the films.

These possibilities are discussed below in the light of simple theoretical treatments and experimental results.

7.3(1) Change in the number of conduction electrons

The Fuchs-Sondheimer theory treats film conductivity (σ) in terms of its thickness (d) and electronic mean free path (ℓ_o) and is expressed as

$$\sigma = \frac{K}{\phi(K)} \sigma_o = \frac{K}{\phi(K)} \frac{ne^2\ell_o}{m v} \qquad (7.3)$$

where $K/\phi(K)$ is some function of $K = \frac{d}{\ell_o}$ as given in equation (1.3), and the other letters have their usual meaning. If it is assumed that the only effect of chemisorption is to alter the number of charge

carriers (n), and the other quantities d, m, e and ℓ_o remain the same, then the relative change in film conductivity ($\delta\sigma/\sigma$) is obtained on differentiating equation (7.3) and dividing, as

$$\frac{\delta\sigma}{\sigma} = \left[\frac{\delta n}{n} - \frac{\delta\bar{\nu}}{\bar{\nu}}\right] \qquad (7.4)$$

From the Sommerfeld theory, n and $\bar{\nu}$ are related by equation (1.1), and therefore

$$\frac{\delta\bar{\nu}}{\bar{\nu}} = \frac{1}{3}\frac{\delta n}{n} \qquad (7.5)$$

Combining equations (7.4) and (7.5) one gets

$$\frac{\delta\sigma}{\sigma} = \frac{2}{3}\frac{\delta n}{n} \qquad (7.6)$$

Thus theoretically a 3% change in the number of charge carriers will result in a 2% change in the film conductivity.

Suhrmann et al.[78] in 1957 found that the decrease in the film conductance $\Delta\sigma$ depends upon the number of gas molecules n_g adsorbed on the film (itself made up of N metal atoms) and was empirically expressed as

$$\frac{\Delta\sigma}{\sigma} = \alpha\frac{n_g}{N} \qquad (7.7)$$

where σ is the conductance of the clean film and α a small number. A significance was attached to the rationalised α values that each adsorbed molecule immobilises α conduction electrons. This led to considerable speculation concerning the nature of the chemical bond in

adsorption. The interpretation of α values calculated from the above relation (7.7) assumes that each adsorbed molecule has an equal effect on the film resistance i.e. the films are uniform and the grain boundary resistance is negligible. But as a rule, evaporated films are generally porous and their resistance is largely determined by the bridges or boundaries between the small grains. For such films the contribution of an adsorbed atom to the change in resistance will depend on its position on the film surface. Zwietering, Koks and van Heerden[79] have given an entirely different explanation for the resistance change on adsorption with such films. They suggested that each adsorbed atom withdraws an electron, which exerts a long range effect, extending over a distance comparable to an electron mean free path, hence adsorption on a massive grain could affect the resistance of the bridges or boundaries. They have deduced certain types of bonding between metallic film surfaces and chemisorbed gases by relating α values with the effective valency of the metal atoms and the number of chemical bonds formed per adsorbed molecule.

Ehrlich[80] has demonstrated from a theoretical expression that it is possible to understand the resistance changes of the magnitude observed experimentally without invoking the long range effect, by considering adsorption only on the bridges or grain boundaries of porous films. To bring the same change in resistance, a deactivation of only a small fraction of one conduction electron per adsorbed molecule on the bridges is required, instead of deactivation of 2-3 electrons per molecule when the adsorption is considered on the whole film surface.

7.3(2) Effective decrease in film thickness

It has been suggested that chemisorption of gases causes surface atoms to alter their spacing with respect to the bulk due to complex compound formation with surface atoms i.e. the wave functions of the metal surface atoms are disturbed, thus losing the property of

metallic conduction. Owing to this the surface layer is eliminated from the conduction process, which results in an effective decrease in film thickness[81,82].

Theoretically, resistance R of a film is inversely proportional to the product of its thickness d and conductivity σ, and is given by the equation:

$$R = \frac{c}{d\sigma} = \frac{c}{d\sigma_o} \frac{\phi(K)}{K} = \frac{c\bar{v}m}{ne^2\ell_o} \frac{1}{d} \frac{\phi(K)}{K} \qquad (7.8)$$

where C is a constant of proportionality. For thick films (K > 1), the function $\phi(K)/K$ reduces to $(1 + \frac{3}{8K})$ and thus the equation (7.8) simplifies to

$$R = \frac{c\bar{v}m}{ne^2\ell_o} \frac{1}{d} (1 + \frac{3\ell_o}{8d}) \qquad (7.9)$$

Now, if it is assumed that on chemisorption the surface atomic layer is eliminated from the conduction process i.e. the effective thickness of the film is decreased, then the relative change in film resistance due to a change in its thickness (assuming the other quantities remaining constant) is obtained by differentiating equation (7.9) with respect to thickness and dividing as

$$\frac{\delta R}{R} = - \frac{1+(3\ell_o/4d)}{1+(3\ell_o/8d)} \frac{\delta d}{d} \qquad (7.10)$$

From this it is apparent that a 3% change in thickness of a film with K = 2, will change its resistance by about 3.5%.

Geus[83] has qualitatively discussed the observed results for conductivity changes of tungsten and iron films due to the chemisorption of hydrogen, nitrogen and carbon monoxide in terms of the decrease in

the effective cross-section of the films and a change in the specular reflection coefficient 'P'.

7.3(3) Resistance change due to a change in surface scattering

On adsorption, the nature of a film surface and its surface potential are changed, and therefore a change in the surface property of electron scattering (i.e. specular reflection coefficient 'P') is expected. Since the resistance of a thin film is largely controlled by the diffuse reflection of the conduction electrons at the film surface, a change in the latter will significantly affect the resistance. Horiuti and Toya[76,77] have theoretically treated the problem of resistance change on hydrogen adsorption due to a change in the reflection coefficient 'P'. Unfortunately, their mathematical analysis seems to be invalid as they took a wrong expression for the film conductivity (see Appendix I). However, an approximate change in the film resistance due to a change in the reflection coefficient 'P' can be deduced from a simple expression as follows.

The modified form of equation (7.9) including the parameter 'P' for thick films (see eq. 1.6) is

$$R = \frac{cm\bar{\nu}}{ne^2\ell_o} \frac{1}{d} \left(1 + \frac{3(1-P)}{8K}\right) \qquad (7.11)$$

On differentiating this equation with respect to 'P' (assuming other quantities are independent of P and constant) and dividing, one gets

$$\frac{\delta R}{R} = - \frac{3}{8K+3(1-P)} \delta P \qquad (7.12)$$

From this simple expression a 5% change in the resistance could be demonstrated for a film with K = 2 and p = 0.3, if on adsorption the film surface is completely reduced to diffuse scattering.

7.3(4) Tunnelling conduction

The effect of adsorption on the tunnelling conduction mechanism is discussed theoretically by Ehrlich[80], in terms of a change in the rate of electron tunnelling across gaps between islands of a patchy film with a change in work funcion. A film will conduct by tunnelling if the thickness of the metal bridges (connecting the metal islands) and the gap width is smaller than 100 Å. The islands are not supposed to be completely isolated from each other (otherwise the individual islands would not be at fixed potential). For such a film, conductivity is expressed by equation 14 of the first chapter.

On adsorption the surface dipole layer on the walls of the gap, i.e. the work function, is changed and hence also the conduction across the gap. These two changes could be determined from logarithmic differentiation of the equation 1.14 with respect to ϕ. The result given much earlier by Ehrlich[80] is

$$\frac{\Delta\sigma}{\sigma} = \frac{\Delta\phi}{\phi}\,(0.5 - 4.63 \times 10^{7}\ \phi^{\frac{1}{2}}\ d) \qquad (7.13)$$

From this it can be easily seen that 0.1eV change in ϕ for a metal with a work function of 4.5eV would change the resistance by about 11% for a gap of 5 Å.

The change in conductivity of discontinuous metal films due to change in work function produced by chemisorption has been measured experimentally by Fehlner[84]. Substituting these two quantities in equation 1.14, he calculated the inter-island distance d, which was found to agree with the published value. Indirectly he established that the major contribution to the resistance change of a discontinuous film on adsorption is due to this mechanism.

7.4 Conclusion

Which mechanism predominantly contributes to the resistance of a continuous evaporated polycrystalline film is still ambiguous, due to the porosity and grain boundaries (possibility iv) found in these films. Hence unless this is elucidated, deductions concerning chemical bond formation and gas-metal interaction are difficult. However, from careful experimental results, the fractional change in resistance due to the number of adsorbed gas molecules per metal atom i.e. the α value can be calculated when certain assumptions are made that:

(i) The only effect of chemisorption is to change the number of conduction electrons and atoms. However chemisorption has other effects. Gases with high heats of adsorption, such as oxygen are known to cause considerable sintering of films even after they have been annealed, and this may affect the resistance of the films.

(ii) The conductivity is a bulk property of the metal, i.e. every film metal atom is assumed to contribute an equal amount to the film conductivity. This will be true when the contact resistance between the particles i.e. the grain boundary resistance is negligible and the films are uniform i.e. they are considered as slices of bulk metal.

The calculated α values could be interpreted in terms of the chemical bond between the adsorbed gas molecule and the metal atoms, if two further assumptions are made that:

(i) The adsorption takes place in a single mode which is the same on all exposed crystal faces. It will be valid when the gas is adsorbed either entirely as atoms or entirely as molecules and the adsorbed entity makes equal number of bonds with each site.

(ii) Each adsorbed molecule has an equal effect on the film resistance. It will apply when adsorption takes place mainly on the outer surface of the film, where all adsorption sites may be approximated

as equal in their effect on the film resistance.

In the light of these various possibilities, the changes in electrical resistance due to interaction of hydrogen and oxygen with erbium will be critically discussed in Chapter XI, and also to what extent these assumptions are justified in interpreting α values in terms of simple electronic interaction.

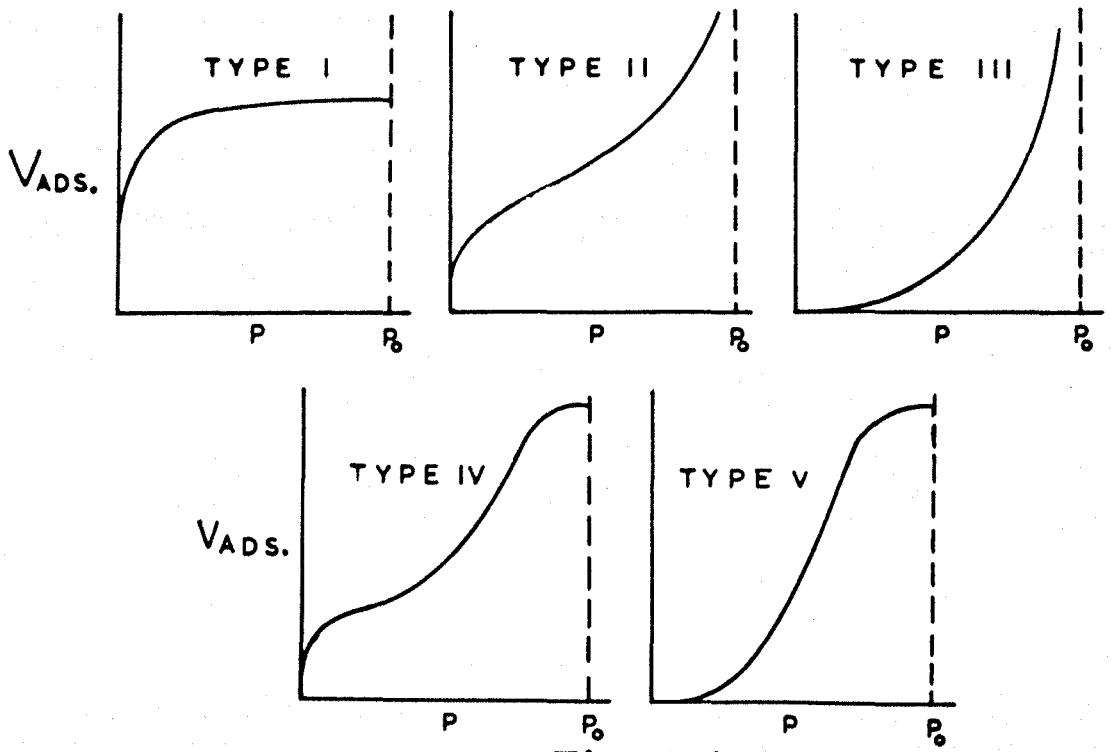

Fig. 24

THE FIVE TYPES OF PHYSICAL ADSORPTION ISOTHERM. P_0 IS SATURATION VAPOUR PRESSURE.

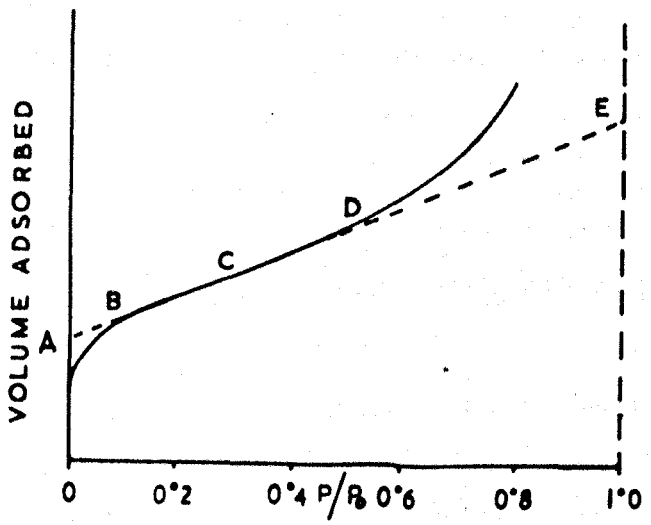

LOCATION OF THE POINT B AND OTHER ARBITRARY POINTS ON A PHYSICAL ADSORPTION ISOTHERM.

Figure 25

CHAPTER VIII

PHYSICAL ADSORPTION ISOTHERMS AND SURFACE AREA MEASUREMENTS

8.1 Adsorption isotherms

In adsorption studies the amount adsorbed v as a function of pressure p and temperature T may conveniently be plotted in the form of an adsorption isotherm

$$v = f(p)_T \qquad (8.1)$$

The amount of adsorbate adsorbed at equilibrium pressure depends on the nature of adsorbent and adsorbate, and below the critical temperature of the latter, p,v curves vary widely as reported by several authors, but following Brunauer et al.[85], these isotherms could be classified in five basic shapes shown in Fig. 24. Qualitative information about the adsorption mechanism, and a semi-quantitative measure of surface coverage of the adsorbate, have been drawn from the shape of these curves.

Type I are obtained for the systems where adsorption ceases after a monolayer is formed. The rest all represent multilayer adsorption. Type IV and V are obtained for the adsorption on highly porous adsorbents and the flattening of the curves at high pressures are attributed to a capillary phenomenon.

Adsorption data have also been plotted for pressure as a function of temperature, keeping volume constant, or for volume adsorbed as a function of temperature, keeping pressure constant. These curves are called adsorption isosteres and adsorption isobars respectively. Since the present experiments were performed at constant temperatures, only the isotherms are described in detail.

8.2 Some related definitions and analytical expressions for surface area measurements

An important application of physical adsorption is in estimating surface area and hence the surface roughness of the adsorbents. Before going into details of methods of surface area measurements, it would be better to define precisely the various definitions and terms involved.

The term specific surface area Σ attached to adsorbents is defined as the surface area per unit mass of the adsorbent. It is generally expressed in square metres per gram.

The monolayer capacity v_m, is defined as the quantity of adsorbate which would be required to cover the adsorbent with a monomolecular layer only. The definition is ideally defined, because observations have revealed that adsorption in the second and higher layers takes place before the first layer is completed. Hence v_m is numerically the total amount in the first, second or higher layers, such that the amount in the second and higher layers is just equal to the amount necessary to fill the vacant places in the first layer. It is commonly expressed as cubic centimetres at STP per gram of adsorbent. These two quantities just defined are related as

$$\Sigma = 0.269\ \sigma_m\ v_m \qquad (8.2)$$

where σ_m is the molecular area in square Angstroms, which one adsorbed molecule would occupy in the completed monolayer.

The true surface area of a film may be estimated by multiplying the number of molecules in v_m necessary to cover the given surface with a monolayer by σ_m of the adsorbate.

When an adsorbate is brought in contact with an adsorbent in vacuum, a part of the adsorbate is adsorbed, and part of it fills up the evacuated space surrounding the adsorbent and the pore spaces or capillary within the adsorbent. In order to know the real volume adsorbed (i.e. the real number of molecules adsorbed), it is necessary to know the volume of this "dead space". It is measured by using a gas that is not adsorbed at the experimental temperatures. Helium has been found most suitable for this purpose as no error could be introduced due to its adsorption at temperatures as low as liquid nitrogen temperature.

8.2(1) Surface area by the Langmuir isotherm equation

Up to the beginning of the year 1938, the Langmuir equation[86] was the only expression used for the estimates of v_m. The original equation derived by kinetic reasoning is given in the following form

$$\frac{p}{v} = \frac{p}{v_m} + \frac{1}{b\, v_m} \qquad (8.3)$$

where b is a constant. On plotting p/v versus p, a straight line would be obtained having slope $1/v_m$ and intercept $1/(b\, v_m)$.

The assumptions underlying this equation are as follows:

(i) Atoms or molecules of the gas are adsorbed as a whole onto definite points of attachment on the surface of the adsorbent.

(ii) Each point of attachment can accommodate one and only one adsorbed atom.

(iii) The energy of an adsorbed atom is independent of the site and of the presence or absence of other adsorbed atoms.

Although these asuumptions are unrealistic, the isotherm equation yields a very approximate value of v_m, but only for those

adsorbents exhibiting monomolecular adsorption i.e. type I isotherms. Hence the expression could not be applied to metal-like adsorbents which give multilayer physical adsorption. The Langmuir expression has been applied to calculate v_m values for the lower part of multilayer adsorption isotherms, but the results show poor agreements.

8.2(2) The Point 'B' Method

In an attempt to determine the surface area of an iron catalyst by physical adsorption of different gases, Emmett and Brunauer[87] in 1937 located five arbitrary points on their isotherms as shown in Fig. 25. Point A is the intercept of the linear portion of the isotherm when extrapolated to zero pressure, B the beginning, C the mid point and D the end of this linear portion. Point E is the intercept of the linear portion on extrapolation to the saturation pressure. Assuming that each point corresponded to v_m, the surface area was calculated from each isotherm. It was observed that the surface areas calculated from values corresponding to point B were deviating very slightly from the mean value. They also calculated heats of adsorption as a function of amount adsorbed using the Clausius-Clapeyron equation and concluded that point B corresponds to monolayer capacity.

Several investigators have attempted to use this Point B method for evaluating surface area and found more or less reliable agreement. Halsey[88] has attached a significance to Point B, that it is located where the affinity of the surface for the gas is changing most rapidly and later on he developed a mathematical analysis for the Point B method.

The Point B method gives a reliable estimate of surface area but it has major shortcomings, that at least five points are required on the isotherm and that these must be properly spaced over the range

of relative pressure, and secondly it is often difficult to know the exact location of point B on the wide knee.

8.2(3) The BET Method

Until 1938 there was no unified theory which could describe both the monomolecular and multimolecular layer adsorption isotherms. It was as the outcome of the generalisation of localised monolayer treatment that Brunauer et al.[89] derived the expression which is capable of describing type II and III isotherms, depending on the value of the constant involved in it, and is an analytical means of locating point B. The multimolecular adsorption theory of Brunauer, Emmett and Teller, in short known as BET theory, makes the following assumptions:

(i) Each molecule adsorbed in the first layer serves as a site for the adsorption of a molecule into the second layer, and so on.

(ii) Mutual interaction forces between adsorbate molecules are neglected similar to Langmuir's assumption.

(iii) The evaporation-condensation properties of the second and higher layers are the same as those of the surface of the bulk liquid adsorbate, which means apart from that of the first layer, the heat of adsorption of the second and higher layers is equal to the heat of liquification of the adsorbate ie.

$$E_2 = E_3 = - - - - = E_L$$

(iv) Arbitrarily, the surfaces of the adsorbents are assumed to be homogeneous.

Brunauer et al.[89] derived the equation on kinetic reasoning and in its simple or '∞' form is given below

$$\frac{p}{v(p_o - p)} = \frac{1}{v_m C} + \frac{(C - 1)}{v_m C} \frac{p}{p_o} \qquad (8.4)$$

where v_m has its usual meaning; v is the volume of gas adsorbed (reduced to STP) at a pressure p, p_o is the vapour pressure of the adsorbate at the temperature of the experiment, and C is a constant which depends on the energetic nature of the adsorbate-adsorbent, and on further simplification is given by

$$C = \exp (E_1 - E_L)/RT \qquad (8.5)$$

Equation 8.4 results a straight line on plotting $P/[v(p_o - p)]$ against p/p_o with a intercept of $1/(v_m C)$ and a slope of $(C - 1)/(v_m C)$. Thus from the BET plot, the surface area and approximate heat of adsorption can be calculated.

For the adsorption in capillaries and pores in the case of porous adsorbents, where the adsorption is restricted to a limited number of n layers instead of infinite, Brunauer et al.[85] derived a similar equation involving three unknown constants. This equation is sometimes referred to as BDDT equation and has been of primary importance in determining the surface area of highly porous solids.

The BET equation describes successfully both the II and III type of isotherms depending on the value of C. It has been shown that as C diminishes, the knee bend in type II isotherm occurs progressively nearer the origin until at a value of about 2, it coincides with it. This means transition from II to III will occur when $(E_1 - E_L)/RT \approx 0.7$. Thus it is easy to understand that when $E_1 >> E_L$, molecules will not be adsorbed into the second and higher layers until the first layer is filled and hence a sharp knee bend will be observed at $v = v_m$. The qualitative interpretation of type III isotherm on the BET basis is that when $E_1 << E_L$, molucules will tend to aggregate into clusters

several molecular layers thick leaving large gaps of bare surface. The theory is not applicable above the critical temperature of the adsorbate as the assumptions involved in its derivation do not hold. Also the forces of condensation are responsible for multimolecular layer adsorption, above the critical temperature a unimolecular layer exists.

8.2(3-a) Shortcomings of the BET theory from the point of view of surface area measurement

The BET theory, though based on oversimplified suppositions, very well describes the second type of isotherm within the relative pressure range of 0.05 to 0.3 for nitrogen, but below 0.05 and above 0.3 the theory predicts low and high adsorbed amounts respectively.

In its original derivation, the surface of an adsorbent has been assumed homogeneous i.e. all surface sites have the same potential energy. Practically, the surfaces of adsorbents (especially evaporated polycrystalline films) are inhomogeneous in nature. There are most attractive sites (the sites of low potential energy) where adsorption occurs first and the less active sites (where the potential energy is maximum) which come into play in the later stages of adsorption. It was suggested that at lower relative pressure i.e. at lower surface coverage inhomogenity plays the vital role and the BET theory deviates from the practical results. Zettlemoyer and Walker[90] introduced a rough idea of the surface inhomogenity in the BET theory by assuming adsorbent surfaces composed of two uniform patches, each characterised by a different C constant. Their theory fits fairly well the experimental data at lower coverages, but the equation becomes a three constant equation.

At relatively high pressures the first layer is presumably almost filled and then there is random distribution of piles of molecules in the second and higher layers. Due to this concentration

of molecules, the mutual interaction between the adsorbate molecules predominates, which has been neglected in the BET theory. Assuming that at relatively high pressure i.e. above two monolayers, all surface sites of the adsorbent are covered by the adscrbate and thus its inhomogenity is smoothed out, then for the incoming molecule the adsorbent surface will be taken as homogeneous. Taking also into account the lateral interaction, Frankel[91] (for the condensation of the vapour into a thin liquid film), and later independently Halsey[92] and Hill[93] developed a theory for adsorption isotherms, which conveniently fits the experimental results of higher coverages. The theory is known as the Frenkel-Halsey-Hill slab theory or in short FHH theory. The general form of this theory is a bit difficult to test but the simple version of it given by Halsey[92] could easily be tested.

Thus it seems that the BET theory fails to account for the observed isothermal data at lower relative pressure because of the surface inhomogenity, and at higher relative pressures because of the mutual interaction of adsorbed molecules. Hence in between these two extreme limits the contributions due to these factors probably mutually balance and the BET theory gives good agreement with the observed data.

Several other modifications in the BET theory have been made by taking into account the layer by layer decrease in heats of adsorption[94],and the decrease in the area available for adsorption in successive layers[95]. All these modifications involve some other parameter and are often difficult to test.

Whatever the physical basis, theoretical shortcomings and the range of its applicability, the theory is at its best in the middle adsortpion region i.e. in the range preceding and following the building up of a monolayer. This fact enables one to estimate the surface

area to a good approximation. For large values of the constant C, both the BET and Point B methods give agreeable results.

In surface area studies of practical adsorbents like molecular sieves and powders, nitrogen is widely used as an adsorbate at liquid nitrogen temperature, because of its high saturation vapour pressure (760 torr) at this temperature. The use of krypton as an adsorbate has been found successful[96] for the smaller surface area adsorbents. It has added advantages that the error involved in determination of the monolayer capapcity v_m is reduced as it occurs at lower equilibrium pressure, and also the range of equilibrium pressure for which the BET theory is valid lies between 10^{-3} and 10^{-1} torr, which is the range of an ordinary Pirani gauge.

8.2(3-b) Single point BET method for surface area measurement

For high values of C, (C - 1)/C reduces to unity and $1/(v_m C)$ reduces to zero, then the equation 8.4 becomes

$$\frac{p}{v(p_o - p)} = \frac{1}{v_m} \frac{p}{p_o} \qquad (8.6)$$

which means the BET plot passes through the origin and v_m can be calculated from the inverse of its slope. Thus only one experimental point is required. The above relation can also be arranged as

$$v_m = v\left(1 - \frac{p}{p_o}\right) \qquad (8.7)$$

Thus it is very quick and easy to estimate v_m from a single observation without the BET plot.

8.3 Modern views on physical adsorption

The main feature of recent physical adsorption studies has been direct experimental proof for the specificity of inert gas interaction with metal surfaces[97]. Specificity i.e. sensitivity to

surface structure of an adsorbent, has been recognised in many ways[97]; (a) by the change in the free energy of adsorption of an inert gas arising from, say, the pre-adsorption of hydrogen or carbon monoxide, i.e. by a change in the shape of the adsorption isotherm and different BET v_m values, (b) by observing different changes in work function when the same inert gas was adsorbed on different crystal planes of the metal and (c) by making use of the field emission microscopic and low energy electron diffraction (with carbon adsorbents) studies of physically adsorbed surfaces.

This specific nature of the physical adsorption of inert gases had made methods of surface area measurement complicated. The application of the BET equation to physical adsorption isotherms has been extensive, but this basically ignores the specific nature of physical adsorption and assumes close packing of adatoms on the surface. In order to obtain absolute surface area values the monolayer capacity must be multiplied by the cross-sectional area of the adsorbed molecule. This is usually determined either directly from the liquid or solid packing of the adsorbate, or indirectly by comparing its v_m value with that of some standard adsorbate for a given adsorbent and taking a known value of the cross-sectional area σ_m of the latter. Brennan, Graham and Hayes[98] have suggested that the determination of cross-sectional areas by these methods is incorrect and that their data indicate an equal number of adatoms of krypton and xenon adsorption on the same surface i.e. a consequence of topographical specificity. Anderson and Baker[99] refer to adsorption at surface sites as a lattice packed monolayer. Ehrlich and Hudda[100], and Rootsaert et al.[101] (by field emission microscopic studies), and recently Lander and Morrison[102] (by low energy electron diffraction) have demonstrated the importance of the co-ordination number of a substrate site in the adsorption of the inert gases. The relatively large energy of activation for

surface diffusion observed for krypton and xenon on tungsten[101] and different work function values of argon, krypton and xenon on individual crystal faces of tungsten[103, 104] are further evidence that these adatoms are located on surface sites.

The different σ_m (Xe) values estimated[105] earlier on different adsorbents i.e. 20.2 $\AA^2$ on carbon black, 18.2 $\AA^2$ on silver iodide and 27.3 $\AA^2$ on anatase (using nitrogen as the reference adsorbate with σ_m (N_2) = 16.2 $\AA^2$ and adopting the BET method), are perhaps the results of specific adsorption of xenon on these different adsorbents. Hence it is born out from these results that in estimating a surface area by physical adsorption of inert gases and applying the BET method, the appropriate value, that is called the best value of cross-sectional area, must be assigned to the adsorbate molecule for the given surface.

CHAPTER IX

THE SECOND VACUUM SYSTEM, EXPERIMENTAL DEVELOPMENTS AND PROCEDURE

9.1 Introduction

A clean surface when exposed to open atmosphere is subjected to 3×10^{23} molecular impacts per square centimetre per second. Some of the atoms or molecules remain associated with the surface while others rebound elastically. The process of adsorption continues until the surface is covered with many layers of molecules. The time taken for a monolayer to form on the surface is inversely proportional to the surrounding pressure. For nitrogen at a pressure of one torr the time taken to form a monolayer is roughly 10^{-6} sec, at a pressure of 10^{-10} torr it is approximately five hours. Therefore for the experimental study of adsorption of gases with metal films, an ultra-high vacuum of the order of 10^{-9} torr or less is desired to allow sufficient time to take the observations before the film is contaminated by the residual atmosphere. Hence, the material for the construction of a vacuum system should be so chosen that its vapour pressure should be as small as possible.

9.2 The vacuum system

The study of adsorption by erbium films was made in a stainless steel vacuum system, evacuated by sorption and sputter-ion pumps. A sketch of the vacuum system used is shown in Fig. 26. The ion pump (FJD 50) was first connected to a stainless steel cross-piece, the other three ends of which were separately connected to a mass spectrometer (Vacuum MS10) head, an extension for sorption pump via bakeable and non-bakeable metal valves, and through a wide stainless steel valve to an adsorption vessel. The mass spectrometer provided

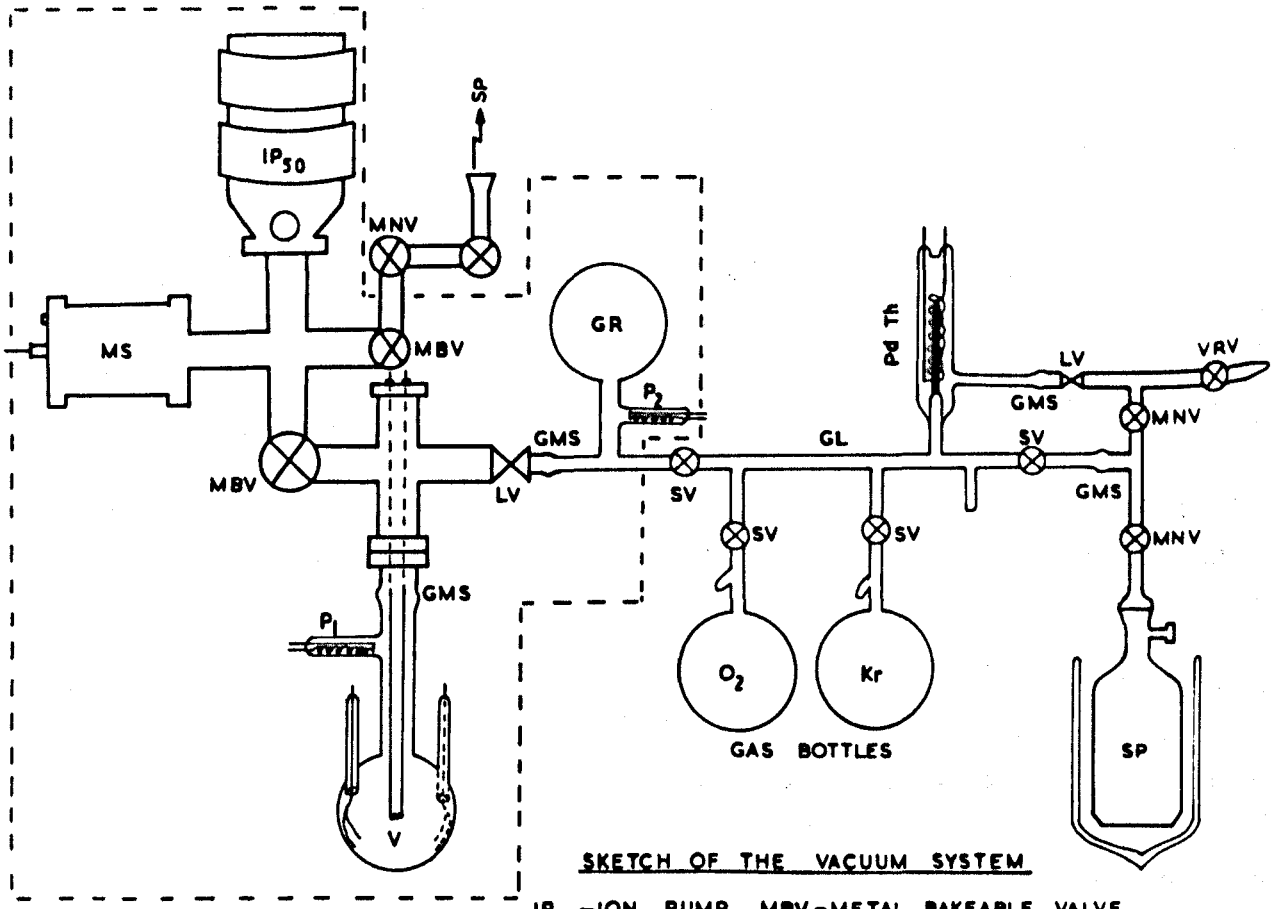

SKETCH OF THE VACUUM SYSTEM

IP_{50} – ION PUMP, MBV – METAL BAKEABLE VALVE, GMS – GLASS METAL SEAL, $P_{1,2}$ – PIRANI GAUGES, LV – LEAK VALVE, MS – MASS SPECTROMETER, MNV – METAL NON BAKEABLE VALVE, GR – GAS RESERVOIR, GL – GAS LINE, SV – SPRINGHAM VALVE, Pd Th – PALLADIUM THIMBLE, SP – SORPTION PUMP, DOTTED BOUNDARY – BAKEABLE TO 250°C.

Figure 26

useful information about the constitution of the residual atmosphere and the partial pressure of individual gases. The wide metal valve separated the ion pump from the adsorption vessel when pure gases were introduced into it for adsorption by the film. The adsorption vessel was joined to this valve via another stainless steel cross-piece, the opposite end of which was used for providing electrode feedthroughs for an evaporation filament, and the remaining end to a bakeable leak valve. Doses of pure gases were introduced into the adsorption vessel from a gas reservoir by briefly opening and then closing this leak valve. All the metal components were joined together with "Conflat" flanges and copper gaskets. This manifold was placed on a thick asbestos sheet on the top of a table made from Dexion angle-iron, and under a baking oven.

A gas handling system was joined to the high vacuum system via a glass to metal seal next to the metal leak valve. This gas handling system was constructed from pyrex glass, and high vacuum greaseless Springham valves were used. A 250 ml spherical pyrex vessel was used as a gas reservoir (GR), in which gases taken from pure gas bottles (British Oxygen Co., grade X) were expanded. To measure the pressure of this expanded gas a bakeable Pirani gauge was attached to this reservoir. The reservoir was joined to a gas line (GL) via a Springham valve, and each gas bottle was joined to this gas line via another Springham valve. Hydrogen, purified by passing through a heated palladium thimble, could also be admitted to this gas line, and the other end of this line could be connected to a sorption pump or rotary pump in order to evacuate it, as shown in Fig. 26. To avoid the possibility of explosion due to mixture of atmospheric oxygen with hydrogen, the thimble envelope was first evacuated by the sorption pump to a pressure of about 10^{-3} torr and then hydrogen was introduced into it under a pressure not exceeding 5.0 cms of mercury

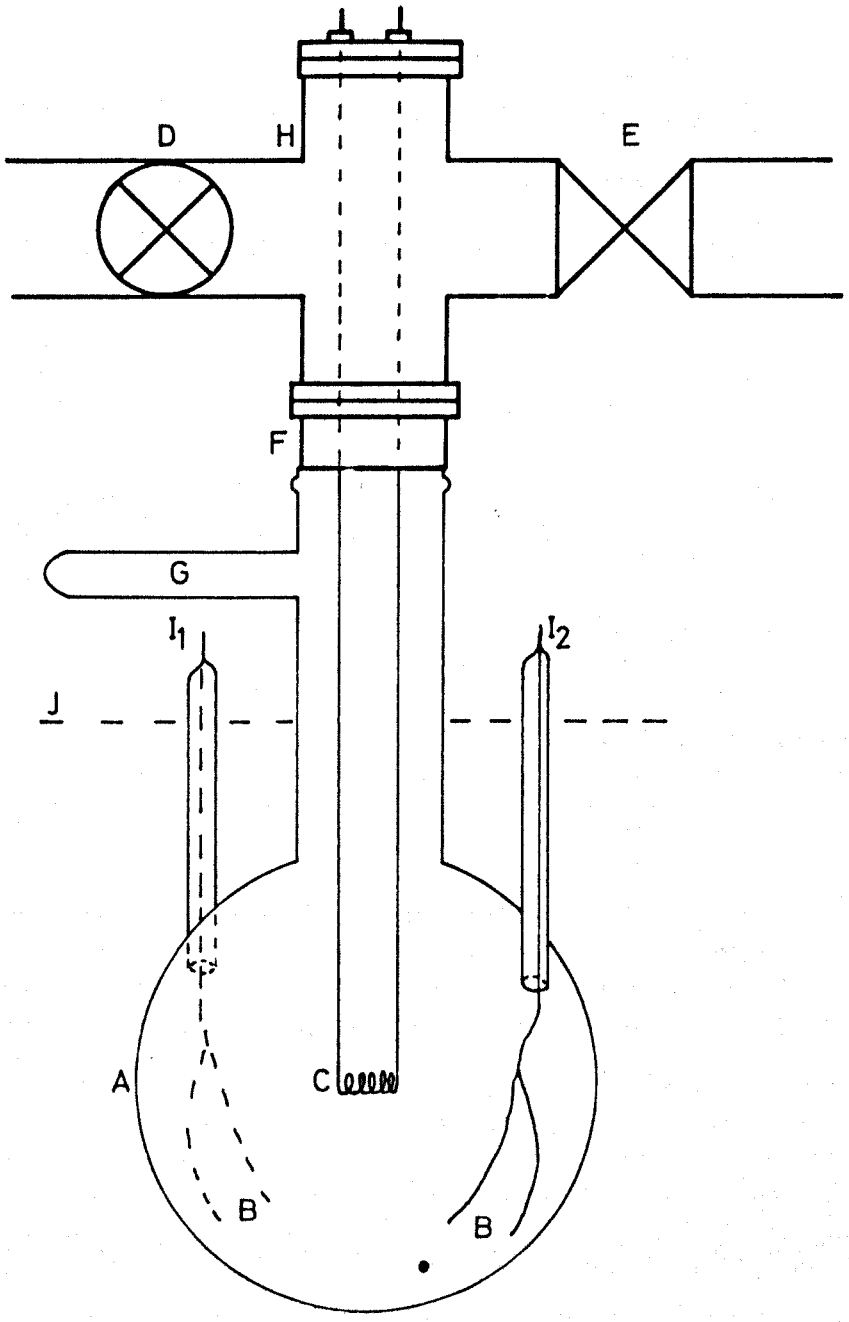

Figure 1 Pyrex adsorption vessel. A 500ml pyrex sphere. B platinum wires.
C molybdenum helix. D bakeable valve. E bakeable leak-valve.
F glass to metal seal on stainless steel flange. G pirani gauge.
H stainless steel crosspiece. I_1, I_2 film resistance terminals.
J liquid bath level.

Figure 27a

column above the atmospheric pressure. After the purified hydrogen was collected in the reservoir, the residual gas in the thimble envelope was pumped out. Inert gases are not pumped by the ion pump, so such gases were pumped by the sorption pump after the adsorption study was over. The sorption pump is inactive for many gases like hydrogen, neon and helium; these gases were pumped by an oil filled rotary pump, which was attached to the gas handling system via an 18" long stainless steel flexible tubing and a metal liquid nitrogen trap.

The adsorption vessel and the reservoir were pumped by the ion pump to a pressure of 10^{-9} torr, or less, and the gas line was pumped by the chilled sorption pump to a pressure of 10^{-3} torr. Before the gas was expanded in the reservoir, the gas line was evacuated many times and flushed with the pure gas.

9.3 Construction of the adsorption vessel

A 500 ml spherical pyrex flask was chosen as an adsorption vessel. Because of its spherical geometry a metal film deposited on the inside wall of it by a molybdenum filament (C) at its centre will be of uniform thickness. A simple diagram of the adsorption vessel is shown in Fig. 27a. To make electrical contact with the experimental film for measuring its resistance, two thin platinum wires (B, 0.3 mm in diameter) in 'V' shape were fused into the inside wall of the vessel. The tip of each inverted 'V' was then joined to a glass-tungsten seal via a thick nickel wire. These glass-tungsten seals were attached to two glass limbs of about ten cm long. After fusing these platinum electrodes, the vessel was annealed at 550°C overnight. This vessel was then joined to a removable $2\frac{3}{4}$" stainless steel flange via a glass-metal seal. A bakeable Pirani gauge was attached to the neck of this vessel for measuring the pressure of reacting gases. Two such identical adsorption vessels were made, which are shown in photograph 27b.

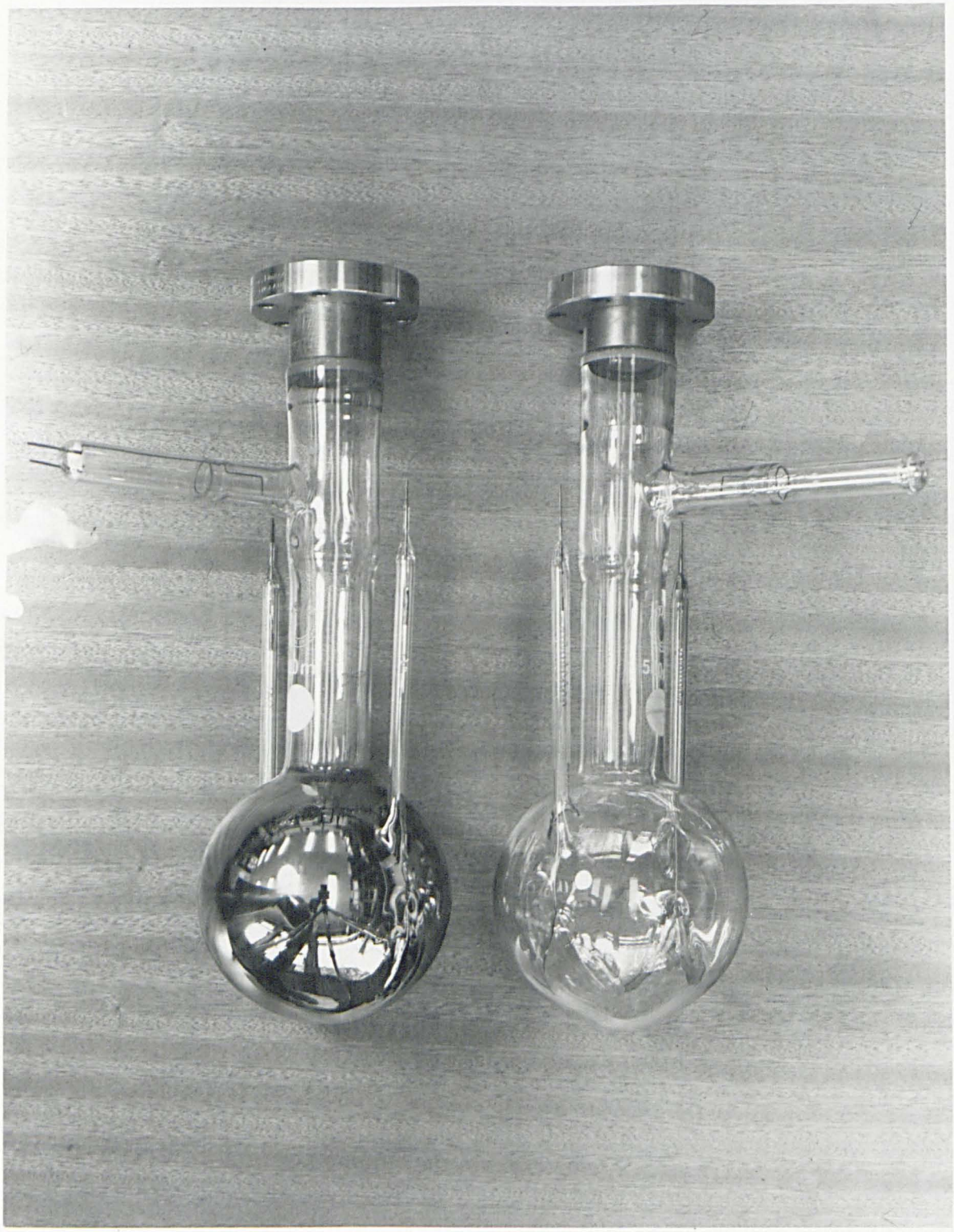

Photograph of the adsorption vessels.

Figure 27b

In the first experiment, one adsorption vessel failed to make electrical contact with the film. It was noticed that the film cast a shadow along the contact wires, as the latter were not properly fused into the glass wall and were resting on the inner surface. Thus good electrical contacts were obtained in this adsorption vessel when these platinum wires were refused and were painted with liquid platinum (Matthey Bright Platinum GA) and fired at about 500°C.

With this vacuum system and the adsorption vessels many successful experimental runs were performed, but some technical difficulties arose. The mass spectrometer was used near the pump (without any valve in between) and not on the side of the gas reservoir. With this arrangement the purity of the incoming gas could not be checked before its adsorption by the film. Also, the long metal cross-piece next to the ion pump reduced its pumping speed and it took a long time to pump the reservoir through the narrow orifice of the leak valve. Secondly, the Springham valves, used in the gas handling system, were good on the high vacuum side but they had a high leakage rate on the other side. The gas bottles, after being opened and kept for a long time, were found to be contaminated with the atmospheric gases and thus needed frequent replacement, so it was desirable to have some better quality valves. Finally, both the Pirani gauges on the adsorption vessel and gas reservoir were calibrated at room temperature, but when the adsorption vessel was placed in a low temperature bath, the attached Pirani gauge was found to read a slightly different pressure than the true pressure. Probably it was cooled due to cold draughts from the low temperature bath, and its compensating resistor was at room temperatree. Keeping these problems in view, the whole vacuum system was redesigned and improved.

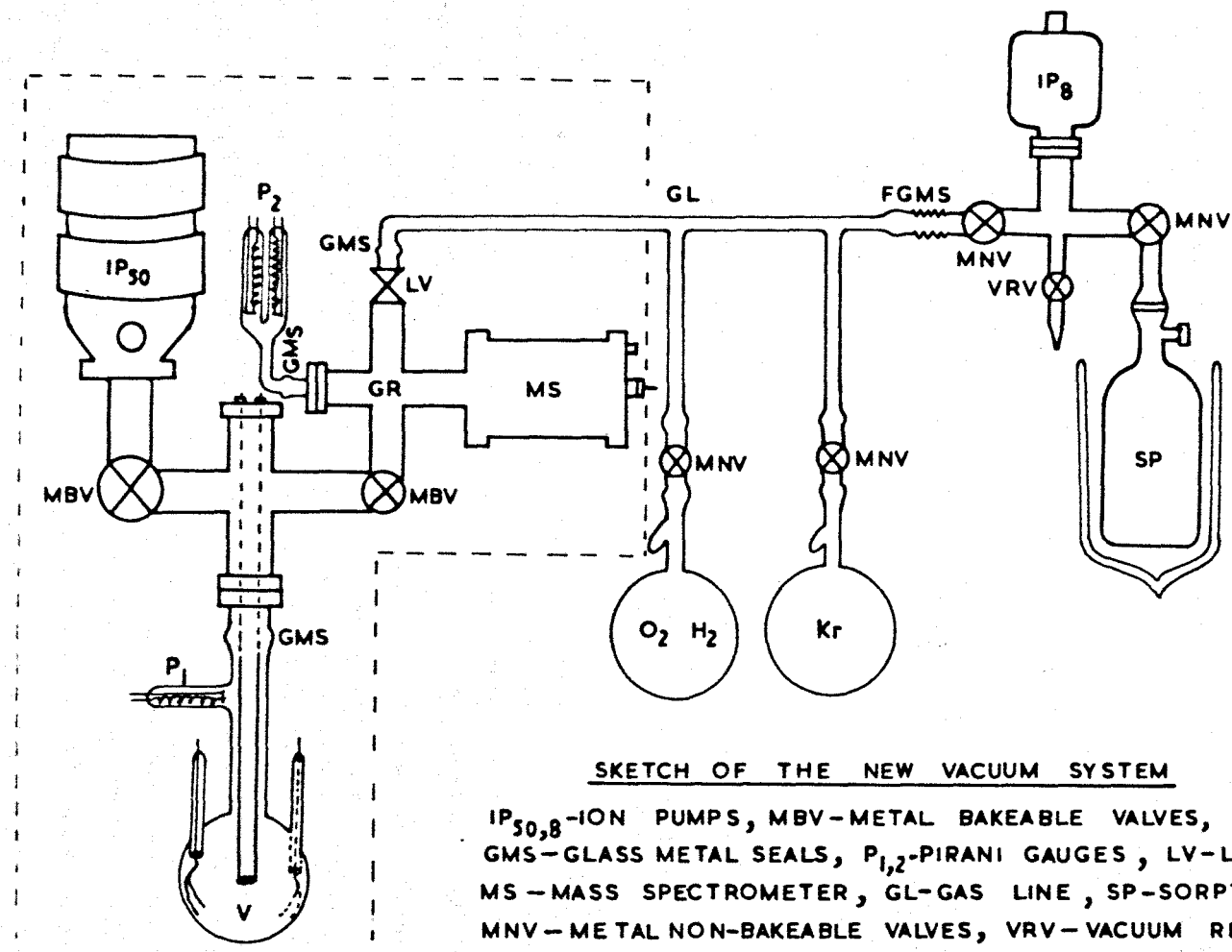

SKETCH OF THE NEW VACUUM SYSTEM

$IP_{50,8}$-ION PUMPS, MBV-METAL BAKEABLE VALVES, GMS-GLASS METAL SEALS, $P_{1,2}$-PIRANI GAUGES, LV-LEAK VALVE, MS-MASS SPECTROMETER, GL-GAS LINE, SP-SORPTION PUMP, MNV-METAL NON-BAKEABLE VALVES, VRV-VACUUM RELEASE VALVE, FGMS-FLEXIBLE METAL-GLASS SEAL, V-ADSORPTION VESSEL, GR-GAS RESERVOIR, O_2/H_2 PURE GAS BOTTLES, DOTTED BOUNDARY-BAKEABLE TO 250°C AND PUMPED BY IP_{50}.

Figure 28

9.4 The new vacuum system

The modified new vacuum system is shown in Fig. 28. In this arrangement the sputter-ion pump was directly connected to the adsorption vessel via the wide metal valve to improve its pumping speed. The gas reservoir was a stainless steel cross-piece, the four ends of which were separately joined to a sensitive Pirani gauge (P_2), The mass spectrometer (MS), the metal leak valve (LV) and a metal valve. The adsorption vessel was joined between the wide metal valve and the above mentioned metal valve through another metal cross-piece. Up to the leak valve, the whole system was pumped by the ion pump, and was placed on the top of the experimental table with the adsorption vessel vertically downwards.

A glass tube gas line (GL), with pure gas bottles, was attached to the main vacuum system by a glass to metal seal next to the leak valve, and was pumped separately by an 8 litre ion pump. This small ion pump was connected to a metal T-piece, the other two ends of which were separately joined to this gas line (via a flexible metal-glass seal next to a metal non-bakeable valve) and to a sorption pump (via another metal non-bakeable valve). The unadsorbed gas left in the adsorption vessel, reservoir and the gas line was pumped by this chilled sorption pump and the ion pump. Each gas bottle was isolated from the gas line by a small metal valve (Vacuum Generators, Ltd., type GH7). Pure hydrogen and other gases were directly obtained from break-seal pyrex bottles, and the palladium thimble was not used, as even when it is at room temperature diffusion of hydrogen always occurs and thus it does not act as a good valve.

The main features of this new system were to use a more sensitive Pirani gauge (Edwards Type G5C-2, power supply model 8/2) capable of reading accurately up to 10^{-4} torr, and better gas handling valves with metal bellows in them. Doses of pure gas from the

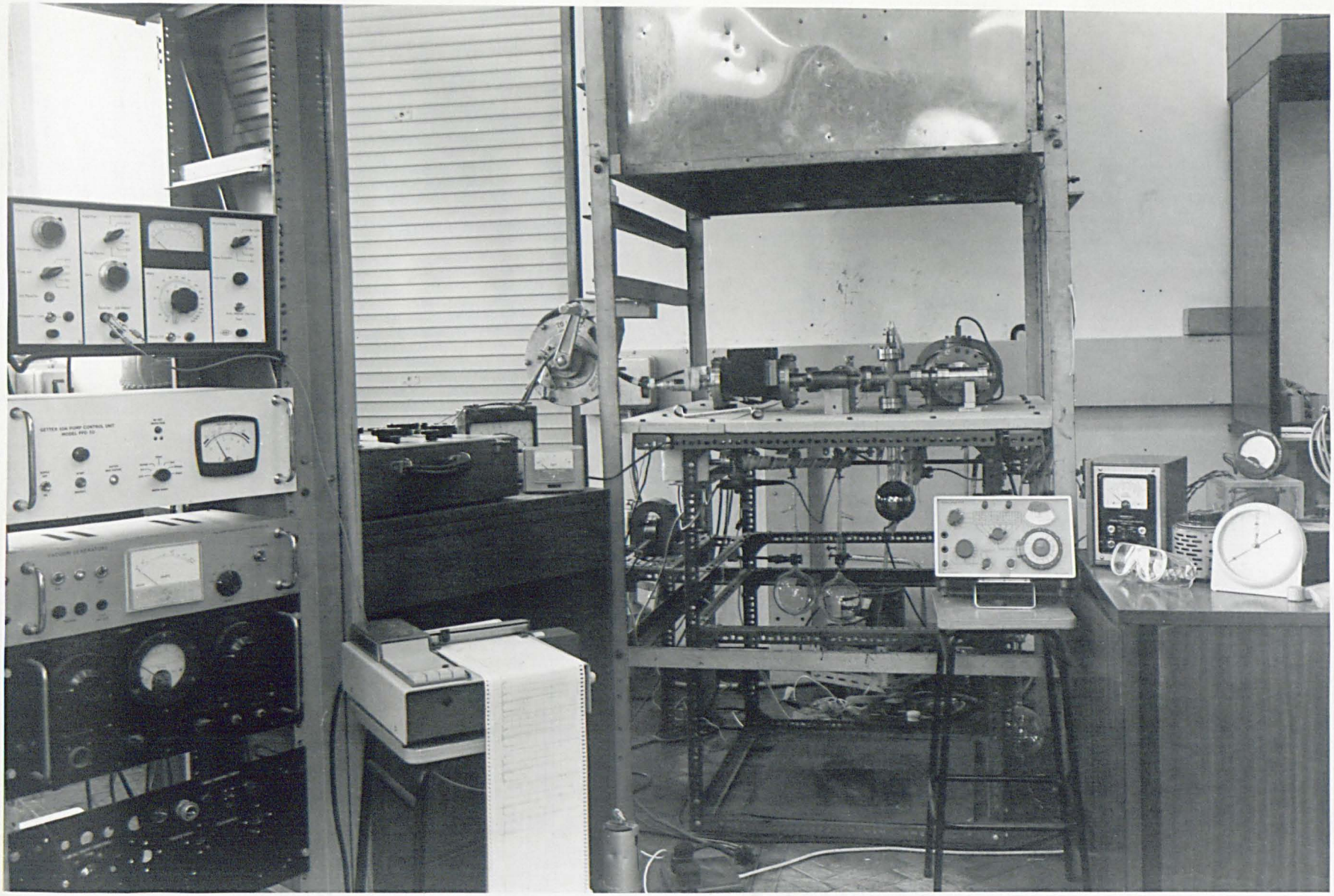

General photograph of the whole vacuum system.

Figure 29

reservoir were introduced into the adsorption vessel, through the bakeable metal valve and it was kept open throughout the period of adsorption of the dose. Thus the same Pirani gauge on the reservoir was used for studying initial and final pressures of each dose, and hence the error due to temperature difference was eliminated. The mass spectrometer on the reservoir could now be used to check the purity of gases before their adscrption. Photograph 29 shows the side view of this new system along with the general electronics to measure various quantities.

9.5 Experimental Developments

9.5(1) Design of big baking oven

Without a bake the high vacuum system attained a vacuum of the order of 10^{-8} torr. To get a vacuum better than 10^{-9} torr, an oven was designed to bake the main system including the ion pump and the gas reservoir. The outer structure of this oven was the same as previously used in the department, but the inner structure and the distribution of heating elements were completely changed. This distribution of the heating elements is shown in Fig. 30a. The whole of the oven (40" x 40" x 40") was heavy one and could be lowered down on to the experimental table and lifted up by means of a winch. The oven could attain an equilibrium temperature of 250°C with three variable heating elements and of 500°C with all the seven elements. Ion pump magnets have an upper limit of baking temperature of 300°C, and therefore a small insulating shell was made to cover the pump magnets during baking of the system. When equilibrium was attained in the course of the baking period, the insulating shell was ineffective in keeping the magnets at lower temperature, and hence the baking temperature of the upper system was limited to about 250°C.

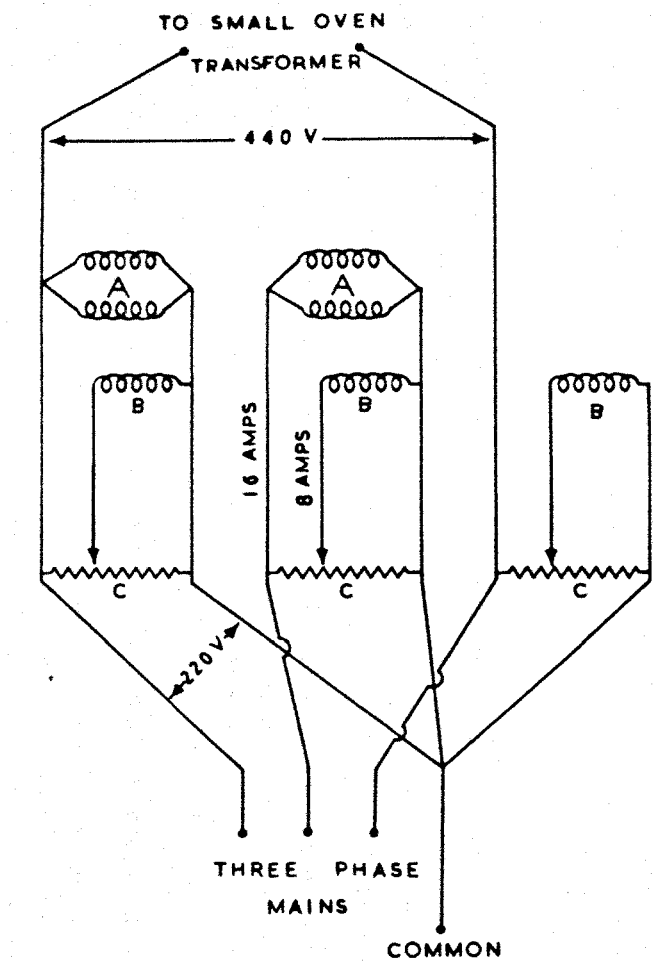

WIRING DIAGRAM FOR BIG OVEN.
A AND B ARE HEATING ELEMENTS, C VARIACS.

(a)

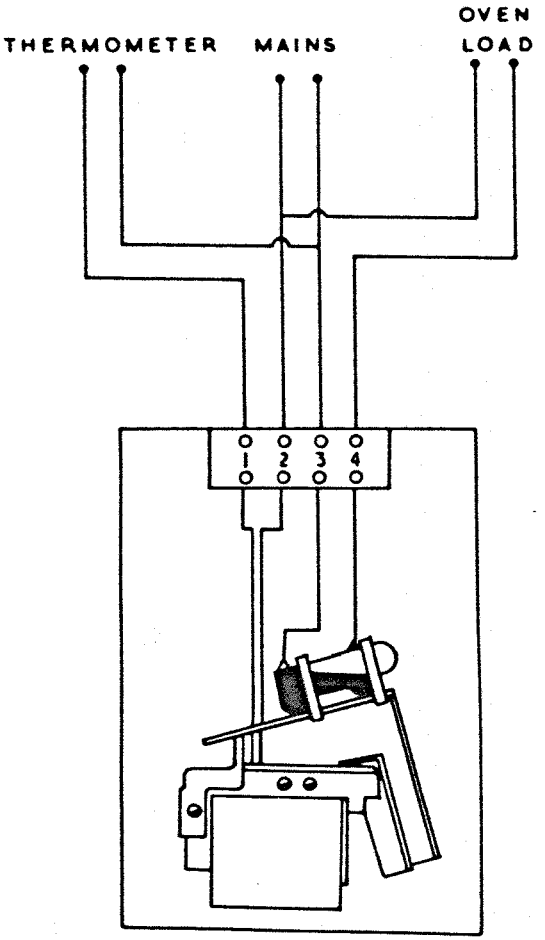

WIRING DIAGRAM FOR RELAY.

(b)

Figure 30

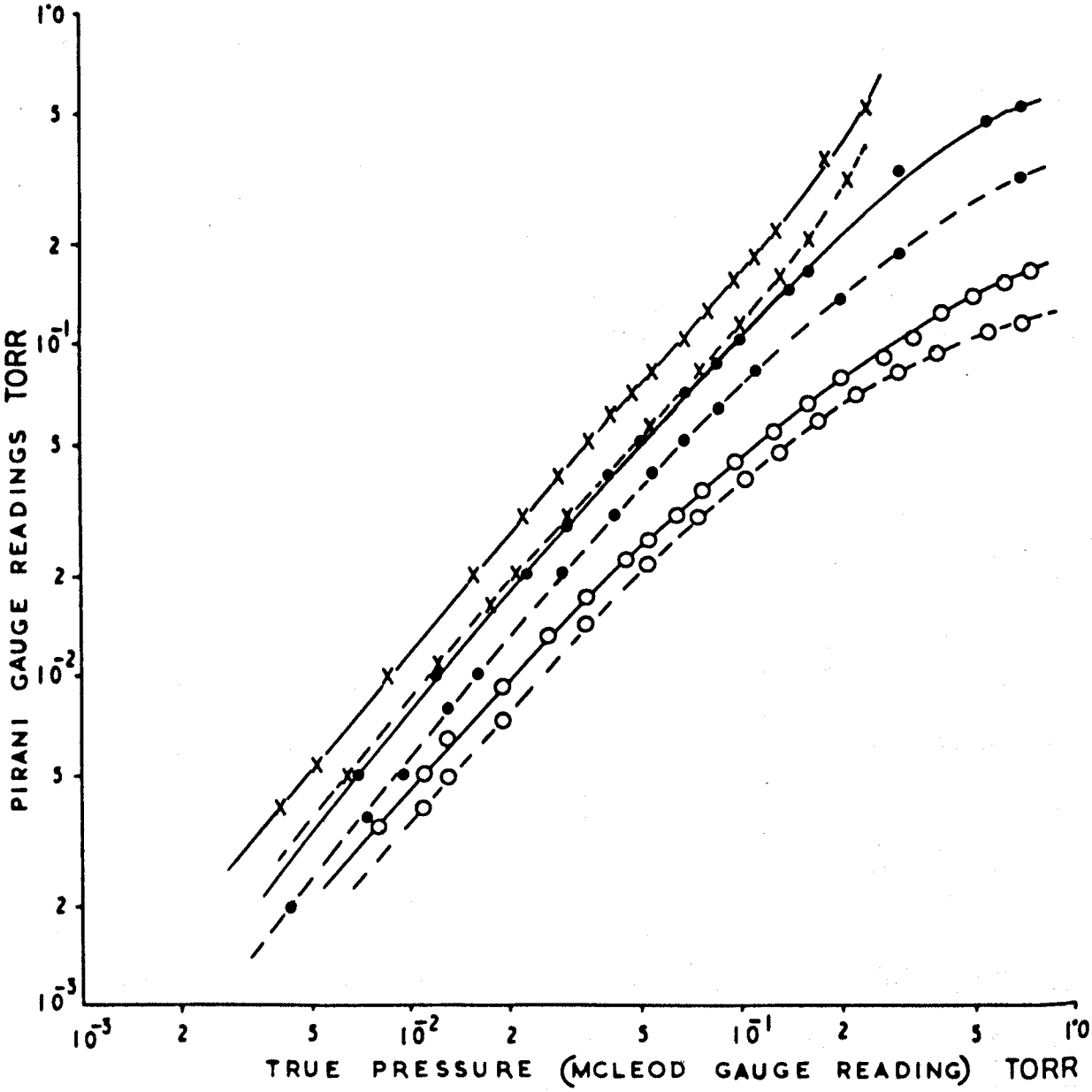

CALIBRATION CURVES FOR ADSORPTION VESSEL PIRANI GAUGE (———), AND GAS RESERVOIR PIRANI GAUGE (– – – –).
●—AIR, X—HYDROGEN, O—KRYPTON.

Figure 31

9.5(2) The adsorption vessel's baking oven

The adsorption vessel was under the experimental table which could not be baked by the big oven, and hence another small oven was designed to bake it. The temperature of this oven was controlled by a Rototherm thermometer and a mercury relay switch, the wiring arrangement of which is shown in Fig. 30b. This oven could easily give a temperature of 450°C under equilibrium conditions.

9.5(3) Calibration of the Pirani gauges

The Pirani gauges along with their bridge circuits supplied by the manufacturer (Edwards High Vacuum, Ltd.) were supposed to be calibrated for dry air. But a slight adjustment of resistors in the bridge circuits to adjust the lower or upper scale changes the calibration. Moreover, due to the different thermal conductivity of different gases, the pressure indicated by the meter differs remarkably from the true pressure from gas to gas. Thus both the Pirani gauges on the reservoir and adsorption vessel were calibrated against a McLeod gauge for dry air, hydrogen and krypton. The calibration curves for both the gauges are shown in Fig. 31.

9.5(4) Quantitative estimate of bulk erbium in the films

Erbium is a heavy active member of the rare-earth group, which consists of 15 chemically similar elements occupying a single position in the periodic system between barium (element 56) and hafnium (element 72). Rare earths are also known as lanthanons and readily form oxalates which are insoluble in oxalic acid and in dilute mineral acids. This characteristic reaction permits the separation of the lanthanons from other elements. If only one lanthanon is present, then it could be estimated gravimetrically as its oxide on igniting its oxalate, or volumetrically on titrating its solution in sulphuric acid with a standard solution of potassium permanganate. The latter, commonly

called the oxalate-permanganate method[106], was adopted for the quantative bulk estimate of erbium in the experimental films.

The erbium film, deposited on the inside wall of the adsorption vessel, was dissolved in dilute hydrochloric acid (approximate 0.1 N) and a colourless solution of erbium chloride was prepared. This solution was then heated to boiling. To this boiling solution was added slowly, with rapid stirring, about 25% its volume of a hot, saturated oxalic acid solution (1 N). Erbium oxalate was precipitated as a pale pink coloured heavy crystalline suspension and it settled down at the bottom of the flask. This suspension was gently boiled for a few minutes, allowed to cool to room temperature, and set aside for overnight.

The next day, the precipitate was filtered and washed first with the saturated oxalic acid solution and then thoroughly with distilled water. Erbium oxalate so obtained was dissolved in 10N sulphuric acid and a colourless solution of its sulphate was obtained. This was then diluted to about five times its volume and heated to boiling. This hot solution was titrated with standard potassium permanganate solution, prepared a day before the titration. The normality of this solution of $KMnO_4$ was adjusted within the range of 0.025 to 0.04N (i.e. 0.79 to 1.26 grams of it per litre of solution). The various chemical reactions taking place are represented by the following chemical equations:

$$2\ Er + 6\ HCl = 2\ ErCl_3 + 3\ \uparrow H_2$$

$$2\ ErCl_3 + 3\ H_2C_2O_4 = \underset{\text{pale pink precipitate}}{\downarrow Er_2(C_2O_4)_3} + 6\ HCl$$

This is washed, filtered and dissolved in H_2SO_4

$$5\ [Er_2(C_2O_4)_3 + 3\ H_2SO_4 = Er_2(SO_4)_3 + 3\ H_2C_2O_4]$$

$$3\ [5\ H_2C_2O_4 + 2\ KMnO_4 + 3\ H_2SO_4 = K_2SO_4 + 2\ MnSO_4 + 10\ CO_2 + 8\ H_2O]$$

$$5\ Er_2(C_2O_4)_3 + 24\ H_2SO_4 + 6\ KMnO_4 = 5\ Er_2(SO_4)_3 + 3\ K_2SO_4 + 6\ MnSO_4 + 30\ CO_2 + 24\ H_2O$$

Thus 6 molecules of potassium permanganate (948.24 parts by weight of $KMnO_4$) are utilised by 10 atoms of erbium (1672.60 parts by weight of erbium) to complete the reaction. From the erbium oxalate and potassium permanganate titration, the weight of $KMnO_4$ was known and thus the metal erbium in the film was quantitatively estimated.

Previous to bulk erbium estimates of experimental films, some test experiments were performed with known amounts of erbium dissolved in dilute hydrochloric acid. Estimates of bulk erbium less than five milligrams failed (presumably due to low solubility product of ions in solution), but for higher concentration up to 40 milligrams it was estimated within a mean error of about 0.5%. However, it was found convenient to detect the small amount of erbium in thin films when more erbium of known amount was added to the original solution.

9.6 Experimental procedure

Before each experiment, the main vacuum system including the ion pump, adsorption vessel and the gas reservoir was thoroughly baked for about a week at 250°C. The gas line was also baked at about 100°C by heating tapes. During baking of the system, the pressure as measured by the ion pump current was not allowed to increase above 10^{-7} torr. After the bake, the upper part of the vacuum system was cooled slowly to room temperature and the adsorption vessel was still kept above 100°C

and thus the residual gases were drawn into the pump. Simultaneously degassing of the evaporation source (a helical molybdenum filament containing a pure erbium pellet - purity mentioned in Section 2.8) was started and it was left degassing for about two days just below the evaporation temperature of the metal. After the source filament was thoroughly degassed, the lower oven was switched off, and the adsorption vessel was placed in a constant temperature (295^{o}K) water bath, and then a background pressure of 10^{-9} torr or less was always achieved. Occasional mass-scans taken with this base pressure showed water vapour, hydrogen and carbon monoxide to be the predominating residual gases, as shown by a typical analysis in Fig. 23. The high partial pressure of hydrogen and water vapour in the system is probably due to baking of the ion pump, as Rivière and Allinson[107] have also reported hydrogen and water vapour to be the major constituents of the evolved residual gases due to baking of sputter-ion pumps.

A thin film was deposited during the long degassing of the metal, but the resistance of these films was very high (K ohm range) as compared to those of the experimental ones (15 - 90 ohms). The experimental films were deposited at a slow rate of evaporation (5 to 10 Å/min) from weighed amounts of erbium metal resting in the filament at the centre of the vessel. The mean film thickness was estimated from its mass and its apparent geometrical area; its mass was known from the mass of the original metal in the filament, and was checked by quantitative volumetric analysis of the film after the experiment was over. Except for the first two runs, the whole metal in the filament was evaporated. During the film's formation its d.c. resistance was continuously measured by a universal bridge. After the deposition of the film was over, its resistance was monitored by passing a constant current (100 micro-amps) through it (from a constant voltage power supply) and by measuring the potential drop across the two leads

(I_1 and I_2) by a sensitive potentiometer. A maximum of one micro-watt was applied to the films to avoid thermal effects. The accuracy of this d.c. bridge for resistance measurement was ± 0.01%.

The object of this work was to measure the effect of chemisorption on the film resistance, consequently the films should be annealed and allowed enough time to completely stabilise their resistance before exposure to the gases. In a separate experiment, the resistance of a film was measured for about two hours after its deposition, and only a 2% change in resistance was observed at the residual pressure of less than 10^{-9} torr. This observation and the results of surface area measurements before and after the experiments indicated that the films were well annealed during their formation. Hence the films were not specially annealed, and 20 to 25 minutes after the evaporation when the resistance became steady, the film adsorption vessel was isolated from the pump and doses of pure gases were introduced by briefly opening and then closing of the leak valve in the first arrangement, and by leaving open of the metal valve in the second arrangement. There was negligible adsorption of hydrogen in the empty vessel when it contained neither a pellet of erbium nor a film.

Upon completion of the gas interaction with the film, the unadsorbed gas was sometimes pumped by the sorption pump and then by the ion pump, and sometimes directly by the ion pump. On repumping, when the residual pressure fell in the region of 10^{-9} torr, the film adsorption vessel was again isolated from the pump and immersed in a liquid nitrogen bath for surface area measurements. The true surface area of the films was estimated from the physical adsorption of krypton at 78°K, using the BET method. The volumes of the adsorption vessels had been precisely found by filling them with distilled water, and the volume of the gas reservoir had been found by expanding helium in them

in separate experiments at room temperature. When the adsorption vessel was immersed in liquid nitrogen to the level 'J' in Fig. 27a, it was necessary to correct the pressure readings for the temperature gradient from A to H, and this was also determined in the same experiments with helium. A blank experiment without a film showed that the inner surface of the adsorption vessel had a roughness factor of 2.36.

The changes in electrical resistance of erbium films, caused by the sorption of hydrogen and oxygen, and their interpretations are discussed in the next chapters.

CHAPTER X

RESULTS AND QUALITATIVE DISCUSSION

10.1 Introduction

The changes in the electrical resistance of erbium films, caused by the sorption of hydrogen and oxygen, have been measured as a function of the ratio of the numbers of gas atoms to surface and bulk metal atoms. These films varied in their thickness from 110 to 630 Å, and all had positive temperature coefficient of resistance. The interaction with each gas was studied at room temperature and at various lower temperatures. The effects on resistance of the interaction of atomic and molecular hydrogen with films pre-covered with oxygen, and of oxygen with a film which had previously interacted with hydrogen, have also been studied. To avoid repetition, the results and their discussion are arranged together in each section.

10.2 The results of surface area measurements

The surface area of the films was measured from the physical adsorption of krypton at 78°K, using the BET method. A minimum of five increments of krypton were admitted and from the previous volumetric calibration of the apparatus, the amount adsorbed at each stage was calculated. The value[108] p_o = 2.0 torr, was used for the saturation vapour pressure of krypton at liquid nitrogen temperature, and measurements were made up to a maximum relative pressure of 0.09, but linearity of the BET plot was obtained up to only about 0.06. The v_m calculated from the BET plot was always found to be slightly greater than the v_m corresponding to the Point B, and the former values are used throughout. The value of 19.5 $Å^2$ for the cross-section of the adsorbed krypton atom was employed to convert the values of v_m to surface areas.

In Fig. 32, typical adsorption isotherms and the corresponding BET plots are drawn together for two films (8 and 14), to show the accuracy of the experiments and the validity of the BET equation within the limited relative pressure range. The measured film areas were between 8 - 16 times the real surface area of the adsorption vessel (i.e. 19 - 38 times its apparent geometrical area). In Fig. 33, the film surface roughness factor (R.F.) i.e. the ratio of the measured film surface area to its real geometrical area (real geometrical area 755 cm^2 = product of apparent geometrical area 320 cm^2 and 2.36 - roughness of the inner glass surface of the adsorption vessel) is expressed as a function of the mean film thickness, assuming that all the films take the contour of the surface of the adsorption vessel. The least squares method is used (assuming an error is involved in the surface area measurement) to find the best straight line to fit the experimental data, and from this line, a mean specific surface area of 71 ± 18 square metre per gram of erbium is calculated. This large value of the specific surface area suggests that the experimental films are rough and porous, and that the dimensions of some of the porosity (i.e. capillaries, grain boundaries and dislocation lines etc) in the films are possibly comparable to the size of a krypton atom (4 Å), and therefore the krypton physisorption also measured the surface area of this broad porosity. However, it is very common to observe a large surface roughness factor for evaporated polycrystalline metal films and values as large as 50 to 100 have also been reported in the literature[79,1].

10.3 Adsorption of hydrogen at room temperature (295°K)

Figure 34 shows typical results for the proportionate change of resistance $\Delta R/R_o$ as a function of dosage and time for film No. 3. The resistance increased to a maximum at A and then decreased again to

its original value R_o at B. The first few doses on the bare metal film increased the resistance immediately, which remained stable and did not decay. As more hydrogen was added and the resistance approached point A, a longer decay in resistance after each dose was observed. Beyond the point A, further doses increased the resistance momentarily and then the resistance decreased. The rate of this decrease was very fast and more pronounced for a few minutes after the addition of the dose and then it slowed down. After each dose the pressure stayed below the lower limit of the Pirani gauge. The films continued to sorb many doses of hydrogen beyond point B until they were partly saturated and unable to reduce the pressure below 10^{-3} torr in the allowed time; but this was a bulk effect and will be discussed later. After the interaction studied with each film was over, the adsorption vessel was evacuated again, then isolated from the pump for the second time and immersed in liquid nitrogen for the surface area measurement. The surface area of the films was generally measured after the experiments, but a test on one film (film No. 8, see Fig. 32) showed that its original surface area was increased by 22% after interaction with hydrogen, possibly due to a phase change from metal (hcp) to dihydride (fcc).

The atomic ratio H/Er(bulk) was found from the doses of hydrogen adsorbed and the mass of the film. The atomic ratio H/Er(surface) was found from the measured area of the film, and the number of surface sites (7.86×10^{14} per cm^2) was calculated from a relationship suggested by Brennan et al[109], for polycrystalline films. Figure 34b shows $\Delta R/R_o$ (measured at the end of each dose in Fig. 34a) as a function of both these atomic ratios. The results of hydrogen interaction with other films (1,2,6 and 8) were very similar to the results shown in Figs. 34a and 34b for film No.3 and are summarised in Table II.

Summary of resistance changes at 295°K Table II

ROW NO	ADSORBATE	HYDROGEN					OXYGEN		
1	FILM NO	1*	2	3	6**	8**	4	5	13
2	MASS IN MG.	3·1	4·95	17·9	8·0	15·7	10·0	7·4	11·1
3	MEAN THICKNESS IN Å	110	175	630	280	550	350	260	390
4	ROUGHNESS a)	—	—	—	—	12·9	—	—	12·2
	FACTOR b)	9·2	—	15·0	9·6	15·7	—	8·8	13·7
5	SURFACE a)	—	—	—	—	635	—	—	830
	AREA PER MG. b)	2270	—	644	920	768	—	895	925
6	INITIAL RESISTANCE R_o IN Ω	90·07	75·60	14·72	52·30	34·55	29·50	40·0	43·2
7	MEAN DOSE ATOMS X 10^{18}	1·6	2·6	1·3	1·4	1·8		1·1	1·3
8	$\frac{\Delta R}{R_o}$ % AT A	18	15	30	15	19	30	25	42 ⊢
9	$\frac{H}{E_r}$ BULK AT A	0·460	0·234	0·226	0·338	0·268	0·250	0·253	0·235 ⊢
10	$\frac{H}{E_r}$ SURFACE AT A a)	—	—	—	—	1·9	—	—	1·3 ⊢
	b)	0·9	—	1·6	1·7	1·6	—	1·3	1·15
11	SURFACE *** COVERAGE	0·62		1·1	1·35	1·17			
12	$\frac{H}{E_r}$ BULK AT B	0·87	0·29	0·42	0·42	0·51			
13	$\frac{H}{E_r}$ SURFACE AT B a)	—	—	—	—	3·7			
	b)	1·7	—	3·0	2·1	3·1			
14	$\frac{\Delta R}{R_o}$ % AT C	65	40	72	71	64			
15	$\frac{H}{E_r}$ BULK AT C	2·50	0·93	1·94	1·84	1·81			
16	$\frac{H}{E_r}$ BULK AT D	3·10	1·20	2·27	2·20	2·11			
17	∝ VALUES	1·44	2·26	2·32			2·32	2·25	2·82

* IN THIS EXPERIMENT A SMALL PIECE OF ERBIUM WAS LEFT IN THE HELIX AFTER EVAPORATING THE FILM, AND THIS SORBED EXTRA HYDROGEN.

** IN THESE EXPERIMENTS THE FIRST FEW DOSES WERE ADDED AT 78°K.

*** WHEN DECAY BEGAN IN RESISTANCE VERSUS DOSE TIME CURVE.

4, 5, 10, 13-a) FOR FRESH FILMS, b) FOR FILMS AFTER GAS INTERACTION.

⊢ Corresponding values for oxygen at the final point.

For the total change up to point A, a 15% to 30% increase in resistance was observed in different experimental runs. The magnitude of these increases depended partly on the magnitude of the doses and possibly partly on the period allowed for interaction with each dose. A large number of small doses allowed to reach equilibrium one at a time increased the magnitude of this resistance change, while big doses with a comparatively small interaction period decreased it (see Fig. 36b). It seems very likely that this measured increase in resistance up to point A is due to surface adsorption. This decrease in conductivity is not the same as the almost negligible one reported previously by Heckman[54] for the bulk erbium-hydrogen system, since the surface to bulk ratio of his polycrystalline bars was very small. When the interaction of hydrogen with erbium is studied in the form of thin films, the surface to bulk ratio is increased and therefore the surface effect becomes predominant.

For all the films, the measured values of surface coverage - θ (i.e. the ratio of gas atoms to the total surface sites) at point A lie between one and two (see the 10th row of Table II). This indicated that before the maximum change in resistance had occurred a part of the added hydrogen incorporated into the bulk. From the resistance versus dose and time curve (Fig. 34a), it is clear that the decay in resistance began after some doses were adsorbed. It is reasonable to assume the stable value of resistance corresponds to the adsorption of hydrogen on the surface as an anion (shown by the increase in work function of erbium - measured in this laboratory[110]), and the decay corresponds to the bulk penetration as a proton (see Section 10.4). On this hypothesis a mean surface coverage of 1.2 was calculated for all the films (see row 11 of Table II) at the point where decay just began. This θ value of slightly greater than unity is either due to some kind of very small incorporation of hydrogen or most probably due to

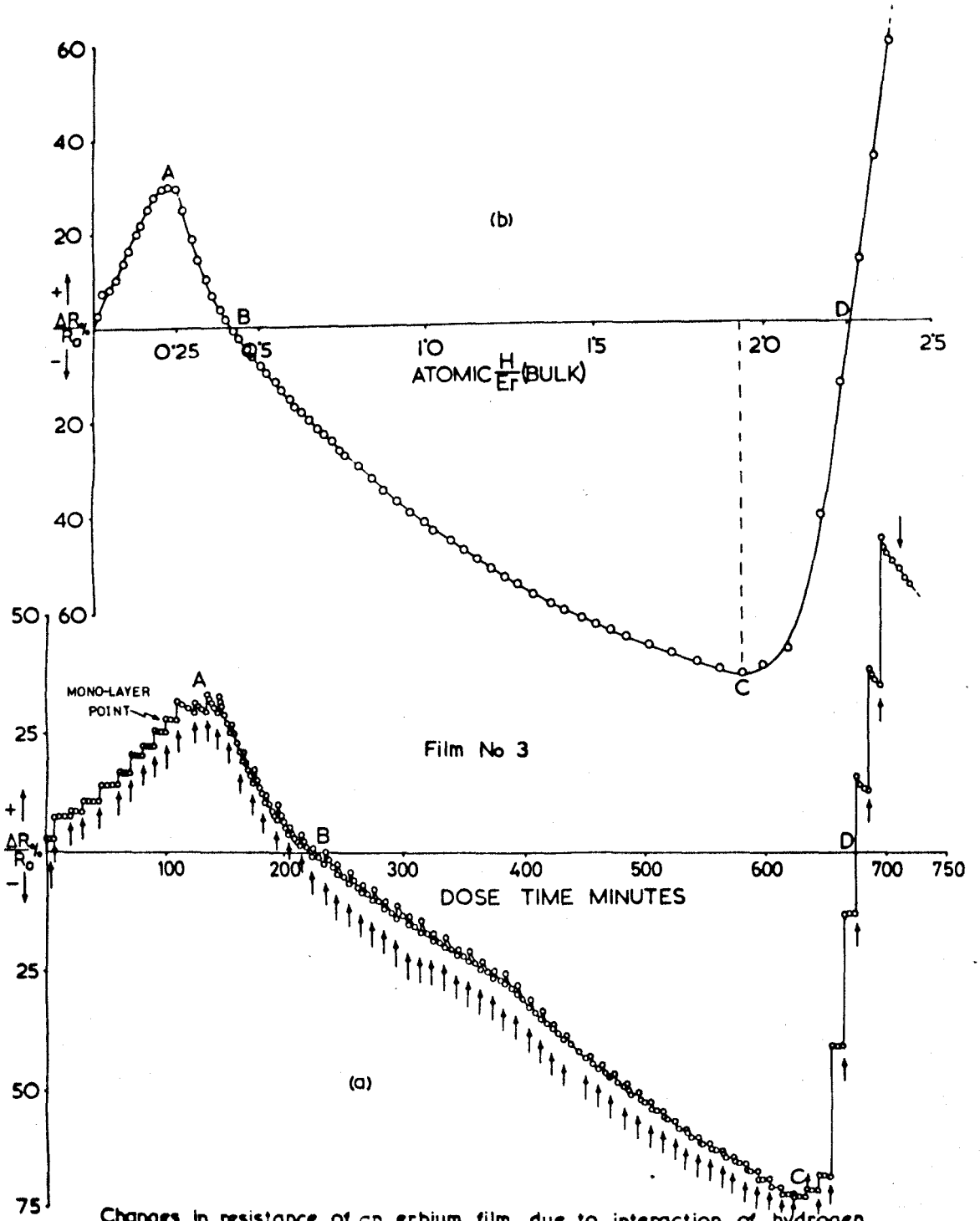

Changes in resistance of an erbium film due to interaction of hydrogen at 295°K. ↑ shows time and position when a dose is added.

(b) Resistance change versus atomic $\frac{H}{Er}$ bulk ratio.

(a) Resistance change versus dose time.

Figure 35

experimental errors (i.e. errors involved in the methods of surface area measurement and surface site calculation etc.), but it showed qualitatively that the incorporation of hydrogen occurred mainly after a monolayer concentration was formed on the surface. However, the surface coverage measured by the physical method is no more than a guide as to the location of species, as even when $\theta < 1.0$, one cannot completely exclude incorporation[111]. Also the problems of whether the penetration of hydrogen occurred partly from each dose before a monolayer was formed, or after it; and which part of the hydrogen incorporated i.e. the newly arriving gas or that which was already staying on the weaker sites, cannot be solved with certainty by the resistance measurements alone as the resistance measures the collective effect of all the hydrogen. Therefore to locate the monolayer point with more certainty some other additional information is essential.

10.4 Bulk sorption of hydrogen at room temperature ($295^{\circ}K$)

The complete picture of the changes in electrical resistance due to adsorption as well as bulk sorption of hydrogen is shown in Fig. 35 for the same film (No. 3). The initial increase of resistance to a maximum at A and then its decrease to the original value R_o at B have already been described in Section 10.3, and the increase was attributed to the surface effect. The resistance continued to decrease beyond point B and it attained a minimum value at C. Depending on the size of the doses, this minimum value was 40 to 72% (see row 14 of Table II) below the original value for the bare films. Further addition of doses caused a rapid increase in resistance without decay with time and in a few doses it approached the original value at D. Beyond the point D, the resistance still increased without decay to about 100% above the bare film value, and after that further uptake of hydrogen became slower and each dose was accompanied by a very large increase of

resistance of magnitude $\Delta R/R_o$ = 15-20 (i.e. 1500-2000% approximately proportional to the size of the dose) with subsequent slow decay. The decayed and stabilized values of $\Delta R/R_o$ in this region were many orders of magnitude greater than the original value.

Up to the point C, all the doses were sorbed so rapidly that no indication of increase of pressure above 10^{-3} torr was observed, it was only beyond the point C that the pressure rose above 10^{-3} torr when the dose was added, but it soon fell below the lower limit of the gauge. The rate of fall of this hydrogen pressure slowly decreased but did not reduce to zero up to the maximum atomic composition (which was quantitatively studied) of about 2.4. In Fig. 35b, the stable value of $\Delta R/R_o$ (after the end of each dose in Fig. 35a) is expressed as a function of the atomic ratio of hydrogen to bulk metal atoms. These atomic ratios at the points where the curve attained the minimum value at C, and again crossed the zero axis at D, are tabulated in rows 15 and 16 of Table II for all the films. For the films which attained equilibrium in the interaction, these ratios could be compared in some respects with the published values for the bulk stable system[54]. The higher values of the ratios at different points in the case of film No. 1, are due the bulk erbium left unevaporated on the filament, which dissolved a considerable amount of hydrogen (as the ratios were calculated from the total amount of hydrogen which disappeared and no allowance could be made for the hydrogen dissolved into the bulk pellet). Film 2 had large doses, and did not attain equilibrium between doses.

An X-ray diffraction study of the bulk erbium-hydrogen system[112] has indicated that the metal changes its structure with hydrogen concentration. This is shown by a phase diagram[113] in Fig. 36a.

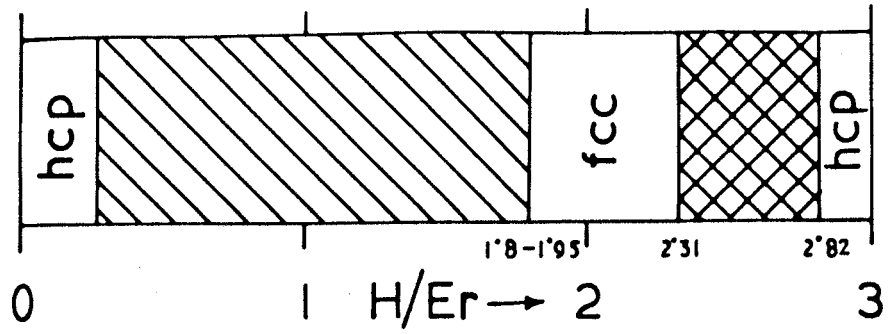

Figure 36a

PHASE DIAGRAM OF BULK ERBIUM-HYDROGEN SYSTEM. HATCHED AND CROSSHATCHED AREAS REFER TO TWO PHASE METAL-DIHYDRIDE AND DIHYDRIDE-TRIHYDRIDE REGIONS. BLANK REGIONS ARE SINGLE PHASE METAL WITH DISSOLVED HYDROGEN, DIHYDRIDE AND TRIHYDRIDE.

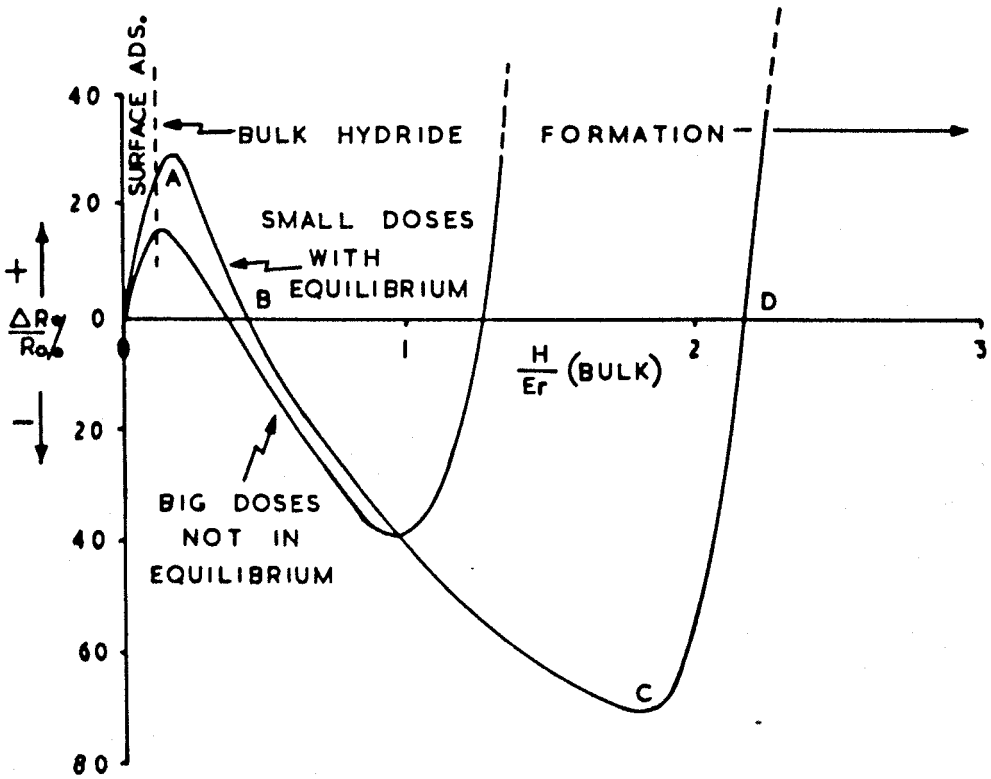

EFFECT OF SIZE OF DOSES ON THE CHANGE OF RESISTANCE OF ERBIUM FILMS WITH COMPOSITION.

Figure 36b

In the beginning and below a certain composition, the metal retains its hcp structure with dissolved hydrogen, and then up to 1.95 atomic ratio[114] (1.8 from resistivity measurements[113]) two phases i.e. metal and dihydride simultaneously exist. At higher concentrations up to 2.31, only a single dihydride phase exists which is fcc. On further addition of hydrogen, it again forms two phases i.e. dihydride-trihydride (up to 2.82), and finally a single trihydride phase (which is again hcp) exists up to the composition 3.0.

The minimum in film resistance occurred at the boundary between the two phase metal-dihydride region and the dihydride region. The conductivity at this point became 3 to 3.5 times the original conductivity of the bare metal films. The atomic H/Er(bulk) ratios, at which the various points (A,B,C and D) occurred, decreased as the size of the doses was increased as shown qualitatively in Fig. 36b. This shows that the bulk interaction was not equilibrated with bigger doses in the period allowed for interaction because of the mild experimental conditions. However, the experiments with the small doses where sufficient time was allowed to reach equilibrium, gave the more reproducible results.

The resistance of the films decreased if the interaction was completed around the point D i.e. in the dihydride region, and the adsorption vessel was put in a liquid nitrogen bath. On the other hand, the resistance was increased for a film which interacted with hydrogen for about five days beyond the point D (possibly formed single phase trihydride) before being cooled to liquid nitrogen temperature. This observation and the magnitude of the measured resistance, suggest that the erbium dihydrides (for which resistance is comparable to that of the bare metal films) are metallic conductors, and compositions near trihydrides (for which resistance is many orders of magnitude greater than that of the bare films) are very likely semiconductors. Thus it

seems possible that in the dihydride region (i.e. after the point D, where the resistance increased and then decayed with each dose) the nucleation of erbium trihydride temporarily takes place (the big increase in resistance) and is followed by its successive decomposition (the slow decay) as the hydrogen pressure is reduced during the uptake of the dose. The equilibrium proceeds very slowly in this region and the bulk composition corresponds to some sort of erbium dihydride with a slowly increasing content of hydrogen. Also with a high content of hydrogen i.e. near trihydride regions, very big jumps in resistance were observed and in one experiment (when the film was exposed to hydrogen at about atmospheric pressure) even the electrical contact was lost, which suggested that near trihydride compositions the film became brittle and cracked. This was readily observed when a pellet of bulk erbium left unevaporated in the filament and which had interacted with hydrogen for a long time, crumbled and fell into pieces when removed from it. During the hydrogen interaction a change in colour of the films was also observed from opaque dark reflecting (metal) to golden light brown (dihydride) and finally to transparent near trihydride region.

The most interesting feature of the results is that for compositions near 1.8-1.9 the resistance is much smaller than that of the bare films. This is surprising as the added hydrogen would increase the scattering centres in the parent metal film. The hydride contains hydrogen ions, hydrogen ion vacancies and metal interstitials randomly distributed in the lattice which would increase the resistance. Hence the decrease in resistance must be due to some other cause, such as extra electrons.

Two models for the rare earth hydrides have been proposed in the literature[54]. In one model the added hydrogen is regarded as an anion and takes one electron from the system. This enables one

reasonably to understand an increase in resistance, but it fails to explain why the resistance decreases from the points A to C. In the second model hydrogen is regarded as protonic and each atom contributes one more electron to the conduction band of the system, thereby decreasing the resistance up to the composition near dihydride. Further increase of resistance beyond H/Er > 2 is assumed to be caused by filling of the conduction band of the system. Electrons are added to the conduction band, and tend to fill it and complete the filling at trihydride. The conduction band ($_5d\ _6s$) of the metal erbium has twelve states and cannot be saturated by the maximum of six electrons (three contributed by each metal atom and three by the three hydrogen atoms). Hence it is necessary to assume that these twelve states split in two sub groups of six states each, and that the lower sub group is filled near trihydride composition. The mechanism which could split the states is not known but it is suggested[54] possibly due to the crystal field effect (Stark effect).

The increase in resistance in H/Er > 2 region could be due to a reduction either in the conduction electrons (anion model) or in the conduction hole population i.e. filling up of the band (protonic model), and hence the resistance measurements alone cannot be used to prove one or the other model. A study of some other properties which distinguish between an electron and a hole would be useful. The recent measurements of Hall coefficient and positron annihilation in rare earth-hydrogen systems[54] have independently rejected the anion model and supported the protonic nature of hydrogen in systems with H/Er > 2.

10.5 Adsorption of hydrogen at low temperatures

As discussed in Sections 10.3 and 10.4, the surface interaction of hydrogen with erbium films at room temperature was followed by its bulk interaction with subsequent di- and trihydride formation. It was

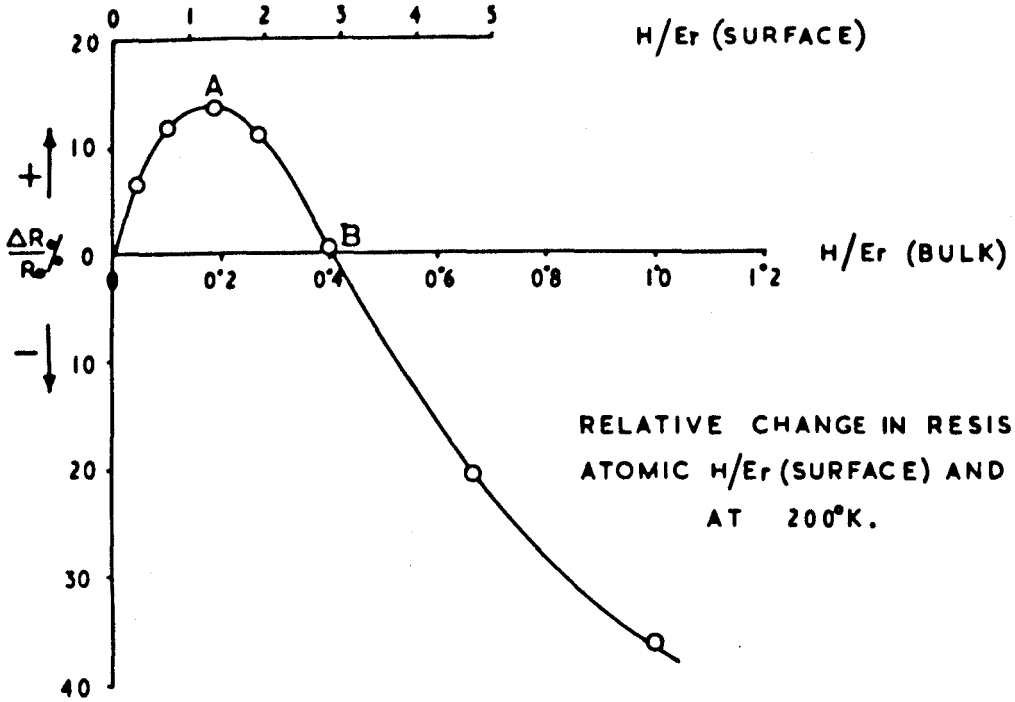

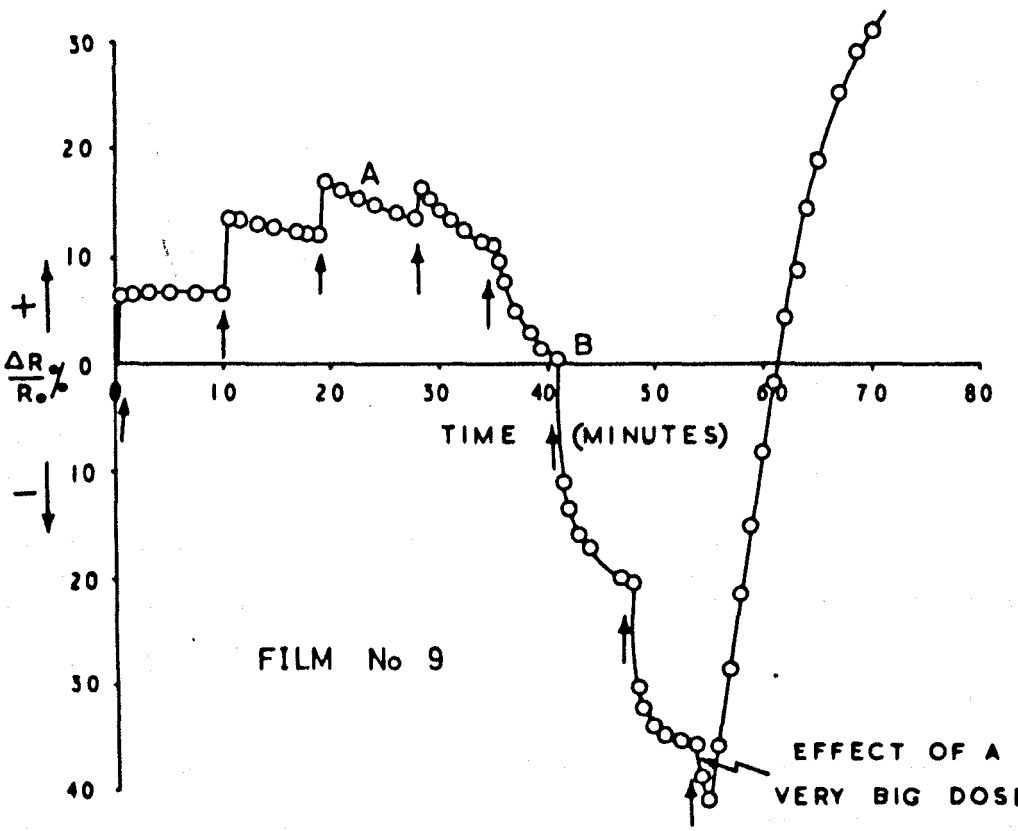

RELATIVE CHANGE IN RESISTANCE VS. HYDROGEN DOSE—TIME FOR AN ERBIUM FILM AT 200°K.

Figure 37

thus thought helpful to study the interaction at temperatures lower than 295°K, where the bulk activity would be reduced and the surface effect might become dominant.

10.5(1) Hydrogen interaction at the temperature of solid carbon dioxide in acetone (200°K)

Cakes of solid carbon dioxide were dissolved in acetone till a saturated solution of solid CO_2 was obtained. The adsorption vessel was put in this cold bath and measured doses of hydrogen were introduced for adsorption. The results obtained with film No. 9 are shown in Fig. 37. The resistance first increased by about 16% at A then decreased to its original value at B. Further doses also decreased it below the original value, but a very big dose (which was beyond the calibration curve for the pressure gauge) reversed the sign of this decreasing resistance before it reached the usual minimum at C. The variation of resistance with composition and its decay during different stages were similar to those of the corresponding stages of hydrogen interaction at room temperature (compare Figs. 37 and 35). Also the atomic ratios H/Er(bulk) and H/Er(surface) measured at the poitns A and B were similar to those measured for the hydorgen interaction at 295°K. Thus the hydrogen interaction at 200°K was similar to the interaction at room temperature, and experiments at still lower temperature were desirable to find out if the bulk interaction could be restricted.

10.5(2) Hydrogen interaction at the melting temperature of iso-pentane

The low temperature bath was prepared by slowly adding liquid nitrogen to iso-pentane and vigorously stirring till the mixture became saturated and some solid iso-pentane was left behind. Two separate experiments (films 10 and 11) were made at this temperature, and the results obtained are shown in Fig. 38. In both the experiments, the resistance first increased by 6-8% and then decreased

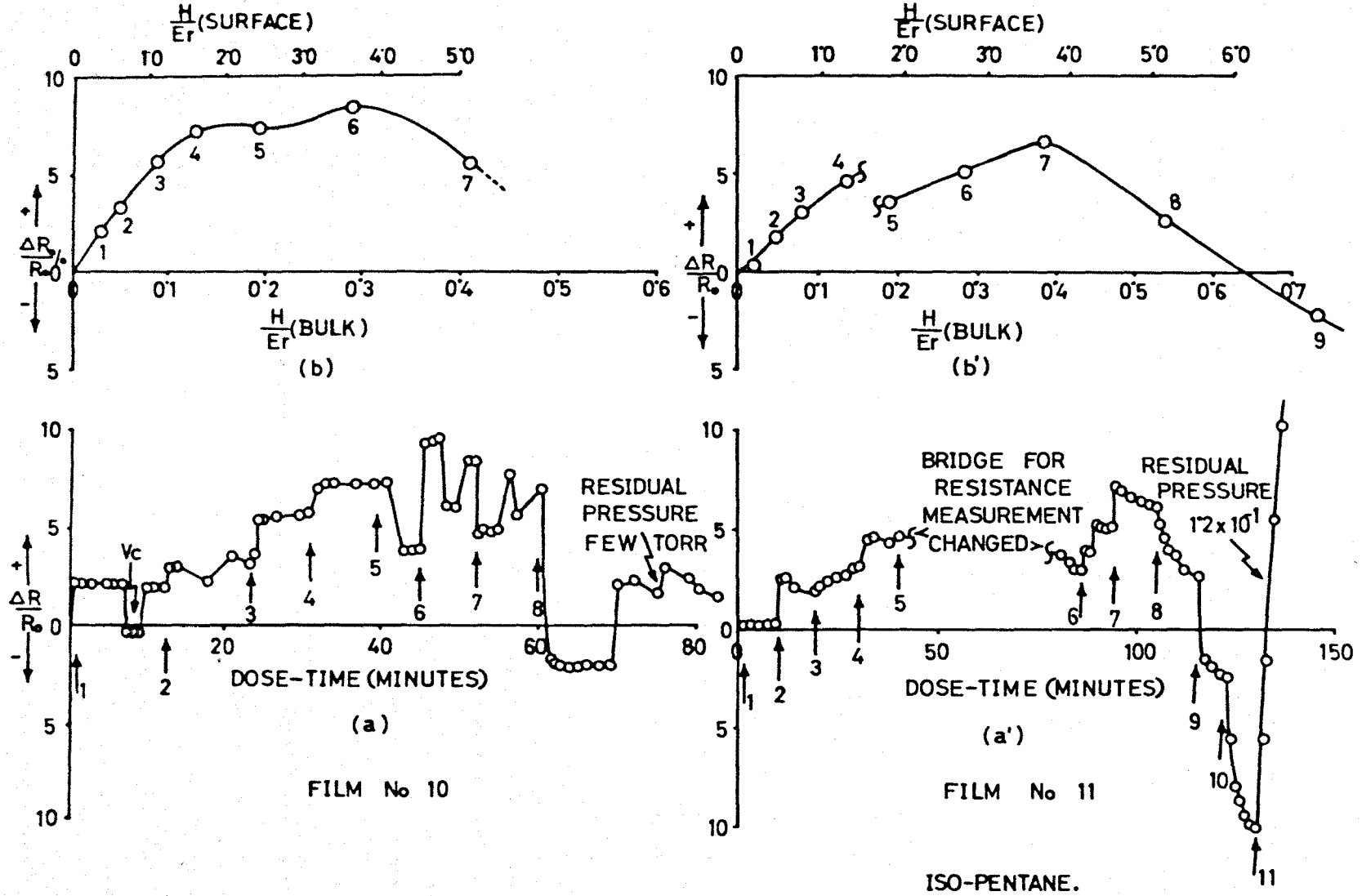

HYDROGEN INTERACTION WITH TWO ERBIUM FILMS AT M.P. OF/a,a') RESISTANCE VERSUS DOSE TIME, b,b') RESISTANCE VERSUS H/Er SURFACE AND BULK ATOMIC RATIOS. NUMBER WITH ↑ REPRESENTS SEQUENCE OF DOSES. Vc-A FLUCTUATION IN RESISTANCE ON VALVE CLOSING.

Figure 38

to its original value in a very irregular manner. After the resistance had attained its original value, it still decreased and then again increased above the original value. In Figs. 38b and 38b', smooth envelopes of the resistance changes are shown as functions of H/Er(bulk) and H/Er(surface) atomic ratios. Because of technical difficulties, the temperature of the cold bath could not be kept constant at the melting point of iso-pentane (113°K). The effect of this is clear from Fig. 38a', in which the measurements took double the usual time (due to a fault in the resistance measuring system) which therefore allowed the temperature of the bath to increase during the experiment; this curve therefore shows a greater decrease in resistance below the original value followed by a greater increase than in Fig. 38a. To know the range of variation of this temperature with time, the temperature of such a bath (in the experiment with film No. 15) was measured by a thermocouple for about 40 minutes and a variation in temperature from 132 to 145°K was noticed. Thus the changes in resistance with composition are inconclusive due to the variation of the temperature of the bath, and experiments at some lower constant temperature are desirable. However, the magnitude of the resistance change at this temperature is smaller than that in experiments at room temperature; possibly the films are less porous (roughness factor 9 and 9.5) than those in the room temperature experiments (R.F. 14 and 15 for films 8 and 15 respectively).

10.5(3) Adsorption of hydrogen at liquid nitrogen temperature (78°K)

Four separate experiments were performed under similar conditions, but the results of hydrogen interaction with erbium films at this temperature were not reproducible. In each experiment, the source was thoroughly degassed as usual and the film was deposited at room temperature with the same rate of deposition. After about 20-25 minutes, the resistance became stable, then the adsorption vessel

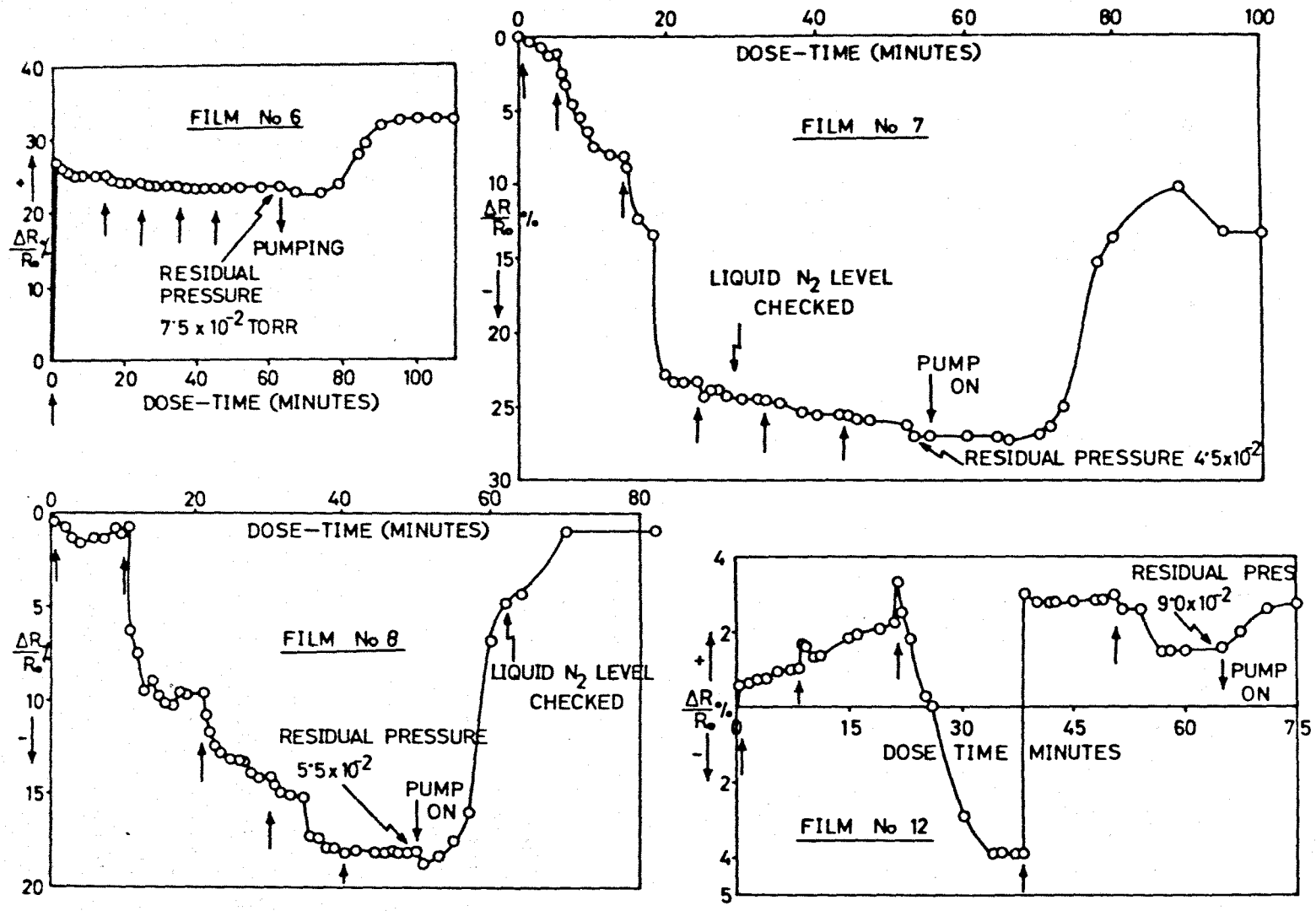

CHANGES IN THE ELECTRICAL RESISTANCE OF EVAPORATED FILMS OF ERBIUM DUE TO ADSORPTION OF HYDROGEN AT LIQUID NITROGEN TEMPERATURE. ↑ SHOWS THE TIME WHEN A DOSE IS ADDED.

Figure 39

was placed in a liquid nitrogen bath, and another 20-25 minutes later when the film attained equilibrium temperature, doses of hydrogen were introduced for adsorption. Very few doses of hydrogen were taken up by the films at this temperature before the residual pressure rose to 10^{-2} torr.

In one experiment, the resistance of the film (No. 6) increased by about 26% with the first dose and then it decreased slightly with subsequent doses but did not approach the bare film value. In another run (film No. 12), the resistance first increased slowly and irregularly to a maximum of about 3% then decreased to about 4% below the bare metal value and then increased again to about 3% above the original value. In the other two experiments with films 7 and 8, the resistance decreased slowly from the beginning and became stable at 27% and 18% below the bare film values respectively. On pumping out the unadsorbed hydrogen after completion of the interaction, the resistance of both the films increased and became stable at 13% and 1% below the bare film values respectively. These observations are shown in Fig. 39 for all the four films.

In two cases (films 7 and 12), film surface areas were measured before the films were exposed to room temperature, and in the remaining cases after hydrogen interaction had again been studied at room temperature. On an average, a surface coverage value of roughly unity ($\theta_6 = 1.1$, $\theta_7 = 1.03$, $\theta_8 = 1.1$ and $\theta_{12} = 1.23$) was measured which indicated that the hydrogen interaction at this temperature was possibly confined to the surface. In spite of the general observation of no resistance change in physisorption, in almost all experiments small irregular changes in resistance were observed during physisorption of krypton. In some cases the resistance initially increased and then decreased, and in some cases it decreased from the beginning, but in the majority of the cases the changes were reversible.

It is evident from the small value of the surface coverage at 78°K that the adsorbate is possibly staying on the surface, but it does not enable one to understand why under similar experimental conditions, the changes in resistance are irreproducible. Pronounced peaks in bulk electrical conductivity[25,26], specific heat capacity[28] and magnetic moment[27] measurements versus temperature have also been reported for bulk metal erbium around this temperautre (78 - 86°K). The bulk metal changes its anti-ferromagnetic state to a paramagnetic state about this temperature. To find out whether these irreproducible changes in resistance at this temperature could be due to this magnetic transition, a bare film in vacuum was repeatedly cooled to 78°K and exposed to room temperature. Most times the film did not recover its original stable values, and in six repetitions its resistance increased irregularly by about 10% at both the temperatures. It is unlikely that these irregular changes in the stable resistance values were due to film contamination, as the residual pressure was less than 10^{-9} torr. This observation, and the small irregular changes in resistance on krypton physisorption, suggest that possibly the films themselves were not stable at this temperature i.e. they were showing residual mixed magnetic states. This type of hysteresis effect was also observed[28b] when thermal conductivity measurements were made with increasing temperature (4.2-300°K) on a polycrystalline bulk erbium sample, i.e. the thermal conductivity values were different (about 6% at 19°K) when the measurements were repeated (twice) on the same bare erbium sample around these magnetic ordering transitions.

In two experiments with films 6 and 8, after the adsorption study at 78°K was over, and when the residual pressure had attained the 10^{-9} torr region, the interaction of hydrogen was again studied at 295°K. On the addition of these extra hydrogen doses, the resistance of each film increased by 15 - 19% at A and then decreased to its original value (that

Figure 40

HYDROGEN INTERACTION AT 295°K OF AN ERBIUM FILM (No 6) WHICH HAD ALREADY ADSORBED HYDROGEN AT 78°K. ARROW INDICATES THE TIME WHEN A DOSE IS ADDED.

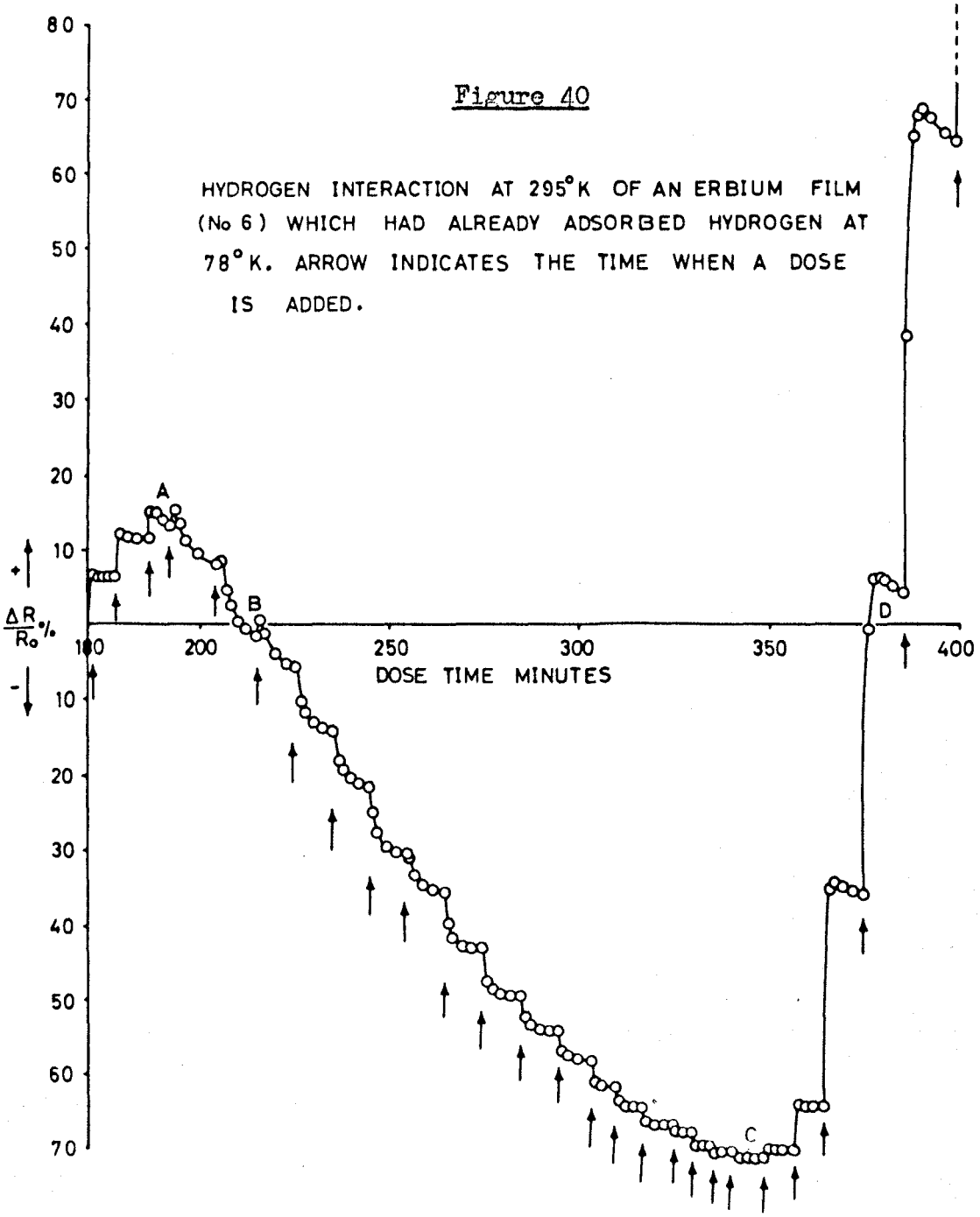

at the beginning of the interaction at 295°K) at B. Beyond the point B, the resistances continued to decrease and attained a minimum value at C (64 - 70% below the stable value at the beginning of the interaction at 295°K). After the point C, more hydrogen caused the resistance to increase rapidly, and it increased beyond its original value as shown in Fig. 40 for film No. 6. This showed that when the films were raised to room temperature after the interaction at 78°K was over, they showed the same behaviour as bare films towards hydrogen. The atomic ratios H/Er(bulk) at which the resistance attained its minimum and maximum values were comparable with those of the bare film hydrogen interaction at 295°K (compare films 6 and 8 with the others in Table II). In calculating H/Er atomic ratios for these films, the amount adsorbed at 78°K has also been included. This 15-19% increase in resistance on the addition of hydrogen at room temperature is again assumed to be due to surface adsorption. A part of the hydrogen chemisorbed at 78°K would have diffused into the bulk on warming the film to room temperature, and the surface sites so left vacant would again be covered with added hydrogen and thus increase the resistance.

10.6(1) Oxygen adsorption on erbium films at 295°K

From the mass spectrometric analysis of the residual gases (Chapter V), it was observed that the partial pressure of oxygen was not reduced significantly during and after erbium film formation, as compared to that of hydrogen which decreased from 10^{-8} to 10^{-11} torr in a few minutes. Thus it was thought advisable to study the oxygen interaction with erbium to understand the inability of erbium films to reduce the partial pressure of oxygen.

Figures 41 and 42 show the effect of oxygen adsorption on the resistance of two erbium films 5 and 13 respectively. With the first few doses, the resistance increased rapidly and then became almost

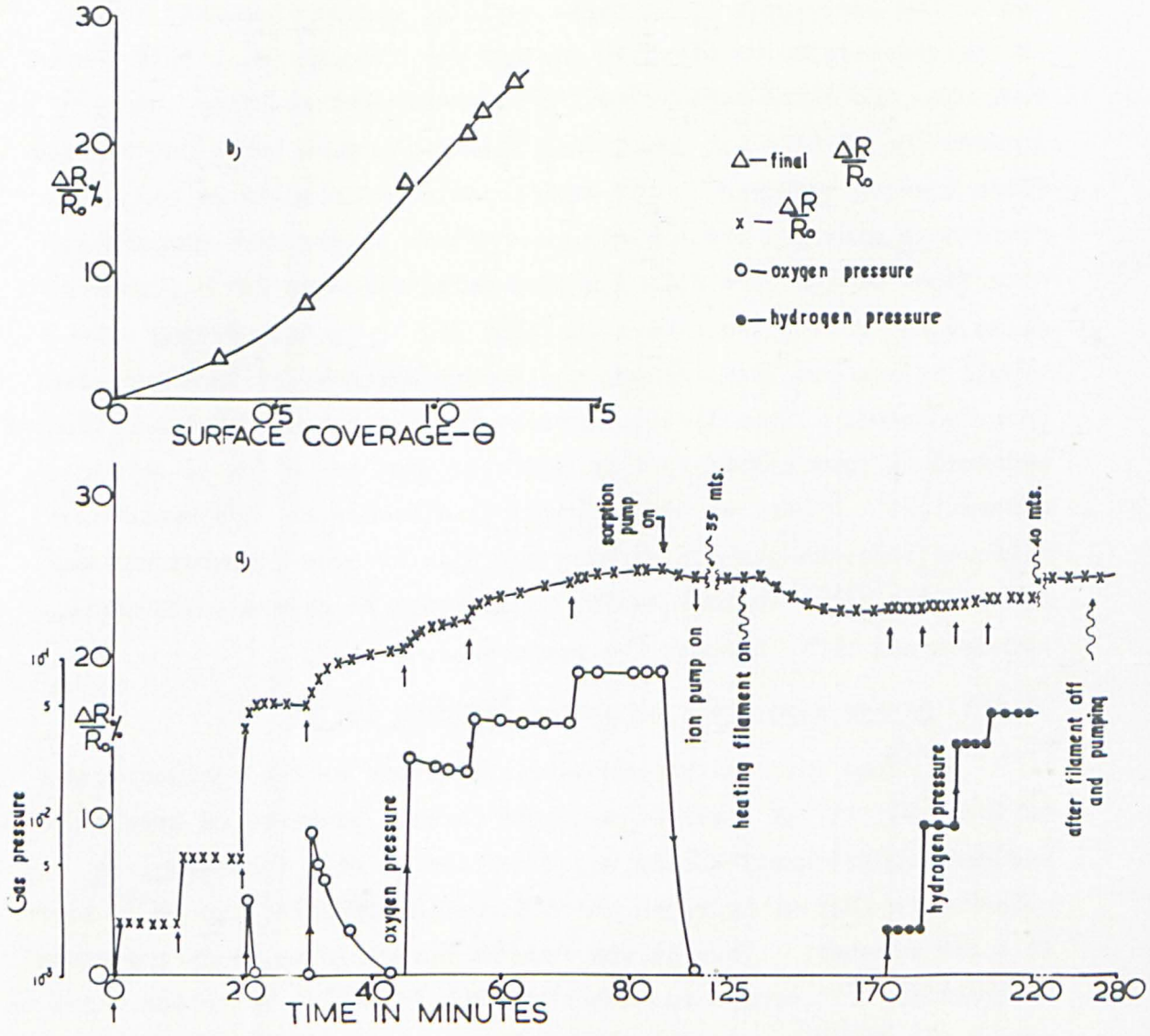

Effect of oxygen on erbium film resistance at 295° K

a) as function of dose and time. Each dose shown by arrow

b) final resistance after each dose as function of surface coverage

Figure 41

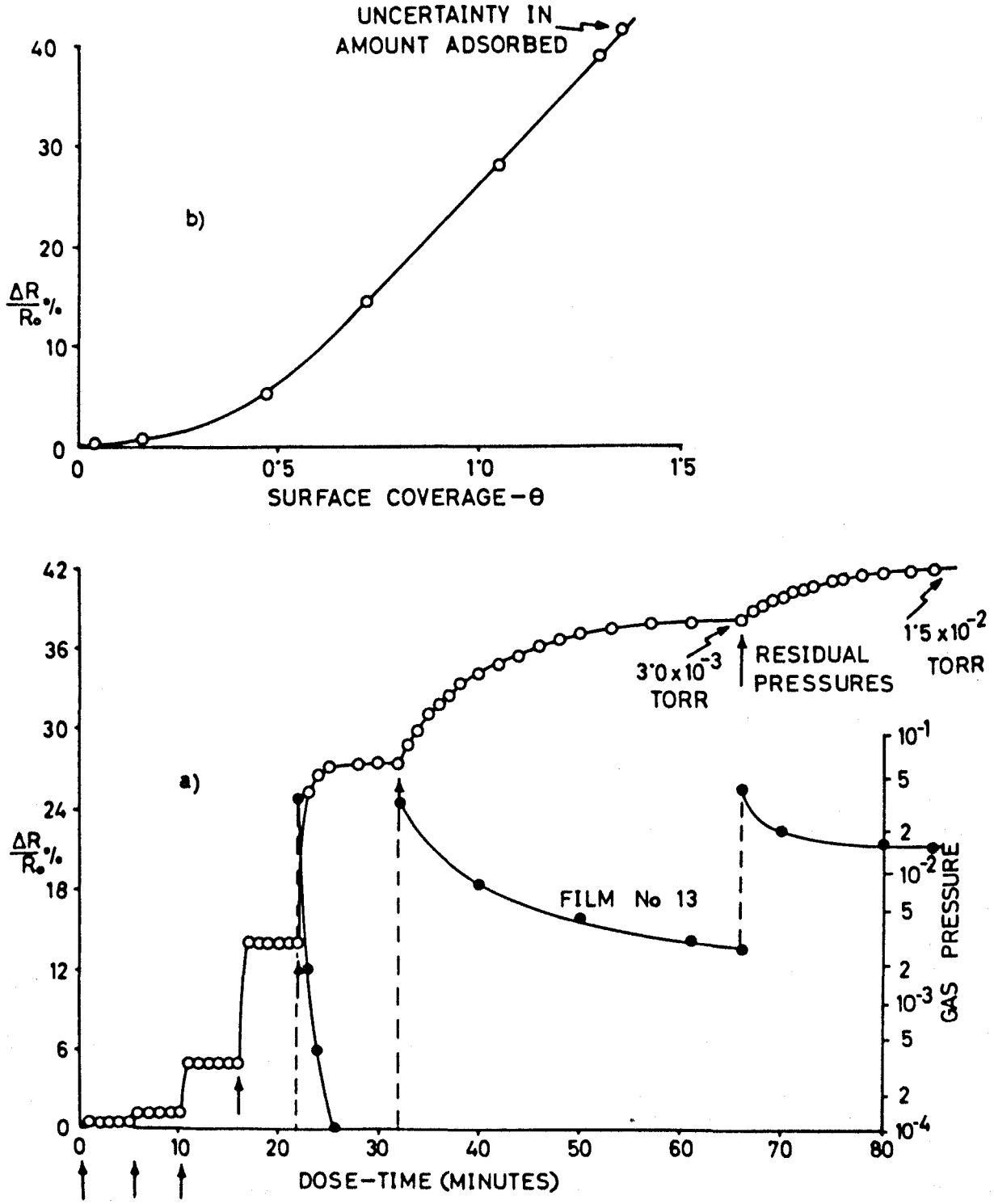

Figure 42

CHANGES IN RESISTANCE DUE TO ADSORPTION OF OXYGEN BY AN ERBIUM FILM AT ROOM TEMPERATURE (295°K).

stable throughout the time of observation of the dose. Subsequent doses also increased the resistance, but the rate of increase of resistance became slower with the number of added doses. Finally after about 6-7 doses of comparable size, the resistance almost became stable at about 25-40% above the bare film value. On pumping out this unadsorbed oxygen, no change in this stable value of resistance was observed.

The first two or three doses were completely adsorbed by the film, but the amount adsorbed from the subsequent doses decreased as the number of doses increased. The first few doses were immediately adsorbed while the next doses took some time for their partial adsorption. This is indicated in Figs. 41a and 42a: for the first two/three doses, the pressure remained below $10^{-3}/10^{-4}$ torr, and also the rate of attaining equilibrium pressure decreased with the number of doses and finally it reduced to zero (for film 5), which showed negligible adsorption of the final dose. From these simultaneous measurements of the changes in film resistance and gas pressure, it follows that the initial increase of the resistance is fast and independent of time (when the uptake of the gas is rapid) and is then followed by a time dependent and slow increase, which is accompanied by a similar slow uptake of the gas. The results of oxygen adsorption on film 4 were very similar to these given in Figs. 41a and 42a for the films 5 and 13, except the magnitude of the maximum resistance change, which was different for the different films, being about 30% for film 4, 25% for film 5 and 42% for film 13.

In Figs. 41b and 42b, final values of $\Delta R/R_o$ (measured at the end of each dose in Figs. 41a and 42a respectively) are plotted as a function of surface coverage-θ. For most of the range of surface coverage the resistance increased monotonically, and did not suggest any

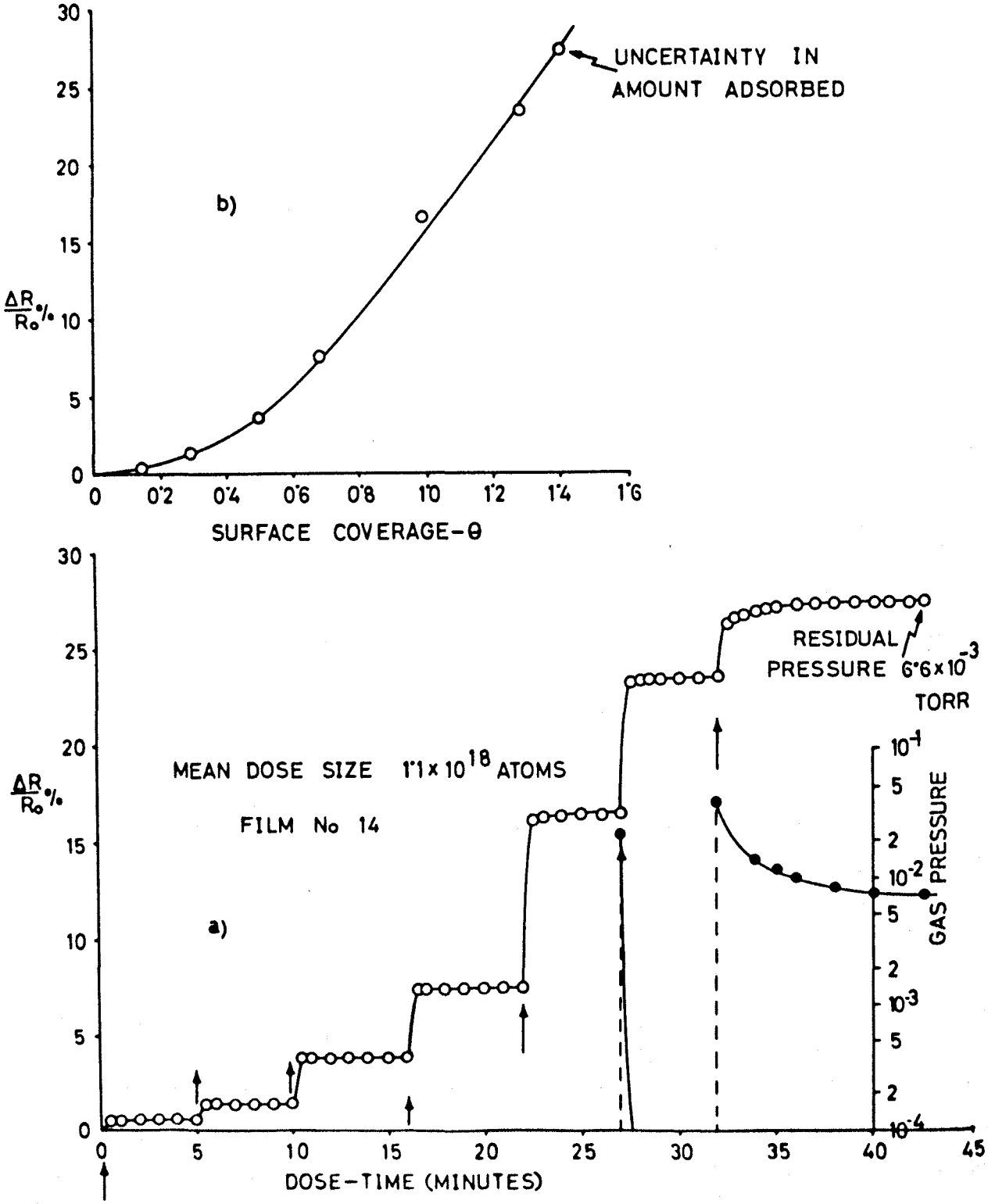

CHANGES IN RESISTANCE DUE TO ADSORPTION OF OXYGEN BY AN ERBIUM FILM AT SOLID CARBON DIOXIDE TEMPERATURE (200°K).

Figure 43

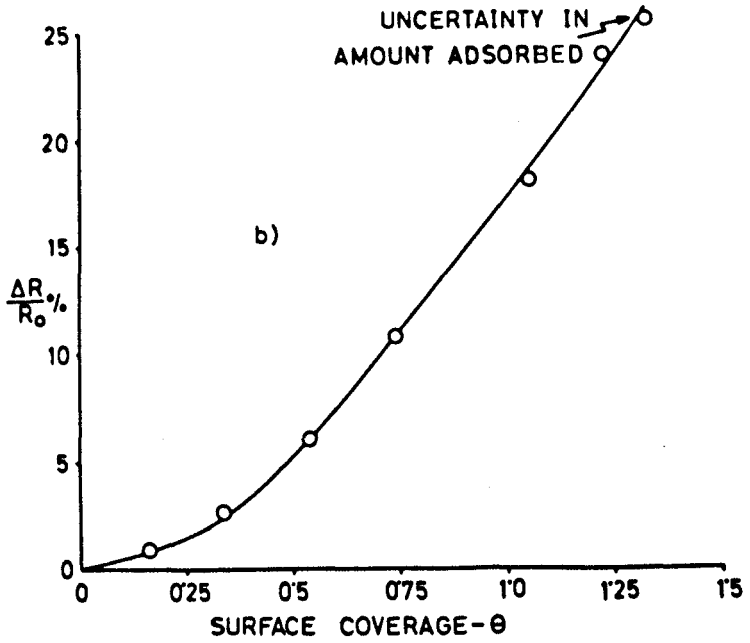

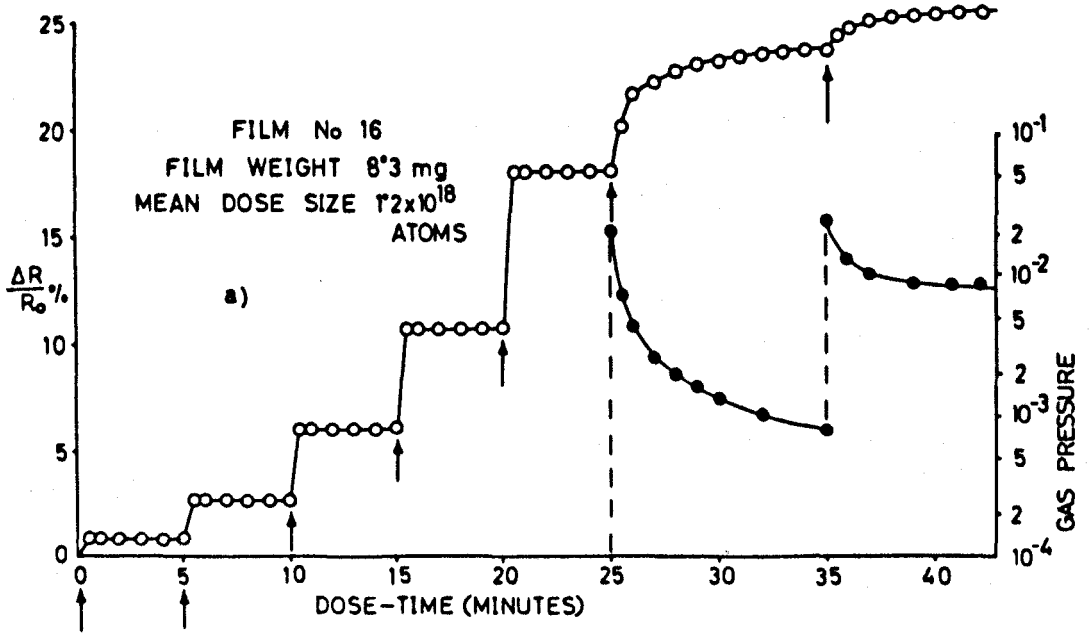

CHANGES IN RESISTANCE DUE TO ADSORPTION OF OXYGEN BY AN ERBIUM FILM AT SOLID CARBON DIOXIDE TEMPERATURE (200° K).

Figure 44

different adsorption laws for the fast changes and slow changes of resistance with time. In both the experiments, the final surface coverage measured is approximately equal (θ_5 = 1.27 and θ_{13} = 1.34), and during the slow increase of the resistance, the quantity of oxygen adsorbed is about 47% and 50% of the total amount adsorbed in the two cases respectively. The complete results for films 4, 5 and 13 are summarised in Table II, except the results of surface area measurement for film 4, which failed due to a technical error.

10.6(2) The adsorption of oxygen at lower temperatures

The study of the resistance changes with dose and time, owing to adsorption of oxygen on erbium films at room temperature, showed that the initial increase of the resistance was fast and independent of time, and in the later stage of adsorption it was followed by a time dependent and slow increase. Also, from the results of hydrogen interaction at the melting temperature of iso-pentane, it seemed that the maximum resistance change decreased as the temperature of the experiments decreased. These raised the author's curiosity to make some experiments on oxygen interaction at temperatures lower than 295°K to find out if the pattern of the resistance change with dose and time, and/or the magnitude of the maximum change would be influenced by the lower temperatures.

Two separate experiments with films 14 and 16 were made at the temperature of solid carbon dioxide in acetone (200°K). The results of oxygen interaction at this temperature are shown in Figs. 43 and 44 for these films. In figs. marked 'a', the resistance changes are plotted as a function of dose and time, and in figs. marked 'b' the stable values of the resistance changes (at the end of each dose) are plotted as a function of the surface coverage. The changes in resistance with dose and time are similar in both the experiments, and they again show the characteristic of the time independent and the time

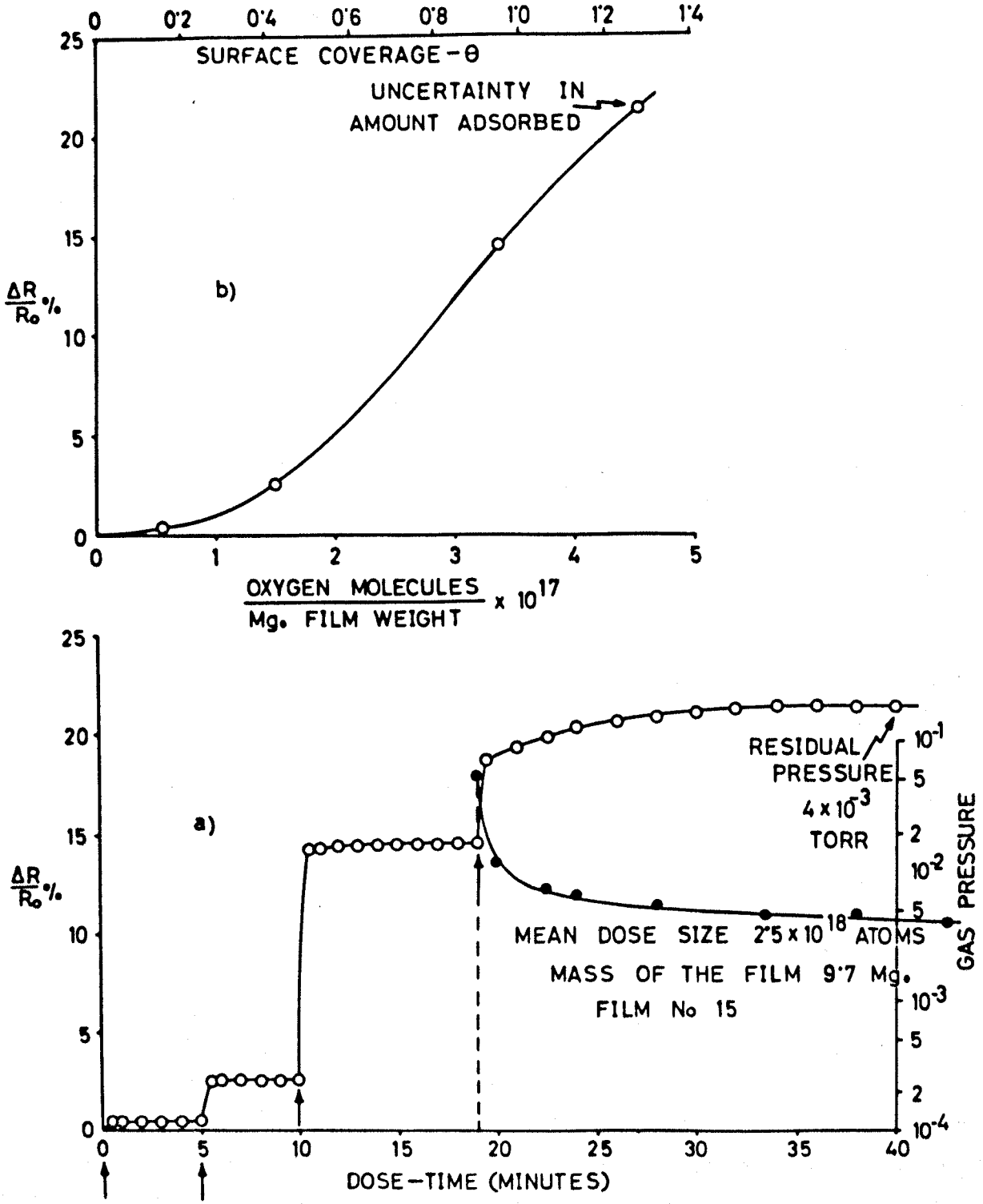

CHANGES IN RESISTANCE DUE TO ADSORPTION OF OXYGEN BY AN ERBIUM FILM AT M.P. OF ISO-PENTANE (TEMPERATURE 132-145°K).

Figure 45

dependent increases and are accompanied by the similar rapid and slow uptake of the gas respectively. During the slow increase of the resistance, the quantity of oxygen adsorbed by the two films was 15% and 20% of the total amount adsorbed in each case, but the measured final surface coverage values (θ_{14} = 1.41 and θ_{16} = 1.32) are comparable with the values measured in the room temperature experiments.

Another experiment with film 15 was performed at a still lower temperature (132 - 145°K) than 200°K. The results obtained are shown in Figs. 45a and 45b, in which the relative changes in resistance and their stabilised values at the end of each dose are expressed as function of dose and time, and the surface coverage respectively. The initial time independent increase of the resistance is still followed by the slow and time dependent increase. The final value of θ = 1.26 (within the experimental errors due to the high residual pressure at the end of the final dose and an uncertainty in the estimate of the exact volume of the adsorption vessel at the temperature of the experiment) is approximately the same as measured in the experiments at other temperatures, and the quantity of oxygen taken up during the slow process is 25% of the total quantity adsorbed. Big doses (approximately two and a half times the usual size of a dose in the other experiments) were introduced to complete the experiment in a shorter time to keep the temperature of the cold bath reasonably constant. In spite of this precaution, the temperature of the bath (measured by a thermocouple) increased from 132 to 145°K in about 40 minutes. Thus more experiments at this temperature were not thought advisable due to the variation of the temperature. However, instead of the one big final dose, if it had been introduced in two small separate doses, the slow process might have begun during the second dose. This would have then decreased the amount of oxygen taken up

during the slow process from 25% to possibly 12% of the total adsorption, which would have been comparable to the amounts taken up during the slow process in the experiments at 200°K.

10.6(3) Discussion - Oxygen adsorption

From these measurements of the changes, due to the adsorption of oxygen at all the temperatures (132-145°K, 200°K and 295°K), it follows that the initial increase of the resistance is fast and independent of time (when the uptake of the gas is rapid), and is followed near saturation of the process by a slow and time dependent increase with a similar slow and time dependent uptake of the gas. This slow increase of resistance may be due to either a surface adsorption (i.e. a natural slowing of the process near saturation as a small number of surface sites and less accessible places will be available near the end) or a bulk sorption (i.e. lattice incorporation and bulk oxide formation). This is difficult to decide by these measurements alone, as both the processes seem to have a similar slow positive effect on resistance. However, the quantitative measurements of the final surface coverage (which is only slightly greater than unity and varied from 1.26 to 1.41) show that bulk oxidation is probably restricted at all the temperatures of study, and the adsorbate is possibly confined to the surface only. Also for most of the adsorption, the monotonous increase of the resistance with the surface coverage (i.e. irrespective of the fast and slow uptake of oxygen) suggests that both types of uptake are similar in their effect on the resistance and are thus most probably surface phenomena.

The slight difference from unity of the value of the surface coverage may be due to errors involved in the methods of surface area measurement and surface site calculation, but its value being always greater than one suggests more likely a small incorporation or diffusion

below the measured surface. Since θ is always constant at all the temperatures of study, diffusion (and adsorption) ~~on~~ *in* the places which are not measured in the surface area by the physical adsorption of krypton, is more likely than lattice incorporation, as the latter (highly activated process) would lead to a smaller value of θ at lower temperatures than at room temperature. These less accessible places should be smaller than 4 Å in dimensions (capillaries of type B, see Fig. 47), where a krypton atom (van der Waals radius[43] 1.98 Å) would not be physisorbed, but oxygen atoms (covalent diameter 1.32 Å) and negative ions (diameter 2.72 Å) could possibly diffuse without any activation energy. This diffusion is a more likely suggestion for a greater than unity value of θ, but with such a small value of θ nearly equal to 1, one cannot reach any other conclusion than the restriction of oxygen to a monolayer i.e. the diffusion (if it is there) is indeed very small.

With decrease of temperature, there is usually a decrease in the total surface coverage after a certain fraction of the surface has been covered by the fast adsorption. This decrease in the quantity of gas adsorbed in a given time during the slow uptake could be interpreted as a slowing of incorporation into the bulk (due to decrease of activation energy and mobility of the adsorbate at lower temperatures). Although such a decrease was observed in the lower temperature experiments, an equal increase occurred in the amount adsorbed during the initial fast uptake, which is unusual. This unusual θ-temperature dependence may arise because the film may be exposing different proportions of crystal planes at different temperatures. Hence, the measured θ alone is possibly inadequate to give some specific significance to the fast and the slow processes, except that both seem to be a surface phenomenon.

For a particular adsorbent-adsorbate combination, the magnitude of the maximum resistance change on adsorption depends on the structure and condition of the bare film, and on the amount and position of the adsorbed species. In the room temperature experiments, the different magnitudes of the resistance changes - 25% for film 5, 30% for film 4 and 42% for film 13 (under similar dose and other experimental conditions), is possibly due to slightly different structures and porosities of the films (R.F. being 9, 10 - from the graph, and 13 for the respective films), i.e. a film with more open defects will possibly undergo a larger change in resistance on gas adsorption.

The surface area of the films was measured after the oxygen interaction, except for one film (No. 13) when it was measured both before and after oxygen adsorption about 12% increase in surface area was observed. A decrease in film surface area has usually been reported on oxygen adsorption with unsintered films, and is hitherto attributed to the sintering of the films due to the high heat of adsorption and to blocking of open capillaries in the films. This observed increase in surface area indicated in the first place that the films were well annealed during their formation, and the slight increase may be due either to a change in the lattice constants of the surface atoms or in the selective nature of the physisorption, as the nature of the surface was changed.

10.7 Hydrogen/Oxygen adsorption on films which had interacted with Oxygen/Hydrogen at 295°K

Upon completion of the oxygen adsorption at 295°K with two films (4 and 5), the unadsorbed gas was pumped out, and when the residual pressure fell in the region of 10^{-9} torr, the films were again exposed to hydrogen at room temperature. In one run (experiment with

film 4) doses of molecular hydrogen were introduced, and in another experiment the film (No. 5) was exposed to atomic hydrogen. Hydrogen was atomised by a red hot molybdenum filament, which was kept red hot in the adsorption vessel for a long time before hydrogen was introduced. A change in the film resistance was observed when the filament was switched on, but it became stable when the film attained an equilibrium temperature. On switching off the filament and repumping the residual hydrogen after the experiment, the resistance again attained the same stable value that it had before the filament heating, so it was evidently a temperature effect. Some four doses of hydrogen of usual size were introduced at equal intervals of time, and the resistance was measured for about an hour, but in both cases no change in the resistance of the films was observed. Also, the pressure of hydrogen in the adsorption vessel increased above 10^{-3} torr with the first dose and then it remained constant. A similar behaviour was observed with subsequent doses as shown in Fig. 41a, which directly gave the idea of no adsorption of hydrogen in any form.

These observations suggested that the hydrogen neither formed a bond with the erbium surface atoms nor with the chemisorbed oxygen. Consequently oxygen seems to have blocked the erbium film surface. A similar behaviour has also been reported with the metals yttrium[115], titanium - see Appendix A, and with molybdenum and copper[116] (in the case of oxygen covered molybdenum and copper films, an interaction with atomised hydrogen was reported).

In another experiment with film 6, after the completion of the hydrogen interaction at 295°K and when the resistance of the film had stabilised in the dihydride region, oxygen adsorption was studied at room temperature. The resistance slowly increased with each dose and the final value of the relative increase in resistance after a few doses was much bigger than that due to oxygen on a bare film. This

showed that the film which had already interacted with hydrogen was still active towards oxygen i.e. hydrogen did not block the film surface as oxygen did. Such extensive interaction has been observed with most of the metals (palladium, rhodium and nickel)[116,117]; with films of molybdenum, displacement of preadsorbed hydrogen with oxygen is reported. However, it was not thought helpful to study such interaction in detail, as in the case of erbium, the interaction is difficult to explain due to the complicated nature of the pre-hydrogen-interacted film surface.

From the thermodynamical point of view, replacement of a pre-adsorbed gas by another is not possible unless the total ΔF is negative (assuming ΔS is small) i.e. the total ΔH is negative. In general, on metals, ΔH for hydrogen is less than ΔH for oxygen, and therefore replacement of pre-adsorbed oxygen by hydrogen would be accompanied by total positive ΔH, i.e. the process would be an endothermic one, which is contradictory to the nature of adsorption. On the other hand, replacement of hydrogen by oxygen is possible, as the process is accompanied by total negative ΔH.

10.8 Conclusion

At room temperature, the surface interaction of hydrogen with erbium is followed by its bulk sorption, and dihydride and trihydride are formed. Experiments on hydrogen interaction with erbium at temperatures lower than 295°K were made to find out if the bulk sorption could be restricted. From the experiments carried out at 200°K, approximately 130-160°K and 78°K, it follows that a temperature as low as 78°K would be needed to restrict the bulk hydride formation. However, resistance changes at 78°K were not reproducible, most probably due to a magnetic transition (AFM-PM) of the bulk metal which takes place around this temperature. At all the temperatures of study (132-145°K, 200°K and 295°K), the oxygen interaction is possibly

confined to the measured surface only. Oxygen is more strongly adsorbed on the film surface than hydrogen i.e. it blocks the surface and makes it completely inactive with respect to both molecular and atomised hydrogen. On the other hand a hydrogen saturated film of erbium (to the stage of erbium dihydride) is still capable of interacting with molecular oxygen.

From the point of view of the large uptake of hydrogen, erbium is an excellent getter. However, because of the brittle nature of its hydrides and the poisoning effect of oxygen, the metal could not be used in the construction of getter-ion pumps, but it could possibly be used as a second stage getter to remove the last traces of hydrogen, which is the major constituent of the residual atmosphere in titanium sputter-ion pumped vacuum systems.

CHAPTER XI

QUANTITATIVE INTERPRETATION OF THE RESULTS, GENERAL REMARKS AND SUGGESTIONS FOR FURTHER WORK

11.1 Introduction

The experimental technique of studying adsorption by measuring the change in electrical resistance of an evaporated thin film as a function of the amount of gas adsorbed on it is simple, but the quantitative interpretation of the results is often difficult and requires many assumptions concerning the film structure and the mechanism by which the gas causes the resistance to change. Hence, unless it is specified which mechanism is predominating, exact deductions concerning chemical bond formation are not possible. However, from the results for the film structure and the electrical properties, a rough idea about the predominating mechanism or mechanisms can be made and the nature of electronic interaction can be speculated.

11.2 Simple quantitative aspect

The different mechanisms for the resistance change on adsorption have been discussed in Section 7.3. An interpretation will be given using two of the mechanisms, as the other mechanisms are of less importance for these continuous films with completely diffuse scattering. The first is that the adsorption of gases causes surface atoms to later their spacing with respect to the bulk, thus losing the property of metallic conduction. The second is that adsorption involves conduction electrons of the metal, thereby changing the concentration of the charge carriers and hence the resistance of the film. If the first two assumptions discussed in Section 7.4 are assumed to be roughly applicable to the results, then the relative change of electrical resistance is expressed by the simple equation 7.7 as

$$-\frac{\Delta\sigma}{\sigma} = \frac{\Delta R}{R} = \alpha \frac{n_g}{N}$$

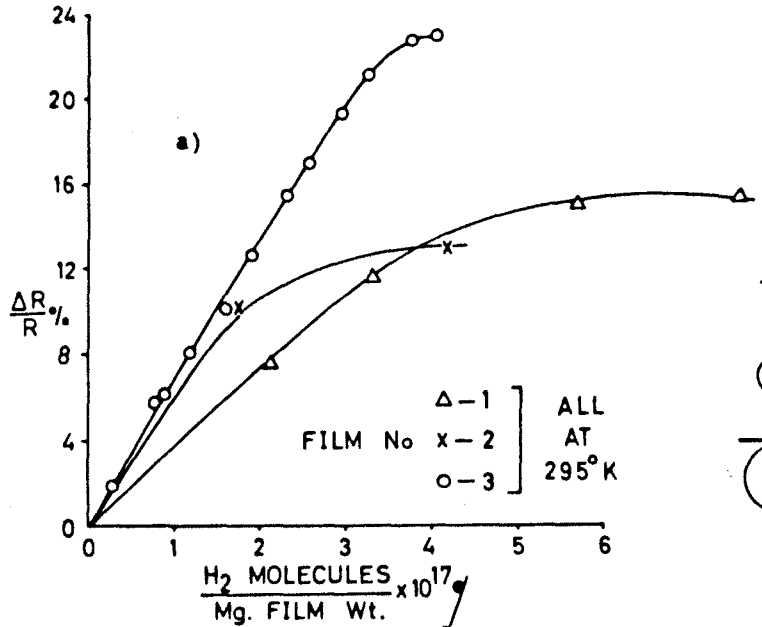

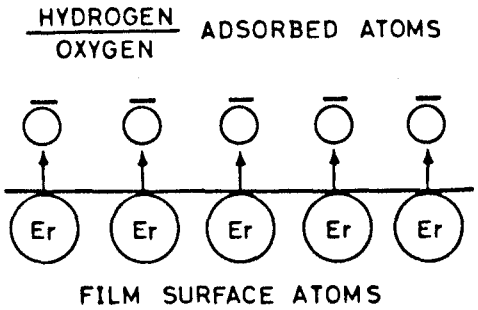

C)

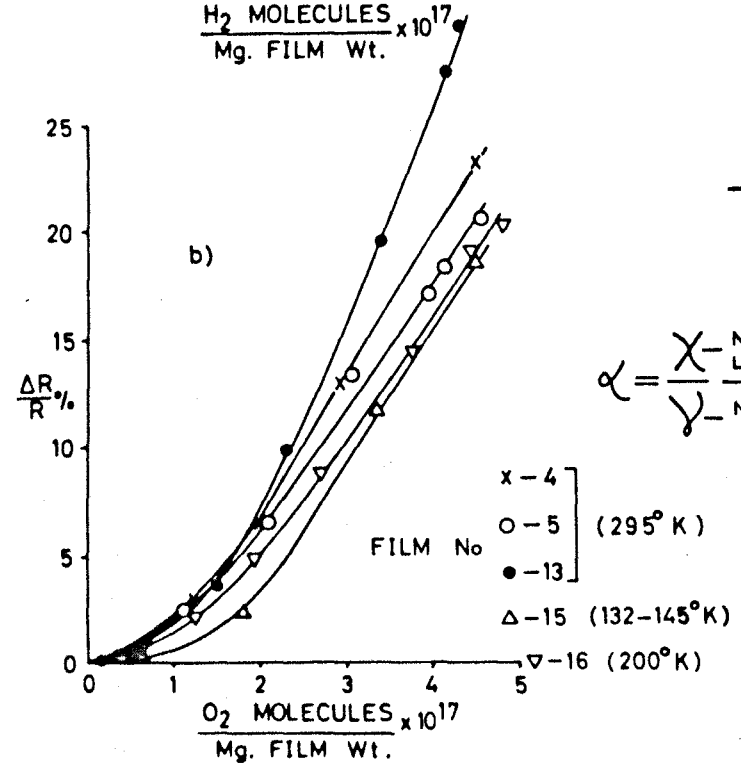

$$-\frac{\Delta\sigma}{\sigma} = \frac{\Delta R}{R} = \alpha \frac{n_g}{N}$$

$$\alpha = \frac{\chi - \text{No OF CONDUCTION ELECTRONS IMMOBILISED BY ONE ADSORBED GAS MOLECULE}}{\gamma - \text{No OF EFFECTIVE CONDUCTION ELECTRONS PER METAL ATOM}}$$

CHANGES IN ELECTRICAL RESISTANCE OF EVAPORATED FILMS OF ERBIUM DUE TO ADSORPTION OF a) HYDROGEN, b) OXYGEN. C) DIAGRAMMATIC REPRESENTATION OF CHEMISORPTION OF BOTH THE GASES.

Figure 46

where $R = R_o + \Delta R$ is the electrical resistance, R_o the initial resistance of the bare film, ΔR the increase of the resistance by the adsorption and the other letters have their usual meaning as in equation 7.7.

Figures 46a and 46b give the relative change in the electrical resistance as a function of the number of adsorbed gas molecules per mg. film weight. In the case of hydrogen adsorption, the relative change in resistance first increases linearly with the number of chemisorbed molecules, then there is a bend in the curve and finally it decreases well below its original value (not shown in the figure). This decrease (and a further increase at higher doses) is a bulk interaction as discussed in Section 10.4. In the case of oxygen adsorption, the curves have a gradually increasing slope in the initial stages and a reasonably straight section during most of the adsorption. From the slopes of these straight parts the fractional change in resistance due to the number of adsorbed molecules per metal atom i.e. the α values can be derived.

The values of α calculated from these curves are shown in Table II. The α values found experimentally for both the gases are approximately 2. These α values could be interpreted in terms of the adsorption bond if the last two assumptions discussed in Section 7.4 are satisfied. The first is valid as the values are calculated from the linear parts of the curves, which signify that there is only one binding state of the adsorbed species on the film surface. The second is also possible, as discussed at the end of Sections 10.3 and 10.6(3), that a large fraction of the adsorbates is restricted to the surface of the film, where all adsorption sites may be assumed equal in their effect on the film resistance.

An interpretation based on the first mechanism would mean that α is simply the number of metal atoms to which the adsorbed molecule bonds (see Appendix II). Then the value $\alpha = 2$ means that each gas molecule forms bonds with two erbium atoms. On the other hand if the second mechanism is assumed to operate, then α is related to the gas metal bond parameters[79] by

$$\alpha = \frac{\chi}{\gamma}$$

where χ is the number of conduction electrons immobilised by the adsorption of one molecule i.e. No. of chemical bonds formed per adsorbed molecule and

γ is the number of effective conduction electrons per metal atom.

For hydrogen, it is reasonable to assume that at room temperature the molecule dissociates in the adsorption process, so that two bonds are formed per molecule, thus χ (hydrogen) = 2. This yields γ value for erbium surface atoms of approximately 1. Thus each erbium surface atom forms one chemical bond i.e. there is only one conduction electron available with each surface atom, contrary to the three valence electrons available with each bulk atom. The calculated value of γ of about unity for the erbium surface atoms yields a value of χ for oxygen of about 2. This means oxygen also possibly dissociates on chemisorption into atoms, and that each atom makes one bond with a surface atom. This is contradictory to the usual observation of two electrons taken by each oxygen atom. Thus either the assumptions involved are not justified due to the unknown structure of the films (i.e. different from that of the bulk) or the model is too simple to reveal the bonding. However, the calculated value of γ of about unity for erbium surface atoms is roughly in agreement with the measured surface coverage value (1.2-1.4) for both the gases. Also the increases in the work function

(of assumed fully covered surfaces) of erbium films due to adsorption of hydrogen[110] (0.53 eV) and oxygen[118] (0.38 eV) are roughly equal in magnitude. Thus for both the gases, chemisorption may be diagrammatically represented as shown in Fig. 46c.

11.3 General remarks

The above conclusion is drawn when a single mechanism of resistance change on adsorption is assumed to predominate over all other mechanisms. It is shown in the following paragraphs that the 30% change in electrical resistance observed in these experiments cannot be accounted for by one predominating mechanism alone, nor even by all the mechanisms operating simultaneously.

In the case of the room temperature hydrogen interaction, the initial increase of resistance has so far been assumed to be due to surface adsorption. The $\Delta R/R_o$(maximum) at A due to adsorption of hydrogen, and the final value of the increased resistance due to adsorption of oxygen, occurred at an average atomic ratio of gas to bulk metal of about 0.25 (see the 9th row of Table II). If the change in resistance on adsorption was solely attributed to a change in the number of conduction electrons of the film metal, then the relative change (decrease) in the number of conduction electrons of the film at this ratio will be 0.25/3 (as each gas atom is assumed to withdraw one conduction electron from the film material, and each bulk erbium atom is assumed to contribute three conduction electrons - see Appendix III). Thus it follows from equation 7.6 that the maximum decrease in conductance of the films would be (2/3) x (0.25/3) i.e. about 5.6% (or 11% if each oxygen atom is assumed to withdraw two conduction electrons of the metal atom), which is much less than the 30% increase in resistance observed experimentally due to both the gases.

The films studied for gas adsorption varied in their thickness from 110 to 630 Å, thus a film of 370 Å mean thickness may be chosen for simple arguments and illustration. If it is assumed that on a statistical average a surface layer 3 to 4 atoms thick was de-metallised due to adsorption of the gases, then from equation 7.10, the increase in resistance for this film ($K = \frac{d}{\ell_o} = 2$, $\ell_o = 185$ Å, see Section 3.3) due to de-metallisation of about 10 Å thick (diameter of an erbium atom 3 Å) surface layer will be about 3%. This is also much less than the observed magnitude of the resistance increase.

On the other hand, if it is assumed that the films originally had some value for the specular reflection coefficient 'P' say a maximum of 0.3 (which is highly unlikely as the measured high resistivity for fresh films of erbium in Section 3.2, shows that the films are probably completely rough), and on gas adsorption the film was completely reduced to diffuse scattering, then from the relation 7.12, a maximum increase in resistance of 5% would be expected. The corrected expression of Horiuti and Toya (see Appendix I) for the resistance change due to a change in 'P' also gives about 7% increase in the resistance of the same film for the same change in 'P'. So this mechanism also cannot alone account for the large observed increase in resistance.

The fourth possibility discussed under Section 7.3 is not applicable to these continuous films as is evident from their comparatively low resistance and positive TCR. A 5% change in the electrical resistance of metal films (reported by many authors on gas adsorption), could be explained by any of the mechanisms discussed above, but there is unlikely to be a 20% to 40% change in resistance even when all the three possibilities mentioned above are assumed to operate simultaneously. It is not unusual to observe such a large change in resistance as Bastl[119] and Kawaski et al.[120] have also reported about 20% and 100% change in resistance of

A DIAGRAMMATIC SECTIONAL REPRESENTATION OF A POLYCRYSTAL EVAPORATED FILM. A SMALL SQUARE REPRESENTS ONE ATOM AND THE HATCHED LINES SHOW DIFFERENT CRYSTAL ORIENTATIONS.

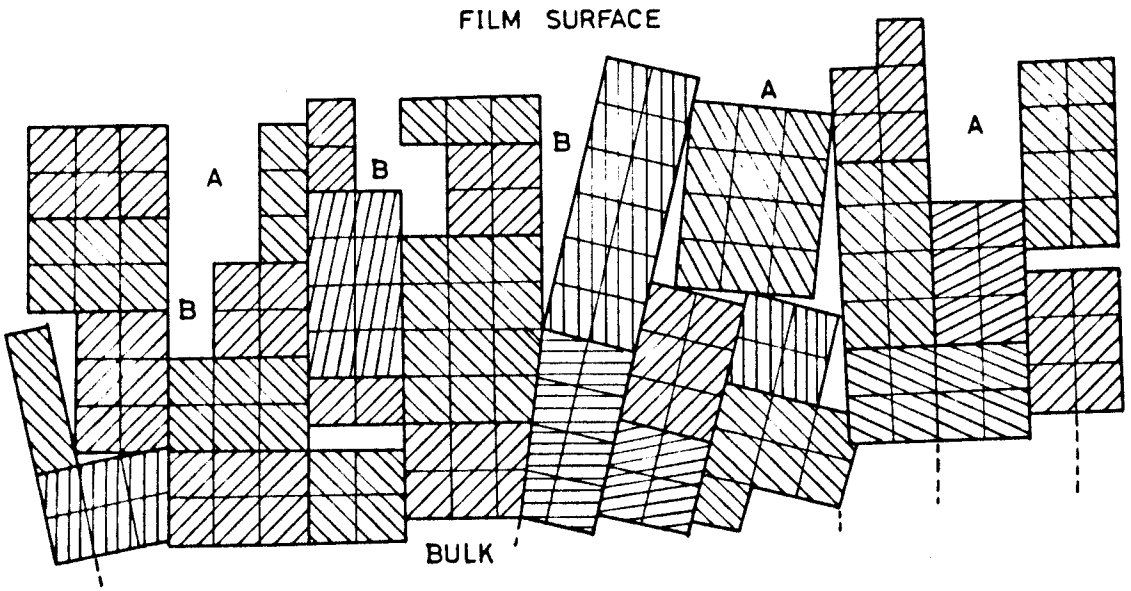

A [Broad capillaries > 4 Å dia. Measured in surface area by krypton physisorption.

B [Narrow capillaries, grain boundaries and dislocation lines etc., < 4 Å dia. not measured by krypton physisorption.

Positions of less accessible places where oxygen and hydrogen atoms could diffuse.

Erbium atomic diameter = 3·5 Å
hcp structure, a = 3·559 Å, c = 5·587 Å

Krypton atomic diameter (vander Waals) = 3·96 Å

HYDROGEN [Covalent diameter = 0·56 Å; Negative ion (H^-) = 2·72 Å

OXYGEN [Covalent diameter = 1·32 Å; Negative ion (O^{--}) = 2·72 Å

Bare films could electrically conduct by electron tunnelling through both the types of capillary (A and B), but on capillary gas adsorption, the potential barrier across it increases which decreases the probability of electron tunnelling and therefore the resistance increases more than the expected theoretically due to the surface adsorption.

Figure 47

molybdenum and titanium films respectively due to oxygen adsorption. Thus in addition to these possibilities there is some other cause which is also contributing to the large observed increase in resistance. All the possibilities discussed above, basically assume the structure of the films to be the same as that of the bulk metal i.e. slices of bulk metal, but in fact, the structure of an evaporated polycrystalline metal film is generally different from that of the bulk metal and it suffers from many structural defects, mainly large grain boundaries, dislocation lines and capillaries etc., as shown in Fig. 47 and discussed at the end of Section 10.2. Small entities adsorbed on an open capillary would make a localised region of high resistance (due to decrease in the probability of electron tunnelling across the gaps) which would reduce the effective cross-section for conduction of the film and thus would increase its resistance enormously. Hence, the most likely cause of the observed big resistance changes is the porous structure of the films, and diffusion and adsorption on open capillaries, grain boundaries and dislocation lines reaching the film surface. Although the study with the electron microscope (Chapter IV) did not give any evidence about the structure of clean fresh films of erbium, it did show that at least the aged films had fine grain sizes and therefore a large area of grain boundaries. The quantity of the adsorbates diffusing in the narrow capillaries i.e. Type B (Fig. 47) is indeed very small but seems to require no activation energy, as the final θ values (for oxygen, and at the point A for hydrogen) measured at all the temperatures of study are approximately equal and very nearly one.

11.4 Suggestions for further work

In the case of polycrystalline evaporated films, quantitative interpretations of the resistance changes on adsorption are complicated due to the various possibilities which could change the resistance. The effect on resistance due to grain boundary adsorption could be reduced

if the adsorption study was made on single crystal epitaxial films at moderately low temperatures. Because of the dependency of resistance on many factors, in addition to the measurements of resistance changes, simultaneous work function measurements or some other type of study would help in interpreting the resistance changes. However, the work function being a surface property, deductions from its measurements alone would be complicated in systems where surface interaction is followed by bulk sorption.

For better understanding of the interaction and comparison with the present results, it would be of interest to study simultaneous changes in the resistance and work function of some other metals (possibly molybdenum) where interaction of hydrogen is restricted to the surface only.

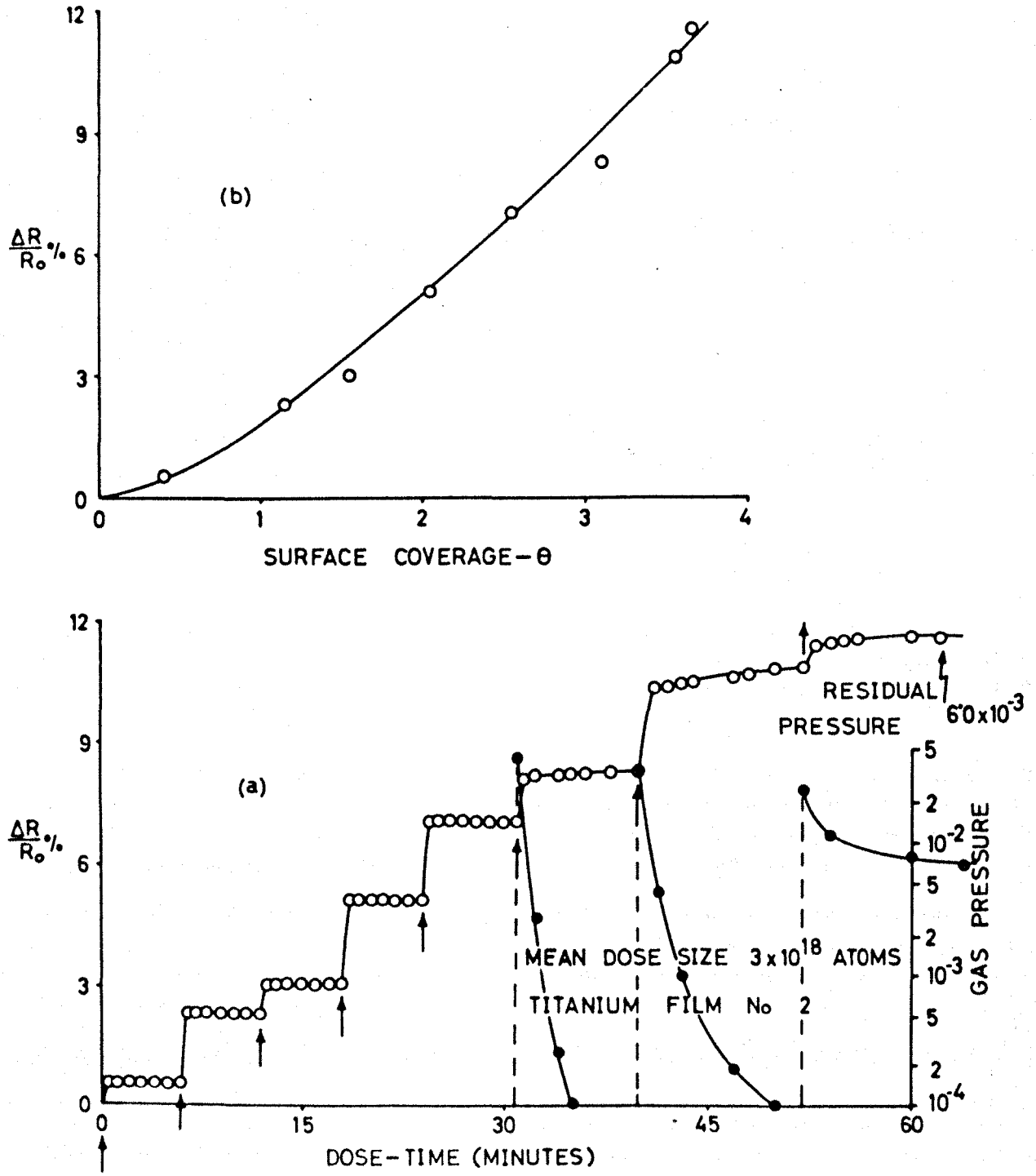

CHANGES IN RESISTANCE DUE TO ADSORPTION OF OXYGEN BY A TITANIUM FILM AT ~~THE~~ ROOM TEMPERATURE (295°K).

Figure 48

APPENDIX A

Summary of the changes in resistance of titanium films due to interaction of oxygen at room temperature (295°K)

Using the same apparatus and the techniques, as described in the second part of this thesis, three separate experiments were performed with titanium films (purity of the metal is quoted as 99.97%), and the results obtained are summarized in table below. The changes in resistance due to interaction of oxygen with all the films were similar, and the results for one of the films (No. 2) are shown in Figs. 48a and 48b as functions of dose and time, and surface coverage-θ respectively.

Film No.	1	2	3
Mass (Mg)	13.2	15.8	5.8
Mean thickness (Å)	935	1115	410
Roughness factor	5.6	7.0	3.0
Surface area (cm^2/mg)	310	335	390
Initial resistance - R_o (Ω)	49.56	36.87	99.25
Final $\Delta R/R_o$ %	14	12	18
Final surface coverage-θ	5.3	3.7	5.6
Oxygen atoms/bulk metal atoms	0.15	0.11	0.20

Remarks:
1. Number of surface sites used for evaporated polycrystalline films of titanium = 1.135×10^{15} per sq.cm.
2. Molecular hydrogen was not adsorbed (and no change in resistance) on the films which were previously interacted with oxygen at room temperature.
3. There seems a little possibility of adsorption of atomized hydrogen on pre-oxygen-interacted films, but no change in resistance was observed.

APPENDIX I

As mentioned in Section 7.3(3), a part of the mathematical analysis of the papers by Horiuti and Toya[76,77] appeared to be invalid. The author wrote to the editor of the volume drawing his attention to these errors, and eventually the authors (H and T) of the original papers sent the table of corrections which is given here. The corrected expression for the resistance change due to a change in 'P' predicts a much smaller change of resistance than was observed (as discussed in Section 11.3).

ERRATA*)

		erroneous	correct
p.28	(4.6)	$\sigma = \sigma_0 \Phi_p(d/l)/(d/l)$	$\sigma_0 = \sigma\, \Phi_p(d/l)/(d/l)$
p.28	(4.7)	$\frac{x}{\Phi_p(x)} = 1 - \frac{3}{2x}(1-p)\int_0^{\infty} \cdots$	$\frac{x}{\Phi_p(x)} = 1 - \frac{3}{2x}(1-p)\int_1^{\infty} \cdots$
p.28	(4.9)	$R(d) = \frac{c'}{d^2}\frac{mv}{ne^2}\left(\frac{d}{l}\right)\{\Phi_p(d/l)/(d/l)\}^{-1}$ or $cR(d)d^2 = (d/l)^2/\Phi_p(d/l)$	$R(d) = \frac{c'}{d^2}\frac{mv}{ne^2}\left(\frac{d}{l}\right)\{\Phi_p(d/l)/(d/l)\}$ or $cR(d)d^2 = \Phi_p(d/l)$
p.29	ordinate of Fig. 4.5	$\sigma_0/\sigma = \left\{\Phi_p(d/l)/(d/l)\right\}^{-1}$	$\sigma_0/\sigma = \left\{\Phi_p(d/l)/(d/l)\right\}$
p.29	(4.12)	$c\delta R(d)d^2 = (d/l)^2/\Phi_p(d/l) - (d/l)^2/\Phi_{p_0}(d/l)$	$c\delta R(d)d^2 = \Phi_p(d/l) - \Phi_{p_0}(d/l)$
p.30	caption of Table 4.1	$(d/l)^2/\Phi_p(d/l) - (d/l)^2/\Phi_{p_0}(d/l)$	$\Phi_p(d/l) - \Phi_{p_0}(d/l)$
p.30	(4.13b)	$\delta R(d)/R(d) = -\frac{\delta p}{2}\{\Phi_{p_0}(d/l)/(d/l)^2\}$	$\delta R(d)/R(d) = -\frac{\delta p}{2}\left[\Phi_{p_0}(d/l)\right]^{-1}$
p.31	ordinate of Fig. 4.6	$(d/\ell)^2/\Phi_{p_0}(d/\ell)$	$\Phi_{p_0}(d/\ell)$
	caption of Fig. 4.6, 2nd line	$cR(d)d^2 = (d/l)^2/\Phi_{p_0}(d/l)$	$cR(d)d^2 = \Phi_{p_0}(d/l)$
	4th line	$(d/l)^2/\Phi_{p_0}(d/l)$	$\Phi_{p_0}(d/l)$

*) Figures in Figs. 4.5~4.8 remain correct and Table 4.1 as well numerically, if the designation of the ordinates of figures, and caption of the above tablo are corrected in accordance with the above ERRATA; that is, the figures were drawn and the table was made by making use of the correct expressions, as checked with reference to Appendix C in the paper of Toya, J. Res. Inst. Catalysis, Hokkaido Univ., 8, 209(1961) or Table 1 of Sondheimer's paper, Advances in Physics 1, 1(1952).

APPENDIX II

Assuming the metallic films have a homogeneous plate-like structure i.e. a slice of bulk metal (second assumption of the first two - see Section 7.4), then the relative decrease in thickness ($\delta d/d$) of the conducting phase would equal the fraction of the metal atoms ($\delta N/N$) involved in the chemisorption bond, if the occupied metal atoms lost their metallic character i.e.

$$\frac{\delta d}{d} = \frac{\delta N}{N} = \frac{\delta \sigma}{\sigma}$$

But,

$$\frac{\delta \sigma}{\sigma} = \alpha \frac{n_g}{N} \qquad \text{(from relation 7.7)}$$

Therefore

$$\alpha = \frac{\delta N}{n_g} = \text{experimental value approximately 2.}$$

APPENDIX III

Contrary to the valence electrons of a monovalent metal, all the free conduction electrons of a multivalent metal are not equally effective in the electrical conduction process i.e. they are considered to occupy more than one band with different effective masses. Thus the effective number of conduction electrons (participating in the bulk conductivity) per metal atom is not necessarily equal to the valence electrons (e.g. 3 in the case of erbium) and is generally less. For example, the effective number of conduction electrons per metal atom of transition metals is of the order of one-half per metal atom (see A.H. Wilson, 'The theory of metals', Section 9.5, Cambridge University Press, 1965).

LIST OF SOME SYMBOLS

(other than those universally accepted)

d	thickness of a continuous metal film, and inter-island separation of a patchy film
e	charge of an electron
ℓ_o	electron mean free path in bulk metal
m	mass of an electron (m^* effective mass)
n	number of free electrons per unit volume of a metal
n_g	total number of gas molecules adsorbed on a film
N	total number of metal atoms in a film
p	pressure of a gas in torr
p_o	saturated vapour pressure of a gas in torr
P	specular reflection coefficient of electrons at film boundaries
r	average linear dimensions of an island
$R = R_o + \Delta R$	electrical resistance of a metal film
R_o	initial resistance of a bare metal film
ΔR	change in the electrical resistance of a metal film
T	absolute temperature
v	volume of a gas in cubic centimetre at STP
v_m	monolayer capacity in cubic centimetre at STP
$\bar{v}$	velocity of an electron at the surface of the Fermi distribution
α_o	temperature coefficient of resistance of a bulk metal
α_f	temperature coefficient of resistance of a metal film
α	a gas-metal adsorption parameter i.e. a ratio of the relative change in film resistance to the number of gas molecules adsorbed per metal atom of the film
χ	number of conduction electrons immobilised by the adsorption of one gas molecule

γ	number of effective conduction electrons per metal atom
σ_o, ρ_o	electrical conductivity and resistivity of bulk metal
σ, ρ	electrical conductivity and resistivity of a metal film
σ_m	cross-sectional area of an inert gas molecule in physical adsorption i.e. molecular area in sq. Angstrom
ε	dielectric constant of vacuum-substrate
Σ	specific surface area of an adsorbent in square metres per gram
ϕ	work function of a metal
$\phi(K)$	a function of the ratio of film thickness to bulk mean free path
K	ratio of film thickness to bulk mean free path
θ	surface coverage i.e. the ratio of numbers of gas atoms to the total surface sites of a film.

LIST OF FIGURES AND TABLES

(front page number shown in brackets)

References

1. Neugebauer, C.A., Adv. Vacc. Sci. Tech., Proc. 3rd Internal. Vacc. Congress (1965), Pergamon Press, Oxford, 1, 29, (1966).
2. Thomson, J.J., Proc. Camb. Phil. Soc., 11, 120, (1901).
3. Fuchs, K., Proc. Camb. Phil. Soc., 34, 100, (1937-38).
4. Sondheimer, E.H., Adv. Phys., 1, 1, (1952).
5. Mayer, H., 'Structure and Properties of thin films' (Eds. Neugebauer, C.A., Newkirk, J.B. and Vermilyea, D.A.), Wiley, New York, 225, (1959).
6. Chopra, K.L., Bobb, L.C., Francombe, M.H., J. Appl. Phys., 34, 1699, (1963).
7. Estermann, I., Schlesinger, T., J. Appl. Phys. 41, 2802, (1970).
8. Lucas, M.S.P., J. Appl. Phys., 36, 1632, (1965).
9. Schwarz, H., Luck, R., Mater. Sci. Engg. 5, 149, (1969/70).
10. Mayadas, A.F., Shatzkes, M., Janak, J.F., Appl. Phys. Letters, 14, 345, (1969).
    Mayadas, A.F., Shatzkes, M., Phys. Rev. B , B1, 1382, (1970).
11. Risnes, R., Sollien, V., Phil. Mag., 20, 895, (1969).
12. Risnes, R., Phil. Mag., 21, 591, (1970).
13. Namba, Y., J. Appl. Phys. 39, 6117, (1968).
14. Minn, S.S., J. Rech. Centre Natl. Rech. Sci. Lab. Vellevue (Paris), 51, 131, (1960).
15. van Steensel, K., Philips Res. Repts., 22, 246, (1967).
16. Neugebauer, C.A., Webb, M.B., J. Appl. Phys., 33, 74, (1962).
17. Hill, R.M., Proc. Roy. Soc., A309, 377, (1969).
18. Kiernan, R., Stops, D.W., Nature, 224, 907, (1969).
19. Hacman, D., 'Basic Problems in thin film Physics' (Eds. Niedermayer, R. and Mayer, H.), Proc. Internal. Symp. 1965, in Gottingen, Germany, 561, (1966).
20. Gerstenberg, D., Ann. der Physik , 11, 354, (1963).

21. Huber, F., I.E.E.E. Trans. Compon. Parts, CP-11, 38, (1964).

22. Ramesh Chander, Howard, R.E., Jain, S.C., Indian J. Pure Appl. Phys., 5, 397, (1967).

23. Friebertshauser, P.E., McCamont, J.W., J. Vacc. Sci. Tech, 6, 184, (1969).

24. Legvold, S., Spedding, F.H., Barson, F., Elliott, J.F., Rev. Modern Phys., 25, 129, (1953).

25. Colvin, R.V., Legvold, S., Spedding, F.H., Phys. Rev., 120, 741, (1960).

26. Green, R.W., Legvold, S., Spedding, F.H., Phys. Rev., 122, 827, (1961).

27. Elliott, J.F., Legvold, S., Spedding, F.H., Phys. Rev., 100, 1595, (1955).

28. (a) Skochdopole, R.E., Griffel, M., Spedding, F.H., J. Chem. Phys., 23, 2258, (1955).
(b) Arajs, S., Dunmyre, G.R., Physica, 31, 1466, (1965).

29. Greaves, C., Vacuum, 20, 332, (1970).

30. Tolansky, S., 'An Introduction to Interferometry' Longmans, London, 161, (1962)

31. Campbell, R.D., Proc. I.R.E.E., Australia, 28, 102, (1967).
Coutts, T.J., Lab. Practice, 16, 161, (1967).

32. Holland, L., 'Vacuum deposition of thin films' Chapman & Hall Ltd., London., 113, 114, (1966).

33. McCracken, G.M., Pashley, N.A., J. Vac. Sci. Tech., 3, 96, (1965).
Lawson, R.W., Woodward, J.W., Vacuum., 17, 205, (1967).

34. Jorgenson, G.V., Welhner, G.K., A.V.S., 10th National Vac. Sym. Trans., The Macmillan Co., New York, 388, (1963).

35. 'Handbook of the Physicochemical properties of the elements' (Ed. Samsonov, G.V.) IFI/Plenum, New York, 315,323,325 (1968).

36. 'High purity metals Catalogue 1765' Johnson, Matthey & Co. Ltd., London, 282, (1962).

37. Lucas, M.S.P., Appl. Phys. Letters, 4, 73, (1964).

38. Chopra, K.L., Randlett, M.R., J. Appl. Phys., 38, 3144, (1967).
39. Nossek, R., Zeits. f. Phys. 142, 321, (1955).
40. Belser, R.B., Hicklin, W.H., J. Appl. Phys., 30, 313, (1959).
41. Pashley, D.W., Adv. Phys., 14, 327, (1965).
42. Caswell, H.L., 'Physics of thin films' (Ed. Hass, G.), Academic Press, New York., 1, 56-57, (1963).
43. 'Handbook of the physico-chemical properties of the elements' (Ed. Samsonov, G.V.), IFI/Plenum, New York, 251,101,98 (1968).
44. Murr, L.E., Phys. Stat. Sol., 24, 135, (1967).
45. 'AEI Vacuum MS10' Tech. Information Sheet, Issue 1, Service/A.501 (1967) and 'AEI MS10' Instruction Manual Publication 2032-69, (Ed. B).
46. Craig, R.D., Harden, E.H., Vacuum, 15, 22, (1965).
47. Bailey, J.R., Nuovo Cim. Suppl. (2), 1, 494, (1963).
48. Hass, G., Vacuum, 2, 331, (1952).
49. Hass, G., Bradford, A.P., J. Opt. Soc. Amer. 47, 125, (1957).
50. Lueckert, J., Vakuum Technik, 10, 1, 40, (1961)
51. Arntz, F., Chernow, F., J. Vac. Sci. Tech., 2, 20, (1965).
52. Klopfer, A., Ermrich, W., Adv. Vac. Sci. Tech. (Pergamon Press, London), 1, 427, (1960).
53. Holland, L., Laurenson, L., Allen, P.G.W., Nature, 192, 749, (1961).
54. Heckman, R.C., Special Report SC-RR-69-571 "Electronic properties of rare earth-hydrides" Sandia Laboratories, Albuquerque, New Mexico., November 1969.
55. Rutherford, S.L., Mercer, S.L., Jepsen, R.L., 7th Natl. Symp. A.V.S., (London), 380, (1961).
56. Pitt, K.E.G., Howard, A.J., Vacuum, 18, 517, (1968).
57. MacRae, A.U., Germer, L.H., Phys. Rev. Letters, 8, 489, (1962).
58. Muller, E.W., J. Appl. Phys., 26, 732, (1955).
59. Oguri, T., J. Phys. Soc. Japan, 19, 83, (1964).
60. Ehrlich, G., Hudda, F.G., J. Chem. Phys., 36, 3233, (1962).
61. Culver, R.V., Tompkins, F.C., Advanc. Catalys. 11, 67, (1959).

62. Riviere, J.C., "Solid State Surface Sci." (Ed. Mino Green), Marcel Dekker, New York, 1, 179, (1969).

63. Suhrmann, R., Advanc. Catalys., 7, 303, (1955).
'Chemisorption',(Ed. Garner, W.E.), Butterworth, London, 106, (1957).

64. Brunauer, S., Emmett, P.H., J. Amer. Chem. Soc., 62, 1732, (1940).

65. Debye, P., Physikal Z. 21, 178, (1920).

66. Keesom, W.H., Physikal Z., 22, 129, 643, (1921).

67. London, F., Z. Phys. Chem. B11, 222, (1930).
Z. physik 63, 245, (1930).

68. Mulliken, R.S., J. Amer. Chem., Soc., 74, 811, (1952).

69. Mignolet, J.C.P., J. Chem. Phys. 21, 1298 (1953).
'Chemisorption' 118, (1957)
(Ed. Garner, W.E.), Butterworths, London.

70. Brunauer, S., 'The adsorption of gases and vapours' Oxford Univ. Press, London, 140, (1945).

71. Hayward, D.O., Trapnell, B.M.H., 'Chemisorption' Butterworths, London., 1, (1964).

72. Elovich, S.Yu., Margolis, L.Ya., Izvest. Akad. Nauk. S.S.S.R., Ser. Fiz. 21, 206, (1957).

73. Smeltzer, W.W., McIntosh, R., Canad. J. Chem., 31, 1239, (1953).

74. Bardeen, J., Phys. Rev., 71, 717, (1947).

75. Mostovetch, M.N., Comptes Rendus Acad. Sci. Paris, 228, 1702, (1949).

76. Horiuti, J., Toya, T., Solid State Surface Sci., (Ed. Mino Green), Marcel Dekker, New York, 1, 1, (1969).

77. Toya, T., J. Res. Inst. Catalysis, Hokkaido Univ. 8, 209, (1960).

78. Suhrmann, R., Wedler, G., Sehliephake, D., Z. Physik. Chem., (Frankfurt), 12, 128, (1957).

79. Zwietering, P., Koks, H.L.T., van Heerden, C., J. Phys. Chem. Solids, 11, 18 (1959).

80. Ehrlich, G., J. Chem. Phys., 35, 2165, (1961).
81. Sachtler, W.M.H., Dorgelo, G.J.H., Z. Physik Chem., 25, 69, (1960).
82. Sachtler, W.M.H., Adv. Vacc. Sci. Tech., Proc. 3rd. Intern. Vacuum Congress (1965), Pergamon Press, Oxford, 1, 41, (1966).
83. Geus, J.W., Surface Sci., 2, 48, (1964).
84. Fehlner, F.P., Adv. Vacc. Sci. Tech., Trans. 3rd Inter. Vacc. Congress, (1965), Pergamon Press, Oxford, 2, 691, (1966).
85. Brunauer, S., Deming, L.S., Deming, W.E., Teller, E., J. Amer. Chem. Soc., 62, 1723, (1940).
86. Langmuir, I., J. Amer. Chem. Soc., 40, 1361, (1918).
87. Emmett, P.H., Brunauer, S., J. Amer. Chem. Soc., 59, 1553, (1937).
88. Halsey, G.D., Disc. Faraday Soc. 8, 54, (1950).
J. Amer. Chem. Soc. 73, 2693, (1951).
89. Brunauer, S., Emmett, P.H., Teller, E., J. Amer. Chem. Soc., 60, 309, (1938).
90. Zettlemoyer, A.C., Walker, W.C., J. Phys. Colloid. Chem., 52, 47 & 58, (1948).
91. Frenkel, J., 'Kinetic theory of liquids', Clarendon Press, Oxford, Sec. 5, Chap. 7, (1946).
92. Halsey, G., J. Chem. Phys., 16, 931, (1948).
93. Hill, T.L., Advanc. Catalys., 4, 211, (1952).
94. Anderson, R.B., J. Amer. Chem. Soc., 68, 686, (1946).
95. Anderson, R.B., Hall, W.K., J. Amer. Chem. Soc., 70, 1727, (1948).
96. Beebe, R.A., Beekwith, J.B., Honing, J.M., J. Amer. Chem. Soc., 67, 1554, (1945).
97. "Encyclopaedic Dictionary of Physics, Supplementary Volume 2" (Ed. Thewlis, J.), Pergamon Press, London, New York, page 1-5, (1967).
98. Brennan, D., Graham, M.J., Hayes, F.H., Nature, 199, 1152, (1963).
99. Anderson, J.R., Baker, B.G., J. Phys. Chem., 66, 482, (1962).

100. Ehrlich, G., Hudda, F.G., J. Chem. Phys., 30, 493, (1959).
101. Rootsaert, W.J.M., van Reijen, L.L., Sachtler, W.M.H., J. Catalysis 1, 416, (1962).
102. Lander, J.J., Morrison, J., Surface Sci., 6, 1, (1967).
103. Nikliborc, J., Dworecki, Z., Acta Physica Polonica, 32, 1023, (1967).
104. Engel, T., Gomer, R., J. Chem. Phys., 52, 5572, (1970).
105. Singleton, J.H., Halsey, G.D., J. Phys. Chem., 58, 330, (1954).
106. Salutsky, M.L., "Comprehensive analytical chemistry", part Ic, (Eds. Wilson, C.L., and Wilson, D.W.), Elsevier publishing Co., London, 444, (1962).
107. Riviere, J.C., Allinson, J.D., Nuovo Cimento Suppl. (2), 1, 520, (1963).
108. Keesom, W.H., Mazur, J., Meihuizen, J.J., Physica, 2, 669, (1935).
109. Brennan, D., Hayward, D.O., Trapnell, B.M.W., Proc. Roy. Soc., A256, 81, (1960).
110. Singh, B., Müller, J., Surplice, N.A., Dutch Journal, Ned. Tijds. Voor Vacuumtechniek, 8, 109, (1970).
111. Roberts, M.W., Recent Prog. Surface Sci., 3, 1, (1970).
112. Pebler, A., Wallace, W.E., J. Phys. Chem., 66, 148, (1962).
113. Heckman, R.C., Hills, C.R., Bull. Am. Phys. Soc., (abstract only given), Fig. 36a, from a private communication of United Kingdom Atomic Energy Authority to Heckman, R.C.
114. Mueller, W.M., "Metal Hydrides", (Eds. Mueller, W.M., Blackledge, J.P., and Libowitz, G.G.), Academic Press, New York, London. 433, (1968).
115. Denison, D.R., Proc. of the 4th Internal. Vacuum Congr. Part I, Conference Ser. 5, Institute of Physics and Physical Society, U.K., 377, (1968).
116. Quinn, C.M., Roberts, M.W., Trans. Faraday Soc., 60, 899, (1964).
117. Ponec, V., Knor, Z., Cerny, S., Proc. of the third Internal. Congress on Catalysis, Amsterdam, 1964, (North-Holland, Amsterdam), 353, (1965).

118. Surplice, N.A., Müller, J., Singh, B., 6th Report on "Ion Source Studies" Contract CON/ALD/11/259133, submitted to United Kingdom Atomic Energy Authority, 16,(Feb. 1971).

119. Bastl, Z., Surface Sci., 22, 465, (1970).

120. Kawasaki, K., Sugita, T., Ebisawa, S., Surface Sci., 7, 502, (1967).